TECHNISCHE UNIVERSITÄT MÜNCHEN

Lehrstuhl für Chemie der Biopolymere

Optimization of Oncolytic Viral Therapy for Hepatocellular Carcinoma

JENNIFER ALTOMONTE

Vollständiger Abdruck der von der Fakultät Wissenschaftszentrum Weihenstephan für Ernährung, Landnutzung und Umwelt der Technischen Universität München zur Erlangung des akademischen Grades eines

Doktors der Naturwissenschaften

genehmigten Dissertation.

Vorsitzender: Univ.-Prof. Dr. A. Skerra

Prüfer der Dissertation:

1. Univ.-Prof. Dr. D. Langosch
2. Priv.-Doz. Dr. O. Ebert

Die Dissertation wurde am 20.07.2010 bei der Technischen Universität München eingereicht und durch die Fakultät Wissenschaftszentrum Weihenstephan für Ernährung, Landnutzung und Umwelt am 16.09.2010 angenommen.

Summary

Oncolytic viruses (OVs) represent a novel biological approach to cancer therapy and are under intense investigation as promising strategies for the treatment of malignancy. Oncolytic virotherapy involves the use of replication-competent viruses that have the intrinsic ability to grow selectively in tumor cells or have been engineered to do so. OVs achieve their tumor selectivity by exploiting abnormalities in cell signaling pathways, which accumulate during malignant transformation, and replicate only in the context of constitutive activation or shutdown of particular transcriptional activities. In particular, many tumor cells harbor defects in interferon (IFN) signaling, resulting in the inability to induce and/or respond to IFN, and therein, tumor escape from anti-viral immune responses is facilitated. RNA viruses have emerged as especially potent oncolytic agents because of their intrinsic capacity to specifically target and destroy tumor cells while sparing the surrounding normal cells and tissues. However, despite encouraging progress in this field, several barriers remain in the development of OV therapy, including relatively poor penetration throughout solid tumor masses, inefficient viral replication in primary cancers in immune-competent hosts, and tumor-specific resistance to virus-mediated killing.

Several strategies are under development to overcome these limitations and improve existing oncolytic vector systems. These strategies can be classified into three major subdivisions: 1) Combination of oncolytic viruses with existing clinical agents for additive or synergistic tumor responses; 2) Virus engineering to modify viral genes or introduce heterologous genes for enhancement of safety or efficacy; 3) Mechanistic studies to better elucidate the means whereby viruses derive their oncolytic specificity and tropism in order to de-target major organs and intelligently design safer next-generation vectors. Advances in genetic engineering and understanding of tumor biology have greatly facilitated the evolution of the field of oncolytic viral therapy, and improved vectors are currently under development.

The work presented here summarizes three publications, each of which represents one of the three strategies for OV development outlined above. All three focus on the treatment of hepatocellular carcinoma (HCC) as a model cancer system, however the principles could potentially be applied to other cancers. The first section describes the combination of oncolytic vesicular stomatitis virus (VSV) with a clinically employed degradable embolization agent. The second section discusses the engineering of the endogenous fusion protein of Newcastle disease virus for enhanced cell-cell membrane fusion, and, hence, enhanced bystander cell killing in HCC tumors. The final portion of this work deals with the characterization of a defect in interferon signaling in HCC cells, which provides a mechanism for the susceptibility of tumor cells to VSV infection and subsequent cell killing. Taken together, this work represents the major areas of recent progress in oncolytic virus development. The three approaches resulted in enhanced oncolytic viral therapy or in the better understanding of the mechanism whereby oncolytic viruses derive their tumor

specificity. This knowledge can contribute to the development of future clinical oncolytic viral agents for cancer therapy.

List of original publications

1. Altomonte, J., Braren, R., Schulz, S., Marozin, M., Rummeny, EJ, Schmid, RM, and Ebert, O. (2008) **Synergystic antitumor effects of transarterial viroembolization for multifocal hepatocellular carcinoma in rats.** ***Hepatology***, 48(6):1864-73.

2. Altomonte, J., Marozin, S., Schmid, RM, and Ebert, O. (2010). **Engineered Newcastle Disease Virus as an improved oncolytic agent against hepatocellular carcinoma**. *Mol Ther*, 18(2):275-84.

3. Marozin, S., Altomonte, J., Stadler, F., Thasler, WE, Schmid, RM, and Ebert, O. (2008). **Inhibition of the IFN-b response in hepatocellular carcinoma by alternative spliced isoform of IFN regulatory factor 3**. *Mol Ther,* 16(11):1789-97.

Abbreviations

OV	oncolytic virus
IFN	interferon
RNA	ribonucleic acid
HCC	hepatocellular carcinoma
VSV	vesicular stomatitis virus
HCV	hepatitis C virus
TAE	transarterial embolizaiton
TACE	transarterial chemoembolization
wt	wild-type
N	nucleoprotein
P	phosphoprotein
M	matrix protein
G	glycoprotein
L	large polymerase
RNP	ribonucleoprotein
BHK	baby hamster kidney
CPE	cytopathic effect
cDNA	complementary deoxyribonucleic acid
GFP	green fluorescent protein
NDV	Newcastle disease virus
NP	nucleocapsid protein
HN	hemagglutinin-neuraminidase
F	fusion protein
PCR	polymerase chain reaction
NK	natural killer cell
RIG-I	retinoic acid inducible gene-1
TLR	Toll-like receptor
IRF3	interferon regulatory factor 3
DCE-MRI	dynamic contrast-enhanced magnetic resonance imaging
PBS	phosphate buffered saline
pfu	plaque-forming units
β-gal	β-galactosidase
$TCID_{50}$	tissue culture infectious dose 50
dsRNA	double stranded RNA

Table of Contents **Page**

1. Introduction

1.1 Hepatocellular Carcinoma

Hepatocellular carcinoma (HCC) represents a major worldwide health concern, ranking among the top five most prevalent malignancies in the world and accounting for over one million cases annually (Parkin 2001). The incidence of HCC has more than doubled over the last two decades (El-Serag 1999; Dyer 2005), and recent reports suggest that the rate of HCC diagnoses will continue to rise, presumably as a consequence of an ever-increasing prevalence of hepatitis C virus (HCV) infection and increased alcohol consumption, as well as rising incidence of obesity and diabetes observed in most industrialized countries (Taylor-Robinson 1997; Deuffic 1998; El-Serag 2003; Dyer 2005). HCC arises from the malignant transformation of hepatic parenchymal cells, usually in the setting of chronic liver disease, such as chronic viral hepatitis, alcoholic cirrhosis, hemochromatosis, and autoimmune hepatitis.

While the incidence of HCC steadily increases, the emergence of new and effective therapeutic agents has remained relatively stagnant. Treatment modalities for HCC with demonstrated survival prolongation are limited to hepatic resection and local-regional ablation procedures for solitary tumors, and orthotopic liver transplantation for solitary or multifocal tumors limited to the liver. Patients with solitary lesions and normal underlying liver function have a 5-year survival rate of up to 52% following hepatic resection, depending on tumor size, vascular invasion, and resection of adequate negative margins surrounding the tumor (Liau 2005). Patients with small solitary lesions who are not candidates for hepatic resection due to poor hepatic reserve from cirrhosis have comparable survival rates (63% at 3-years) following local percutaneous alcohol injection under ultrasound guidance (Livraghi 1992). Other localized tumor ablation procedures are currently under investigation, including cryo-, microwave, and radiofrequency ablation (Popescu 2005). For patients with multifocal tumors localized to the liver, regional approaches, such as orthotopic liver transplantation, offer long-term remission with 3-year survival rates of 39-57% (Merli 2005). However, the majority of HCC cases are detected at an advanced stage, at which time the treatment options are even further limited (Bertolozzi 1995; Mathurin 1998; Llovet 2003). Although surgical resection and liver transplantation are considered to be curative, the majority of patients do not meet the strict criteria designated by such treatments. In general, surgical therapy is indicated only in patients with limited HCC progression (1-3 nodules), without portal hypertension or underlying liver disease (Bruix 1996; Llovet 1999; Arii 2000). The feasibility of liver transplantation is further limited by a shortage of donor livers, resulting in waiting times in excess of 12 months in some Western countries (Keeffe 1998; Yao 2002; Graziadei 2003; Schwartz 2007).

For patients with non-resectable HCC, or patients on the waiting list to receive liver transplantation, local regional therapy using transarterial embolization (TAE) or transarterial chemoembolization (TACE) are considered standard palliative treatment (Bruix 2004; Blum

2005; Miraglia 2007; Schwartz 2007). The rationale for such therapies lies in the dual blood supply feeding the liver. While normal hepatocytes receive the majority of their blood flow from the portal vein, with only about 25% being supplied by the hepatic artery, tumors receive their blood almost exclusively from the hepatic artery (Lein 1970; Ackerman 1972; Kan 1983). TAE and TACE therapies exploit this unique feature by blocking the arterial blood flow in the liver, and thereby delivering a concentrated dose of a chemotherapeutic drug and/or embolizing agent selectively to the tumor, resulting in ischemia-induced necrosis, and enhanced oncolysis due to a prolonged exposure time of the tumor cells to the chemotherapeutic agent (Anderson 1981; Kato 1981; Tancredi 1999). Although it is generally accepted that TAE and TACE techniques result in substantial tumor response after treatment (Chang 1994; Kenji 1997; Bruix 1998; Camma 2002; Llovet 2003; Varela et al. 2007), it is not yet clear whether or not the incorporation of chemotherapy provides an additional survival benefit over TAE alone.

For patients with advanced HCC, the prognosis and response to treatment is poor. Systemic chemotherapy with doxorubicin, mitomycin or 5-fluorouracil has produced response rates of less than 20% with minimal impact on the median survival of 4 months (Simonetti 1997). Recently, sorafenib, an oral multikinase inhibitor of the vascular endothelial growth factor receptor, the platelet-derived growth factor receptor, and Raf, has shown promise for advanced HCC. Early trials indicate the median survival and the time to radiologic progression were prolonged by nearly 3 months for patients treated with sorafenib than for those given placebo; however, the time to symptomatic progression did not differ significantly among the two groups, and it remains to be seen how effective and safe sorafinib will be for treatment of patients with poor liver function (Llovet et al. 2008).

In conclusion, despite incremental advances in palliative treatment options, HCC remains a disease for which only a small proportion of patients are candidates for curative treatments, while the remaining majority of patients face a poor prognosis (Yeung 2005). The development of novel and effective treatment modalities is, therefore, urgently needed.

1.2 Oncolytic viruses as tumoricidal agents

Due to the overwhelming deficit in effective treatment options for HCC, several alternative approaches have emerged. Oncolytic viruses (OVs) represent a novel class of therapeutic agents for cancer treatment, due to their intrinsic ability to selectively replicate and kill tumor cells, while sparing the surrounding normal tissue (Lorence 1994; Coffey 1998; Kirn 2001; Peng 2001). OV therapies are based on the use of replication-competent viruses that have been selected or engineered to preferentially grow in tumor cells. During the process of malignant transformation, genetic abnormalities accumulate to provide cancer cells with growth and survival advantages. OVs exploit such defects in cellular signaling pathways to support their own replication in these cells. A well-characterized example of this

phenomenon is the impaired ability of many cancer cells to secrete or respond to interferon (IFN) in comparison to normal cells, which demonstrate efficient and robust IFN signaling capabilities. While these defects allow tumors to escape from immune surveillance, they also prevent tumor cells from mounting a productive antiviral defense, and, thus, replication of the OV is permitted.

Oncolytic viruses exert their effects both by direct killing of infected tumor cells, as well as via induction of adaptive immune responses, which can boost anti-tumor immunity and lead to destruction of neighboring uninfected tumor cells. Furthermore, viruses can be engineered to express a wide range of therapeutic genes to further enhance the oncolytic potential and tumor specificity. Over the last decade, exponential progress has been made in the development of enhanced OV therapies, and many novel strategies are being explored.

The idea that viruses might be able to kill tumor cells has been reported since the late 19th century. The initial reports were not based on attempts at alternative cancer therapy, but rather, the result of observations that some cancer patients experienced periods of brief remissions following contraction of an infectious disease. The classically sited case involved a 42-year-old woman with "myelogenous leukemia" that went into remission after a presumed influenza infection, reported in 1896 (Dock 1904). Since this case, various other clinical case reports have described the regression of leukemia and Hodgkin's disease coinciding with acquired viral infections, such as chickenpox, measles, and hepatitis (Hoster et al. 1949; Bierman et al. 1953; Pasquinucci 1971; Zygiert 1971; Taqi et al. 1981). It was furthermore reported at the International Cancer Congress in 1910, that a patient suffering from a large cervical carcinoma underwent spontaneous remission of the tumor following the injection of a live rabies vaccine administered after the patient was bitten by a rabid dog (DePace 1912). This was the first known case of an oncolytic response to a live viral vaccine. As a result of these early observations, as well as the advent of in vivo cancer models and in vitro cell culturing technology, research in the field of oncolytic virus therapy accelerated rapidly during the 1950s and 1960s. During this time, clinical studies involving the administration of various human pathogens to cancer patients were undertaken, some of which would seem contradictory to current ethical standards. However, several of these early attempts resulted in moderate success with minimal side effects, including a vaccine strain of rabies virus used in a clinical study involving melanomatosis, which resulted in tumor regression in 8 out of 30 treated patients (Pack 1950), and a trial of adenovirus adenoidal-pharyngeal-conjuctival virus (APC) administered to cervical carcinoma patients, which resulted in localized tumor necrosis in 26 out of 40 patients (Huebner et al. 1956).

Although interest in the field quickly faded in the years following, the past two decades have demonstrated a resurgence in oncolytic virus research, resulting in new attempts at clinical trials. Most oncolytic viruses currently used in clinical trials are derived from adenovirus or herpes simplex virus type 1 (HSV1), with more than 300 patients with solid tumors already treated. The use of a molecularly engineered replication-competent HSV1 to treat glioma was first proposed by Martuza et al. in the early 1990s (Martuza 1991), and has since been

explored by others (Ikeda 2000; Kambara 2005). The generation of recombinant virus rescue techniques allowed attenuated HSV1 vectors with tumor specificity to be engineered, and they were shown to be effective in other tumor models (Coukos 2000; Blank 2002). These have been tested in early-phase clinical trials (Mineta 1995; Miyatake 1999).

In parallel to these HSV1 trials, the concept of using an "oncolytic virus" as a new class of therapeutic agents for cancer treatment was further popularized by McCormick et al. in the mid-1990s, when they reported that adenovirus dl1502 with an E1B-deletion (Barker 1987) was able to preferentially replicate in p53-negative tumor cells in vitro and in tumor-bearing mice, either alone or in combination with standard chemotherapy (Bischoff 1996; Heise 1997). This mutant adenovirus was later re-named Onyx-015 and it has been tested in multiple clinical trials with mixed results. While there were indications of intratumoral viral replication and moderate tumor responses, the anti-tumor effects were more evident when applied with standard cisplatin-based chemotherapy (Nemunaitis 2000; Chiocca 2004). Since then, a variety of conditionally replicating adenoviruses were created by deletion of other endogenous viral genes that are necessary for viral replication in normal cells but dispensable in tumor cells, use of tumor-specific promoters to direct the expression of early adenovirus genes that are necessary for viral replication, or engineered viral coat protein genes with tumor-specific ligands (Wickham 1997; Hallenbeck 1999; Fueyo 2000). In November 2005, the first marketing approval of an oncolytic virus was granted by Chinese regulators for the genetically modified adenovirus H101 for use in combination with chemotherapy in the treatment of late-stage nasopharyngeal cancer (Garber 2006). In addition, other virus-based therapies have shown even greater promise for the treatment of cancer, in particular OncoVEX GM-CSF, which is based on herpes simplexc virus and is now in Phase 3 clinical trials in melanoma. Vectors derived from retroviruses, as well as other RNA viruses such as reovirus, Newcastle disease virus, measles virus and vesicular stomatitis virus, have also been explored for their oncolytic potential due to their inherent tumor specificity (Kirn 2001). However, despite marginal success, a ubiquitous limitation to the successful use of oncolytic viruses to treat cancers is their relatively inefficient replication and spread within the solid tumor mass in vivo. Secondly, neutralizing anti-viral immune responses are elicited within days, which limits the duration of intratumoral replication for oncolytic viruses in immune-competent hosts. These limitations can be partially addressed through the use of viruses with great oncolytic potency and short life cycles, and other viral engineering and combination strategies are being explored to further minimize these issues.

1.3 Vesicular stomatitis virus as an oncolytic virus

Vesicular stomatitis virus (VSV), is an enveloped, negative-sense, single-stranded RNA Rhabdovirus. Because it has inherent tumor specificity due to the attenuated type I interferon responses in most tumor cells, it represents an extremely promising oncolytic agent for

cancer treatment. Additional features contributing to the potential of VSV as an attractive oncolytic virus include: 1. a short life cycle of only 8-10 hours, leading to robust replication in most rodent and human tumor cell types (Stojdl et al. 2000; Balachandran et al. 2001; Fernandez 2002); 2. the ability to molecularly engineer the virus by reverse genetics (Lawson et al. 1995; Whelan et al. 1995) and the genetic stability of the resultant recombinant virus vectors (Schnell et al. 1996); 3. the ability to rigorously test its oncolytic potency and safety in immune-competent laboratory animals bearing syngeneic tumors since they are permissive hosts to this virus (Balachandran 2000; Stojdl et al. 2000; Fernandez 2002; Stojdl 2003); 4. the avoidance of potential complications associated with vector integration into cellular chromosomes because it is a cytoplasmic virus with an RNA genome that does not enter the nucleus and does not have a DNA phase in its life cycle (Rose et al. 2001); and 5. VSV-Indiana, a laboratory strain that has been in research use for decades, is not a pathogen in humans and there are no pre-existing neutralizing antibodies in the general population that can compromise its effectiveness in cancer treatment. Infections in humans are asymptomatic in most cases or result in a mild febrile illness (Letchworth et al. 1999).

VSV replicates in the cytoplasm of susceptible cells, causing cell death as a result of the general shutdown of host RNA and protein synthesis. It was first observed that treatment of human melanoma xenografts with wild-type (wt) VSV in nude mice resulted in regression or growth inhibition of the established tumors, while sparing the surrounding normal cells (Stojdl et al. 2000). Because VSV is known to be extremely sensitive to the anti-viral actions of type I interferons (IFN), it has been postulated that its tumor specificity is the result of defects in interferon signaling in cancer cells (Stojdl et al. 2000). However, it is also recognized that defects in IFN signaling can only partially explain the robust tumor-specific replication of VSV in cancer cells, and, therefore, other mechanisms must exist.

Although VSV has produced encouraging results in several different tumor models, there is a clear need for improvement of available vectors. The development of a "reverse genetics" system for rescue of recombinant negative-sense RNA viruses has provided the opportunity to engineer the genome of VSV for the construction of novel oncolytic vectors.

1.3.1 Generation of recombinant VSV vectors by reverse genetics

The linear, single-stranded RNA genome of VSV, approximately 11kb in size, represents a succession of five individual protein-encoding genes, each defined by an upstream gene start signal and downstream gene end signal. Transcription starts at the very 3' end of the genome producing a leader RNA of approximately 50 nucleotides in length. This is followed by the sequential synthesis of the individual mRNAs, giving rise to a gradient of transcripts, steadily decreasing in copy number toward the template 5'end. The RNA genome of VSV contains five genes in the order 3' N – P – M – G – L 5' (Fig. 1). It has an extremely compact arrangement with only two nucleotides between each of the transcription units encoding the

five mRNAs. The nucleocapsid (N) protein, and the phosphoprotein (P) are encoded in the 3' proximal part of the genome, whereas the catalytic subunit of the polymerase (L) is located 5' terminally. N protein mRNAs are therefore the most abundant mRNA species, whereas transcripts encoding the L protein, which is required in very small amounts, are much less abundantly produced. In between are located genes coding for matrix (M) and the transmembrane envelope glycoprotein (G).

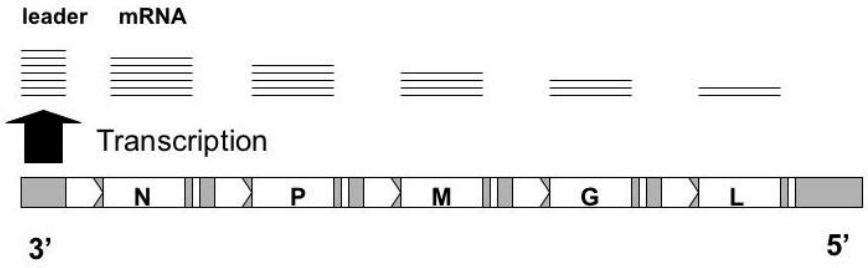

Figure 1. Genome structure and RNA synthesis of VSV. The VSV genome organization containing the five genes (N, P, M, G, and L). Transcriptional start and stop signals are indicated by open arrowheads and vertical boxes, respectively. Attenuation at gene borders produces a gradient of mRNA transcripts.

Replication of the VSV genome is a process distinct from transcription of the gene units, although both processes are performed by the same viral polymerase encoded by the L and P genes. During replication, the polymerase acts in a processive mode in which the internal transcription signals are ignored so that full-length genomic RNAs are produced. The final RNA product is then encapsidated into a ribonucleoprotein complex (RNP), which contains a copy of the positive RNA strand of the VSV genome. When synthesis of the RNP is complete, the anti-genome RNP serves as a template for the polymerase, although exclusively for replication. The newly synthesized genome RNPs may then serve again as templates for both transcription (secondary transcription) and replication. (Conzelmann 1998)

For the generation of infectious recombinant VSV vectors, a reverse genetics system has been established (Fig. 2) (Lawson et al. 1995; Whelan et al. 1995). Using this system, recombinant VSV vectors with modifications to the viral genome, or with foreign transgenes inserted as additional transcriptional units, can be rescued (Schnell et al. 1996; Schnell et al. 1996). To this end, individual plasmids encoding the T7 promoter-driven VSV nucleocapsid protein (pT7-N), phosphoprotein (pT7-P), and polymerase (pT7-L) are transfected into BHK (baby hamster kidney) cells previously infected with vTF7-3, a recombinant vaccinia virus that expresses the T7 RNA polymerase (Fuerst et al. 1986). In addition, a plasmid containing the full-length anti-genomic VSV cDNA with a T7 promoter at the 5' end and a self-cleaving ribozyme at the 3' end (pT7-FL) is co-transfected. Two days post-transfection, the conditioned medium is harvested and filtered to remove the vaccinia virus, which is much

larger in size than VSV, and added to fresh BHK cells. Within 48 hours, a cytopathic effect (CPE) can be observed in dishes of cells in which the virus was successfully rescued.

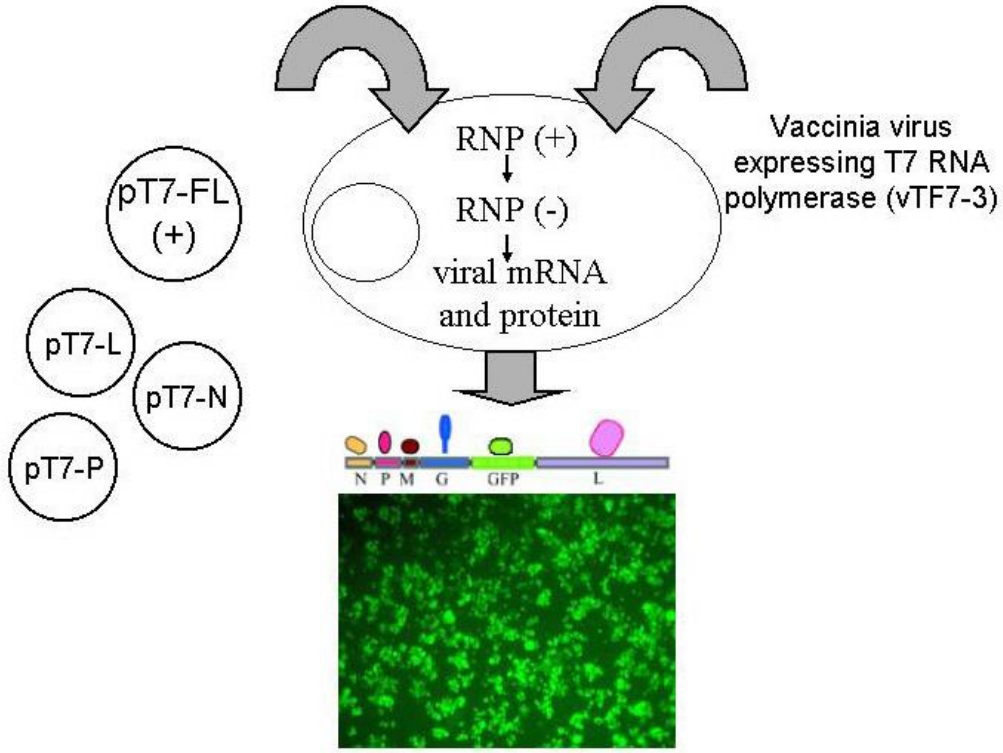

Figure 2. Reverse genetics system for VSV. Briefly, baby hamster kidney (BHK) cells were grown in 10-cm dishes and infected at a multiplicity of infection (MOI) of 10 with vTF7-3. After 1 hour, cells in each dish were co-transfected with an equimolar mixture of T7 promoter-driven plasmids expressing N, P, and L genes, and the full-length anti-genomic plasmid pT7-FL encoding GFP. The cells were incubated at 37°C for 48 hours following co-transfection. The cell supernatant was passed through a 0.2 μm-pore-size filter to remove the majority of vaccinia virus and then applied to fresh BHK cells for an additional 48 hours. Recovery of infectious VSV was confirmed by scanning BHK monolayers for cytopathic effects and GFP expression.

1.4 Newcastle disease virus as an oncolytic agent

Newcastle disease virus (NDV) is a nonsegmented, negative-strand RNA virus of the *Paramyxoviridae* family, whose natural host range is limited to avian species; however, it is known to enter cells by binding to sialic acid residues present on a wide range of human and rodent cancer cells (Reichard 1992). NDV has been shown to selectively replicate in and destroy tumor cells, while sparing normal cells, a property believed to stem from the defective antiviral responses in tumor cells (Balachandran 2000; Stojdl 2003). Normal cells, which are competent in launching an efficient antiviral response quickly after infection, are able to inhibit viral replication before cell damage can be initiated. The sensitivity of NDV to interferon (IFN), coupled with the defective IFN signaling pathways in tumor cells, provides

a mechanism whereby NDV can replicate exclusively within neoplastic tissue (Park et al. 2003).

The oncolytic properties of NDV were first reported by Cassel and Garret in 1965 (Cassel et al. 1965). Since then, NDV has been investigated in many in vitro and in vivo studies for its potential as an anti-cancer therapeutic. Due to compelling pre-clinical data implicating NDV as an ideal candidate for cancer therapy, phase I and II clinical trials have recently been initiated (Csatary 2004; Freeman 2006; Hotte 2007). Several have successfully demonstrated that NDV is a safe and effective therapeutic agent, with no reports of pathologic effects in patients beyond conjunctivitis or mild flu-like symptoms (Nemunaitis 2002). Although the results of these ongoing clinical trials are encouraging, strategies for improving the therapeutic potential of this virus are warranted, and the established system for generating modified NDV vectors through reverse genetics has provided a unique opportunity to achieve this aim. To this end, recent reports have demonstrated the successful use of recombinant NDV vectors engineered to express various transgenes to provide improved oncolytic efficacy (Janke 2007; Vigil 2007).

1.4.1 Characterization of Newcastle disease virus

The nonsegmented, negative stranded RNA genome of NDV is 15.9 kb in length, and the genomic RNA contains six genes encoding at least eight proteins. The nucleoprotein (NP) is the most abundant protein within the virion, and forms the nucleocapsid with the phosphoprotein (P) and the large polymerase protein (L). The genomic RNA together with this nucleocapsid structure create the ribonucleoprotein complex (RNP), which serves as a template for RNA synthesis (Yusoff et al. 2001). The hemagglutinin-neuraminidase surface glycoprotein (HN) and the fusion protein (F) are anchored in the lipid bilayer of the external envelope, while the inner layer of the virion envelope is formed by the matrix (M) protein (Fig.3). Two additional non-structural proteins, V and W, are formed during RNA editing of transcription of the P gene. It has been demonstrated that the V protein is the determinant of host range restriction and functions by antagonizing interferon responses in avian cells, but not in human cells (Park et al. 2003). The W protein is also likely to play a role in replication and pathogenesis of the virus, although its precise function has yet to be understood.

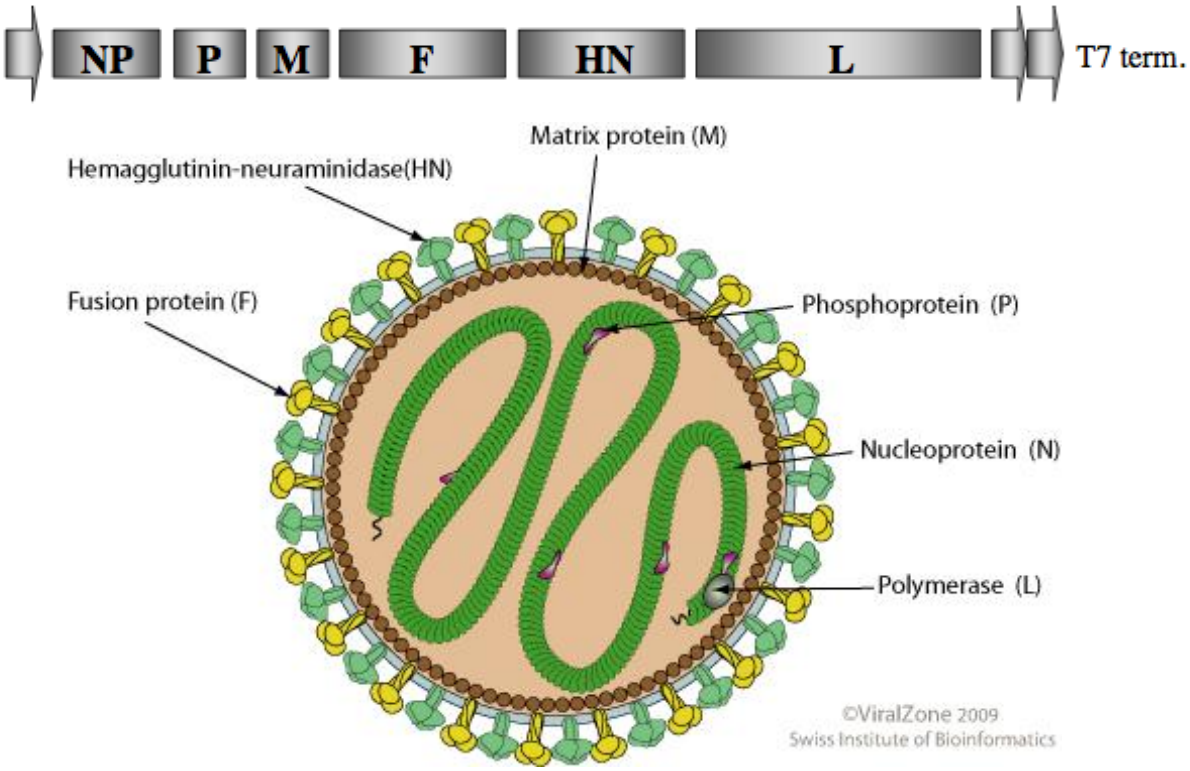

Figure 3. NDV genome and structure of the NDV virion. The NDV genome encodes for six viral genes: N, P, M, F, HN, and L. The N, P, and L proteins form the RNP, while the HN and F are anchored in the external envelope. The M protein forms the inner layer of the viral envelope.

NDV binds to cells via the HN protein, which attaches to host cell receptors containing sialic acid. Binding is then followed by fusion of viral and cell membranes, a process mediated by the F protein. The viral RNA is then released into the cytoplasm of the cell, where replication then occurs. Through this critical process of binding and fusion, the interaction of HN and F is responsible for infectivity and virulence. The HN possesses six glycosylation sites, which contribute to protein folding, stability, maturation, and antigenicity, and together with the F protein, determines the virulence and pathogenicity of the NDV strain. Based on the virulence in infected birds, NDV can be classified into three pathotypes: 1) Lentogenic, which is considered non-virulent, and causes only mild or asymptomatic respiratory disease; 2) Mesogenic, which produces intermediate respiratory and nervous symptoms with moderate mortality rates; and 3) Velogenic, which causes severe gastrointestinal lesions and neurological disease resulting in death of infected birds. The presence of multiple basic amino acids at the cleavage site of the fusion protein precursor (F0) determines the molecular basis of virulence in birds.

1.4.2 Generation of recombinant NDV vectors

The reverse genetics system for generating recombinant vectors has been described in the previous section for VSV. Two days after co-transfection of the full-length NDV plasmid,

along with the helper plasmids expressing NP, P, and L into a co-culture of A549 and primary chicken embryo fibroblasts (CEFs), aliquots of the supernatants are injected into 10-day old embryonated chicken eggs for production of high titers of the rescued virus. Using this technique, several reports have described the enhancement of recombinant NDV vectors through the incorporation of various therapeutic genes. For example, vectors encoding GM-CSF, IFN-γ, IL-2, TNF-α, and the influenza NS1 protein have been reported (Vigil 2007; Zhao et al. 2008; Zamarin 2009).

1.5 Antiviral effects of interferons

Interferons (IFNs) are a group of secreted cytokines, which exert pleiotropic effects on important cell functions, including cell proliferation and modulation of the immune system (Dunn et al. 2006; Stetson et al. 2006). The IFN system provides an extremely powerful potent antiviral response to control virus infections in the absense of adaptive immunity. Based on their amino acid sequences, they are grouped into three classes: type I, II, and III IFNs. Type I IFNs comprise a large group of molecules; however, only IFN-α and -β are induced directly in response to viral infection. Type II IFN has a single member, IFN-γ, and is secreted by activated T cells and natural killer (NK) cells, rather than in direct response to viral infection. The cytokines in the type III IFN group, IL-29, IL-28A, and IL28B, are also induced in direct response to viral infection and appear to use the same pathway as the IFN-α/β genes to sense infection.

IFN-β and/or IFN-α are rapidly induced following the detection of viral nucleic acids in the cytoplasm of cells by intracellular receptors, such as retinoic-acid inducible gene-1 (RIG-I), or after engagement of Toll-like receptors (TLRs) (Yoneyama et al. 2004), and activate a signal transduction pathway that triggers the transcription of a diverse set of genes. These genes are referred to as IFN-inducible genes or IFN-stimulated genes, and together they establish an antiviral response in target cells (Fig. 4). Type III IFNs are also secreted and elicit an equivalent antiviral response to IFN-α/β. However, the role of the type III IFNs is not entirely elucidated, and it seems they do not play an essential role in host survival in response to viral infection.

Interferon regulatory factor-3 (IRF3) is a member of the IFN regulatory transcription factor family, which, upon stimulation and dimerization, translocates to the nucleus and activates the transcription of IFN-α and -β, as well as other IFN-inducible genes (Hiscott et al. 1999). The production of IFN during viral infection leads to the induction of at least three transcription factors (IRF-1, -7, and -9). Positive feedback models have suggested that IRF3 is utilized for induction of primary IFN genes, which then feed back onto cells and induce synthesis of IRF-7, which, in the presence of a continued infection, enhances the transcription of the primary, as well as secondary, IFN genes (Fig. 5).

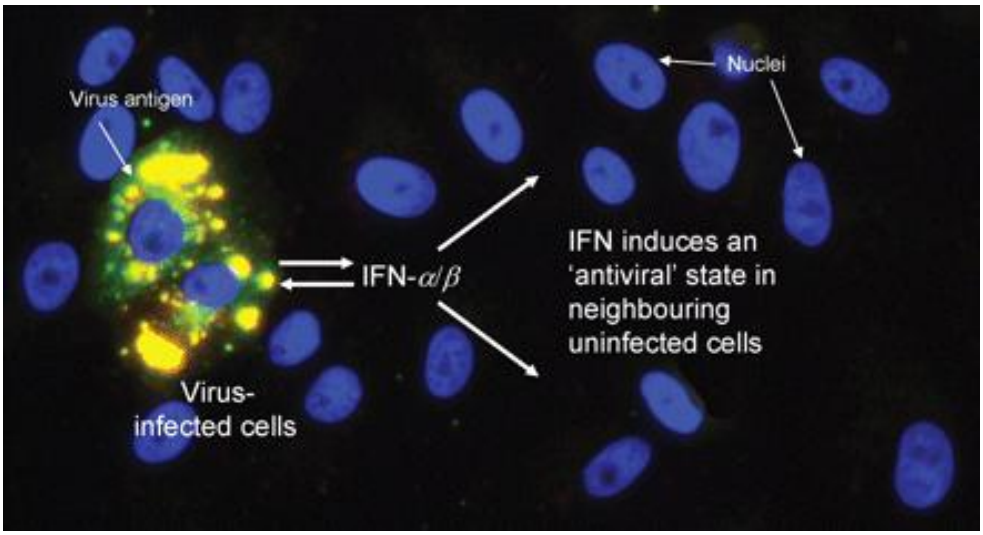

Figure 4. The antiviral state. Cells which are competent in IFN-α/β signaling can detect viral nucleic acids, such as dsRNA, and activate intracellular signaling cascades leading to transcription of IFN-α/β genes. Secreted IFNs bind to their receptors on neighboring uninfected cells, as well as on the initial infected cell, and activate intracellular signaling to induce several hundred IFN-α/β-responsive genes, many of which have direct or indirect viral action. Viruses released from the primary infected cell replicate inefficiently in cells which are in the antiviral state. Figure obtained from (Randall et al. 2008).

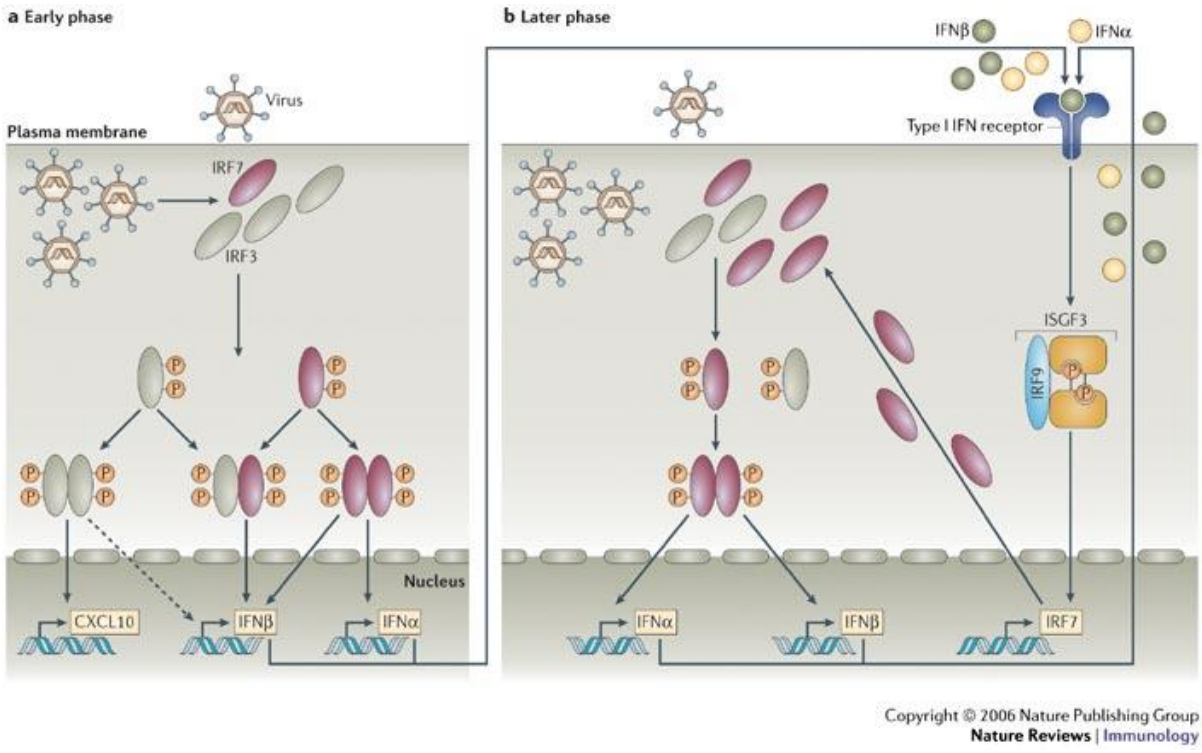

Figure 5. Positive-feedback regulation of type I interferon genes through interferon regulatory factors. A. In the early phase of virus infection, interferon regulatory factor 3 (IRF3) and IRF7 are phosporylated on specific serine residues, resulting in homo-or hetero-dimerization. These dimers translocate to the nucleus and activate transcription from the IFN-α and -β promoters, as well as the CXC-chemokine ligand 10 (CXCL10). B. Secreted IFNs then bind and activate the type I IFN receptor, leading to the activation of IFN-stimulated gene factor 3 (ISGF3), which is a heterodimer of signal transducer and activator of transcription 1 (STAT1), STAT2, and IRF9. Activated ISGF3 then translocates to the nucleus and induces transcription of the IRF7 gene. Activation of this newly synthesized IRF7, following recognition of viral nucleic acids by pattern recognition receptors (PRRs) leads to the expression of large amounts of IFNβ and many IFNα proteins. thereby creating a positive-feedback loop of type I IFN-dependent type I IFN gene induction.

Because of the robustness of IFN signaling in clearing viral infections, there is a tremendous interest in selecting oncolytic viruses on the basis of their ability to circumvent the IFN response in human cells for cancer therapy. The rationale for employing such strategies is that many tumor cells harbor defects in their IFN signaling pathways, and hence, these viruses could be very effective in replicating and lysing permissive tumor cells, while the surrounding normal cells would remain protected. Although oncolytic viral therapies have been under investigation for decades, the entire nature of the IFN defects in tumor cells, as well as other potential mechanisms of tumor selectivity, have not been fully elucidated.

2. Present Investigations

The doctoral work presented here consists of three distinct aims, with the common goal of improving oncolytic viral therapy for hepatocellular carcinoma and gaining a better understanding of the mechanisms which govern the tumor-specificity of these viruses. These goals can be discussed as a review of three manuscripts which were published as a by-product of this doctoral work, and the contents of this work are described below, along with a description of my personal contribution to each manuscript.

1. The first aim was to establish a novel treatment regimen, which combined the therapeutic properties of oncolytic vesicular stomatitis virus with a clinically approved embolization agent. Equal volumes of an embolization agent and a relatively low-dose virus preparation were mixed and applied to HCC tumor-bearing rats by intra-hepatic arterial infusion, and animals were assessed for tumor necrosis, apoptosis, inflammatory cell infiltration, and finally, survival. Although the monotherapy consisting of low viral dose provided no appreciable survival benefit, when administered in combination with the embolization agent, a synergistic prolongation of survival was observed. This survival benefit was demonstrated to result from a combined oncolytic effect resulting from viral therapy and embolization, as well as an increase in inflammatory cell infiltration in response to viral infection of tumor cells, which we hypothesize can boost the anti-tumor immune response in the host.

I contributed to this project by conceptualizing and performing all in vitro and in vivo studies, as well as quantifying intra-tumoral virus titers, performing immunohistochemical staining and all data analysis. In addition, I wrote the original and revised manuscript and prepared all figures.

2. The second aim represents a different approach to enhance the oncolytic efficacy of a virus, involving the introduction of modifications to a viral genome. This process is termed viral engineering. Here we employed the Newcastle disease virus (NDV), which possesses intrinsic tumor specificity, and causes oncolysis of susceptible tumor cells through membrane fusion, resulting in the formation of large multinucleated cells, called syncytia. We hypothesized that we could further enhance the oncolytic potential of NDV by introducing a known modification into the endogenous fusion (F) protein, which would result in enhanced bystander cell killing through augmented syncytial formation. To this end, we employed site directed mutagenesis, as well as the newly established reverse-genetics system for rescuing recombinant NDV viruses, to introduce a single amino acid mutation into the fusion protein of a recombinant NDV vector. We proceeded to characterize this novel NDV vector in vitro and in an in vivo rat model of HCC, to demonstrate the superior ability of the modified vector

to promote cell-cell fusion and subsequent tumor cell death, without compromising safety to the neighboring hepatic cells.

My contribution to this work included the conceptualization of the hypothesis, the establishment of the NDV vector system in the lab, cloning, virus rescue, in vitro and in vivo characterization of the recombinant virus, immunohistochemistry, data analysis, and writing and revising of the manuscript and figures.

3. The third goal was to attempt to further elucidate the mechanism whereby oncolytic VSV maintains its tumor specificity. Gaining a better understanding of the principles which dictate a cell's susceptibility to VSV infection could contribute to a more rational design of future recombinant VSV vectors with enhanced safety profiles, or potentially act as a molecular basis for the selection of HCC patients as candidates for oncolytic VSV therapy in future clinical application. In this study, we identified the presence of a defective splice variant of a key component of the interferon signaling pathway in HCC cells, which results in the impairment of the cell's antiviral response. Over-expression of this IRF3 variant significantly abrogated the IFN-β response to VSV infection and resulted in augmented viral replication. Importantly, we identified this splice variant, not only in tumor cell lines, but also in tissue samples obtained from HCC patients.

I contributed to this work by establishing a chromatin immunoprecipitation assay (ChIP), participating in conceptual discussions regarding the project, and revision of the manuscript.

2.1 Methods

Recombinant viruses. The construction and rescue of the rVSV vector expressing a mutant (L289A) NDV fusion protein (rVSV-F) has been previously described (Ebert 2004). Briefly, BHK-21 cells were pre-infected with a vaccinia vector expressing the T7 RNA polymerase (vTF-7.3), followed by transfection with 10µg of full-length VSV cDNA in addition to plasmids encoding the endogenous VSV N, P, and L proteins using LipofectAMINE 2000 reagent (Invitrogen, Calrsbad, CA). Two days post-transfection, supernantants were filtered onto fresh BHK-21 cells through a 0.22µm filter to remove the majority of the larger vaccinia virus. Any remaining vaccinia virus was eliminated by plaque purification, and the titers of amplified stocks were determined by plaque assays on BHK-21 cells.

To produce concentrated stocks for in vivo experiments, the virus was amplified on BHK-21 cells, and the supernatant was purified by sucrose gradient. Briefly, the cells were infected at an MOI of 0.0001, and 48 hours later, the supernatant was collected and centrifuged to clear floating cells. The supernatant was then subjected to ultra-centrifugation at 24,000 rpm for 1 hour. The pellet was resuspended in PBS and layered on top of a sucrose gradient ranging from 60% to 10%, and ultra-centrifuged for 1 hour at 24,000 rpm. The band containing the virus was carefully collected with a syringe and 20 G needle, and aliquoted and stored at -80^{o}C.

The NDV cDNA sequence was derived from the mesogenic Hitchner B1 strain engineered to express the modified F cleavage site (F3aa), as previously described (Park 2006). The LacZ gene was inserted as an additional transcription unit into the unique *Xba I* restriction site between the P and M genes in the full-length plasmid, pT7NDV/F3aa (a kind gift from Adolfo Garcia-Sastre; Mount Sinai School of Medicine, New York, NY). To generate the recombinant NDV vector expressing the mutant F3aa(L289A) F protein, the pT7NDV/F3aa plasmid was modified by site-directed PCR mutagenesis. To this end, a long forward primer (5'-GGCTTAATCACCGGTAACCCTATTCTATACGACTCACAGACTCAA CTCTTGGGTATACAGGTAACT**GCA**CCTTCAGTCGGGAAC -3') was designed to span amino acid 289, as well as the upstream *Age I* restriction site. The reverse primer (5'-GTCATCTACAACCGGTAGTTTTTTCTTAACTCTCCG -3') corresponded to the non-coding region between the F and HN genes, including a second *Age I* restriction site. The nucleotides substituted in the primers to mutate the amino acid at position 289 from Leu to Ala appear in *bold* font, while sequences corresponding to the restriction sites are *underlined*. The resulting PCR fragment was then purified and digested with Age I, and inserted back into the full-length pT7NDV/F3aa plasmid, thereby replacing the corresponding segment of the endogenous F gene. DNA sequences of all modified plasmids were confirmed by commercial sequencing (Eurofins MWG, Ebersberg, Germany). Viruses were rescued using an established method of reverse-genetics (Nakaya 2001). For simplicity, the rNDV/F3aa-LacZ and rNDV/F3aa(L289A)-LacZ vectors will be referred to as rNDV/F3aa and

rNDV/F3aa(L289A). The rVSV-LacZ control virus was generated as previously described (Shinozaki 2004).

To amplify NDV stocks, 10 day-old embryonated pathogen-free chicken eggs were inoculated with 100 plaque-forming units of virus, and the allantoic fluid was harvested 48 hours later and pooled. The fluid was cleared by centrifugation at 1800 g for 30 minutes, and then subjected to ultra-centrifugation at 24,000 rpm for 24 hours. The pellet was resuspended in Hanks balanced salt solution (HBSS) and layered on top of a sucrose gradient ranging from 60% to 10%, and ultra-centrifuged for 1 hour at 24,000 rpm. The band containing the virus was carefully collected with a syringe and 20 G needle, and ultra-centrifuged for another hour at 24,000 rpm to remove the sucrose. The pellet was resuspended in 3 ml of HBSS and aliquoted and stored at -80^{o}C until use. Titers were determined by $TCID_{50}$ analysis in DF1 cells.

Growth curves. Viral growth in the presence and absence of degradable starch microspheres (DSM; EmboCept®, PharmaCept, Berlin, Germany) was compared in McA-RH7777 cells. The cells were plated in 6-well dishes at $1x10^6$ cells per well, and infected with rVSV-F at a multiplicity of infection (MOI) of 10, mixed with an equal volume of either DSM or PBS in triplicate. After infection at room temperature for 30 minutes, cells were washed three times with PBS, and fresh complete medium was added. Aliquots of supernatant were collected at 0, 8, 16, and 24 hours post-infection, and assayed for viral titer by TCID50 analysis.

Multi-cycle growth curves of wt and M51R mutant strains of VSV were performed on primary human hepatocytes, HepG2 and Huh-7 cell lines. Cells ($1x10^6$/well) were infected at an MOI of 0.01 of the viruses. After adsorption for 1 hour, monolayers were washed three times with PBS and fresh medium was added. Aliquots of culture media were taken and fresh media added immediately at time 0, 8, 16 and 24 hours post-infection. Viral titers were determined by standard plaque assay and each time point represents the average of triplicate experiments. For experiments establishing the activity of IRF3-nirs3 on viral growth, A549 cells were seeded at density of $5x10^5$/well and transfected with 1 μg of pGFP-IRF3nirs3 or the empty vector pGFP-C3. 24 hours post transfection, cells were infected with VSV-M51R at the MOI of 0,01 and viral titers were determined at time 0, 4, 8, 12 and 24 hours post-infection.

Cell proliferation assay. McA-RH7777 cells were seeded overnight in 24-well dishes at $2x10^5$ cells per well, and then infected the following day with rVSV-F at an MOI of 10, mixed with an equal volume of either DSM or PBS. Cell viability was measured at 0, 6, 12, 24, 48, and 72 hours after infection using the MTS tetrazolium compound [3-(4,5-dimethylthiazol-2-yl)-5-(3-carboxymethoxyphenyl)-2-(4-sulfophenyl)-2H-tetrazolium] (CellTiter96® AQ_{ueous} One Solution Cell Proliferation Assay, Promega, Madison, WI). All cell viability data are expressed as a percentage of viable cells as compared to mock-infected controls at each time point.

Interferon sensitivity assay. Primary human hepatocytes (PHH) and HCC cell lines (HepG2, Huh-7, and McA-RH7777) were seeded in 24-well dishes at a density of $5x10^5$ cells/well. Monolayers were mock-treated or treated overnight with Universal type I IFN (PBL) at concentrations of 10, 100, 500, and 1,000 IU/ml. Following the pre-treatment, the cells were infected with either rVSV-LacZ, rNDV/F3aa, or rNDV/F3aa(L289A) at a multiplicity of infection (MOI) of 1. 24 hours post-infection, aliquots of the conditioned media were harvested and subjected to $TCID_{50}$ determination of viral titers.

Luciferase reporter assays. To demonstrate interferon signaling in response to NDV infection, PHH, Huh-7, HepG2, and McA-RH7777 cells were seeded in 24-well dishes at a density of 5×10^5 cells/well. Cells were transfected with a firefly-luciferase reporter plasmid driven by either the IFN-β or ISRE promoter, using Lipofectamine 2000 (Invitrogen; Carlsbad, CA) according to the manufacturers instructions. In addition, to control for transfection efficiency, cells were co-transfected with the Renilla reniformis plasmid. 24 hours post-transfection, the cells were either mock-treated, or stimulated with poly I:C (2.5 mg), universal type I IFN (500 IU), or rVSV-LacZ, rNDV/F3aa, or rNDV/F3aa(L289A) at an MOI of 1. Following overnight incubation, cell lysates were prepared, and the luciferase activities were quantified using the Dual-Luciferase Assay system (Promega, Mannheim, Germany) with a standard luminometer (Turner Designs, Sunnyvale, CA). The relative light units of firefly-luciferase activity were normalized to the constitutively active Renilla luciferase, and presented as the fold-induction of stimulated, compared to mock-treated cells.

To determine the effect of IRF3nirs on IFN signaling, similar luciferase reporter experiments were conducted. Cells seeded in 24-well plates were co-transfected with the IFN-β, IRF3 and ISRE promoter-luciferase reporter plasmids (100 ng), and Renilla reniformis plasmid (10 ng). Depending on the experiments, the following expression vectors were used: phuTBK1, phuTRIF, phuIRF3, phuTLR3 and phuIRF3nirs3 at the indicated amounts. Twenty-four hours later, cells were mock treated or challenged with Poly (I:C), treated with different concentrations of recombinant Universal type I Interferon (PBL Biomedical) or were virus infected according to the experiment. Luciferase activities were quantified as described above.

Quantitation of syncytium formation. Huh-7, HepG2, and McA-RH7777 cells were seeded at a density of 10^6 cells/well in 6-well dishes. Upon attachment, they were infected with rNDV/F3aa or rNDV/F3aa(L289A) at an MOI of 0.1 in triplicate. 48-hours post-infection, the cells were stained using the β-gal staining set (Roche; Mannheim, Germany) according to the manufacturers instructions. For a quantitative assessment, the nuclei were labeled with propidium iodide and counted. The syncytial index was calculated as the number of nuclei per syncytia divided by the total number of nuclei per field of view.

Mean death time (MDT) assay. 10-day old embryonated chicken eggs were infected with serial 10-fold dilutions of NDV vectors, with 5 eggs per virus dose. The eggs were incubated at 37^oC and monitored twice daily for 7 days, and the time at which the embryos were found

dead was recorded. The highest dilution that killed all embryos was considered to be the minimum lethal dose. The MDT was then calculated as the mean time required for the embryos to be killed at the minimum lethal dose.

Animal studies. All procedures involving animals were approved and performed according to the guidelines of the institution's animal care and use committee, and the government of Bavaria, Germany. Six-week old male Buffalo rats were purchased from Harlan Winkelmann (Borchen, Germany), and housed under standard conditions. To establish multifocal HCC lesions within the liver, 10^7 syngeneic McA-RH7777 rat HCC cells were infused as a 1 ml suspension in serum-free DMEM through the portal vein. For embolization experiments, a second laparotomy was performed 21 days post tumor-cell implantation, and animals with visible tumors within the range of 1-10mm in diameter were randomly assigned to the following treatment groups: PBS, DSM, rVSV-F, or combination treatment of rVSV-F plus DSM. All treatments were administered as a 1 ml solution, injected via the hepatic artery. A dose of $1x10^6$ plaque-forming units (pfu) of VSV was used in the monotherapy and combination group. 500 μl of DSM was diluted 1:1 with either PBS or rVSV-F, depending on the treatment group. Representative animals from each group were sacrificed on day 1 and 3 for histology and immunohistochemical analysis of tumor and liver sections. In addition, TCID50 analysis of extracts from snap-frozen tumor samples was performed for quantification of VSV yield on day 1. Finally, animals were followed for survival to compare the therapeutic outcome of each treatment. The animals were monitored daily and euthanized at humane endpoints.

To assess the potential toxicity of rNDV vectors when administered at 10^8 $TCID_{50}$/rat, non-tumor bearing Buffalo rats were subjected to laparotomy for preparation of the hepatic artery, whereby a 1 ml suspension of PBS, rNDV/F3aa, or rNDV/F3aa(L289A) was slowly infused. Body weights were monitored daily from day 0 to 14 days post-treatment. In addition, serum was prepared from whole blood drawn on days -3, 0, 1, 3, 7, and 14 for determination of serum concentrations of GOT, GPT, BUN, and creatinine. All serum chemistry measurements were performed by the Institute for Clinical Chemistry and Pathobiochemistry (Klinikum rechts der Isar, Munich, Germany).

To determine in vivo oncolysis, as well as the intratumoral kinetics of NDV spread, rats bearing multifocal HCC were treated with 10^8 $TCID_{50}$ rNDV/F3aa(L289A) via the hepatic artery as described previously. Five animals were randomly chosen for sacrifice at each of the following time points: 30 min, day 1, 3, or 7. Upon sacrifice, sections of liver and tumor were snap frozen for $TCID_{50}$ determination of intratumoral and intrahepatic viral titers or prepared for histological and immunohistochemical analyses. An additional set of tumor-bearing rats was treated with PBS (n=10), rNDV/F3aa (n=13), or rNDV/F3aa(L289A) (n=14) and followed for survival to compare the therapeutic outcome of each treatment. The animals were monitored daily and euthanized at humane endpoints, and data were plotted as a Kaplan-Meier survival curve.

MR Image acquisition and image analysis. MR images were acquired on a 1.5-T whole body MRI scanner (Philips, Achieva, Netherlands). Buffalo rats bearing multifocal McA-RH7777 HCC tumors, either untreated or treated with transarterial injection of DSM, were subjected to DCE-MRI approximately 30 minutes post-infusion of the embolization agent. Rat livers were imaged individually using a 47mm surface coil (Philips). Axial images were obtained for tumor localization using a T1 weighed 3D gradient echo (GE) sequence (TR = 20 ms, TE = 4.6 ms, flip angle = 30°, FOV = 6.4 x 4.0 cm, imaging matrix = 224 x 179, slice thickness = 1 mm). Contrast dynamics with 3 baseline scans and 27 postcontrast scans were then visualized using an axial T1w 3D GE sequence (TR = 20 ms, TE = 2.9 ms, flip angle = 45°, slice thickness = 2mm) with a time resolution of 28 sec / dynamic. Bolus injection via the tail vein of 0.2 mmol/kg GdDTPA (Magnevist®, Bayer HealthCare Pharmaceuticals) was carried out manually within 2 seconds. Data was quantitatively analyzed using View Forum Software (Philips, Netherlands), by measuring grey scale signal intensities in equally sized regions of interest within tumor nodules and adjacent normal liver tissue.

Interferon (IFN) neutralization assay and IFN resistance. Primary human hepatocytes were plated on collagen-coated 24-well plates at the density of $2x10^5$ cells/well. Monolayers were infected with VSV-wt and VSV-M51R at a multiplicity of infection (MOI) of 1 for 1 hour. After virus absorption, cells were washed 3 times with PBS and, in order to block the effect of type I IFN, incubated with a mixture of 5000 neutralizing U/ml rabbit anti-human IFN-α Ab, 2000 U/ml rabbit anti-human IFN-β Ab and 20 μg/ml mouse anti-human IFN-α/β receptor mAb IFN-αR1β (PBL Biomedical Laboratories). As an isotype control a mouse IgG (DB Pharmingen) was used. At 24 hours post-infection, supernatants were harvested and viral titers assessed by plaque assay.

Primary human hepatocytes and HCC cell lines (HepG2 and Huh-7) were seeded at the density of $1x10^6$ cells/well. Monolayers were mock-treated or treated overnight with Universal type I IFN (PBL) at the concentration of 100, 500 and 1000 IU/ml. Infection with VSV-wt and VSV-M51R mutant, was performed for 1 hour and viral titers were determined after 24 hours.

Chromatin immunoprecipitation (ChIP) assay. Huh-7 cells were transfected with the fusion plasmids GFP-IRF3 and GFP-IRF3nirs3. Chromatin immunoprecipitation was performed from un-stimulated and Poly (I:C)-treated cells using an assay kit following the manufacturers' instructions (Upstate Biotechnology, Lake Placid, NY). Chromatin was immunoprecipitated with an antibody against GFP (Ab290, Abcam). Controls were obtained with an anti acetyl histone H3 or normal rabbit Ig as the immunoprecipitating antibodies. The immunoprecipitated DNAs were amplified by PCR using primers amplifying the human IFN-β promoter (Table 1) and GADPH, as internal control. The samples were amplified for 35 cycles and analyzed by electrophoresis on a 1.5% agarose gel.

Statistical analyses. For comparison of individual data points, a two-sided student t-test was applied to determine statistical significance. Survival curves were plotted according to the

Kaplan-Meier method, and statistical significance between different treatment groups was determined using the log-rank test. Statistical data were obtained using GraphPad Prism 5.0 (GraphPad Software, San Diego, CA). P-values of less than 0.05 were considered statistically significant.

2.2 Synergistic antitumor effects oncolytic VSV therapy in combination with transarterial embolization

Although we had previously demonstrated that VSV administration via the hepatic artery in HCC tumor-bearing rats results in tumor-selective viral replication and oncolysis, treatment efficacy was limited by the inability of the virus to efficiently penetrate the entire tumor mass before being cleared by the host immune response, and the remaining viable tumor eventually relapsed. This limitation encouraged us to seek alternate approaches to improve the therapeutic effect of VSV treatment. To this end, we developed a new treatment modality, involving the combination of recombinant VSV with an embolization agent infused through the hepatic artery in tumor-bearing rats (Altomonte et al. 2008). We termed this procedure "viroembolization".

2.2.1 Hepatic arterial administration of therapeutic agents for tumor specific treatment of multi-focal HCC in rats

As most HCC patients present with advanced disease consisting of multiple tumor nodules and micro-metastases, the feasibility and logistics of applying therapy via intratumoral injections is severely limited. The liver has a dual blood supply, with the portal vein supplying 75% and the hepatic artery contributing 25% of hepatic blood flow. However, malignant liver tumors are supplied predominantly by arterial blood, thereby creating a highly tumor-specific and convenient route of drug delivery. For this reason, hepatic artery infusion is the most commonly employed method for local–regional therapy of HCC in current clinical practice (Mohr 2002). With this knowledge in mind, we have previously established an orthotopic, multifocal HCC model in immune-competent rats, in which we achieve tumor-selective delivery of treatment via infusion through the hepatic artery. Briefly, syngeneic rat HCC cells are injected into the portal vein of Buffalo rats, which results in the establishment of multi-focal hepatic lesions, which are macroscopically visible after approximately 21 days. At this point, therapy can be administered by a 1 ml infusion through the gastroduodenal artery, which then feeds directly into the proper hepatic artery and into the liver, whereby primarily tumor nodules become perfused (Fig. 6).

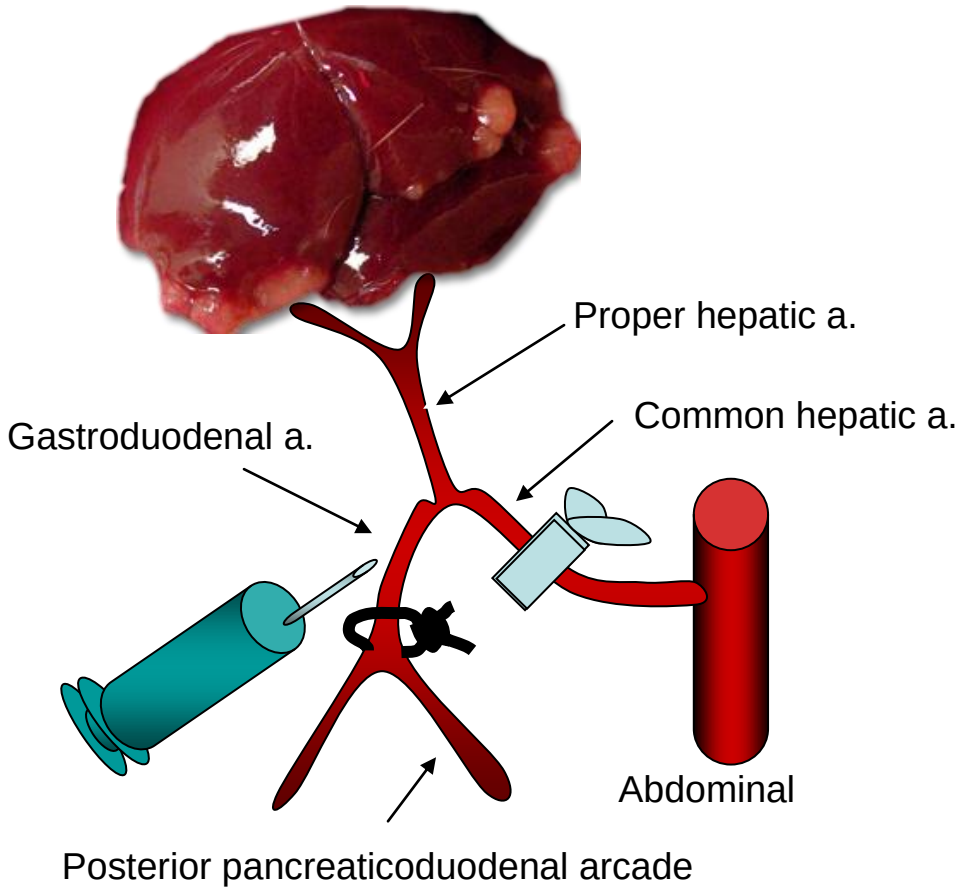

Figure 6. Representative picture of a rat liver with multi-focal HCC lesions super-imposed with a schematic representation of the hepatic arterial infusion procedure. 21 days after tumor cell infusion into the portal vein, 90-100% of rats develop visible multi-focal HCC lesions macroscopically (2-10 mm in diameter, 5 to 10 nodules). The hepatic vessels (common hepatic artery, proper hepatic artery, and gastroduodenal artery) are dissected with the aid of an operating microscope. After ligation of the gastroduodenal artery and temporal block of the common hepatic artery, 1 ml of treatment agent is slowly infused into the gastroduodenal artery. The proximal site of the gastroduodenal artery is then ligated to prevent bleeding, and the clamp on the common hepatic artery is released, thereby resuming normal arterial blood flow to the liver.

2.2.2 Transarterial embolization in multifocal HCC tumor-bearing rats

Transarterial embolization (TAE) techniques have been established and shown to improve the efficiency and tumor selectivity of anticancer treatments. In this study, we utilized degradable starch microspheres (DSM), an embolic agent currently being used for transarterial embolization (TAE) of HCC and metastatic liver tumors in the clinic, which provide transient embolization of the therapeautic agent, before being degraded by serum amylases. DSM were injected as a mixture with a low dose of our previously reported syncytia-inducing VSV-F.

First, to ensure that the DSM delivered transarterially through the hepatic artery was able to successfully embolize multifocal HCC lesions in our rat model, we performed dynamic contrast-enhanced magnetic resonance imaging (DCE-MRI). Approximately 30 minutes after transarterial embolization, rats were infused by tail vein with Magnevist®, a widely-used gadolinium-based MR contrast agent, and imaged on a clinical MR scanner (Fig. 7A).

The data were analyzed in terms of grey-scale intensity over the course of time, and recorded as an intensity plot (Fig. 7B). This plot reveals that in the non-embolized animals there is approximately equal perfusion of tumor and liver tissue, while in the embolized animals only the non-tumorous liver tissue is perfused with contrast agent. These data indicate that hepatic arterial infusion of DSM results in nearly complete embolization of tumors, while having little effect on normal liver perfusion.

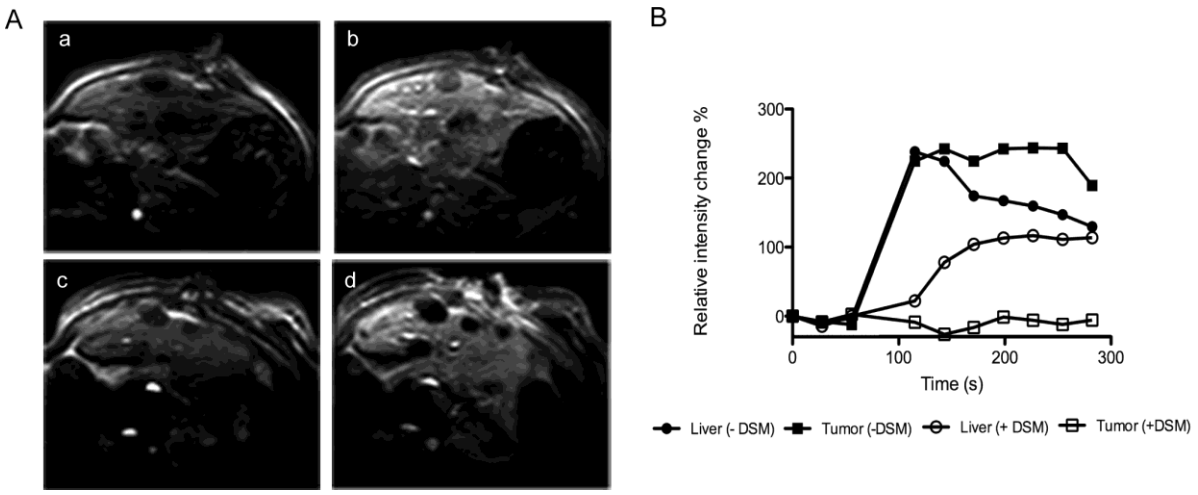

Figure 7. Dynamic Contrast-Enhanced Magnetic Resonance Imaging (DCE-MRI). McA-RH7777 tumor-bearing rats, either non-embolized or 30 minutes after hepatic arterial embolization with DSM, were imaged by DCE-MRI. Panel A, location of tumor nodules was identified using a T1 weighted sequence (a and c), followed by a dynamic gadolinium (Gd) (Magnevist®) enhanced T1 weighted MR acquisition on a clinical 1.5 Tesla scanner, employing a 47 mm surface coil (b and d). Gd was injected manually within 5 sec. Panel B, data was quantitatively analyzed by measuring grey scale signal intensities in equal sized regions of interest of tumor nodules and adjacent normal liver tissue. One representative data set is shown.

2.2.3 Transarterial application of combination therapy using oncolytic VSV and an embolization agent

Next, we proceeded to test the efficacy of viroembolization for the treatment of HCC. After the establishment of multifocal HCC nodules in the livers of Buffalo rats, animals were randomly assigned to receive one of four treatments via hepatic arterial infusion: PBS, DSM, rVSV-F at a 10-fold-lower dose than the MTD ($1x10^6$ pfu), or combination therapy of rVSV-F ($1x10^6$ pfu) plus DSM in equal volumes. Histology on day 3 post-treatment revealed a massive tumor response in the absence of toxicity to the neighboring liver parenchyma, with DSM treatment causing nearly 70% tumor necrosis, and combination treatment resulting in more than 90% tumor necrosis. Further immunohistochemical analyses revealed an increase in apoptosis and inflammatory cell infiltration in viroembolized tumor tissue, providing a possible mechanism for the synergistic response. These results translated to significant

prolongation of survival of viroembolized animals in comparison to those treated with rVSV-F or DSM monotherapy (Fig. 8).

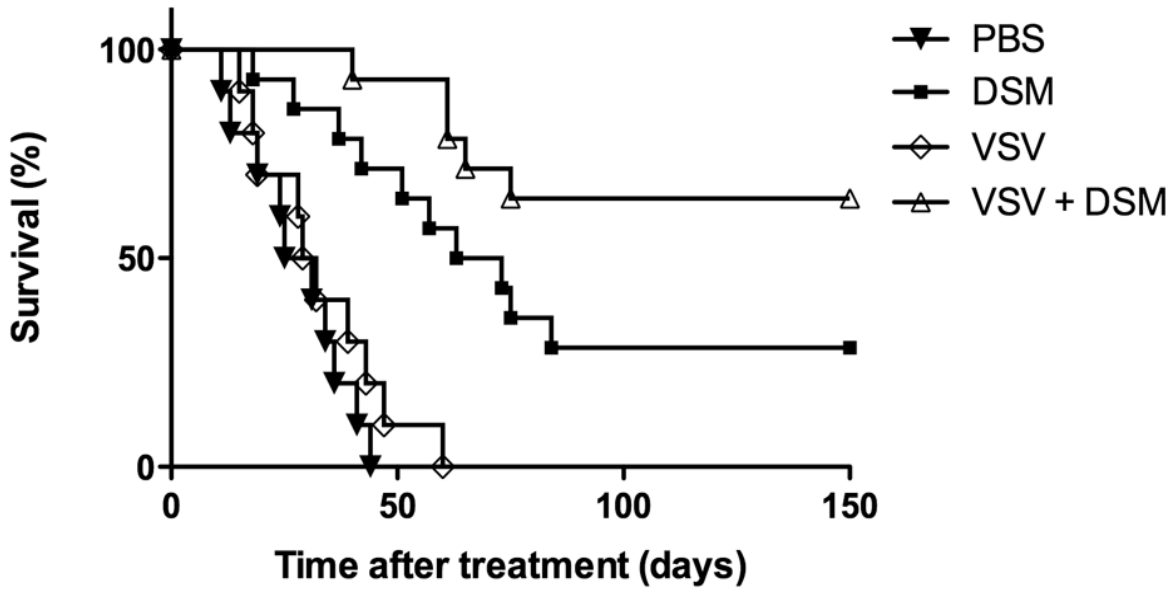

Figure 8. DSM combined with rVSV-F results in significant survival prolongation in HCC-bearing rats. Multifocal HCC tumor-bearing rats were treated with PBS (n=10), DSM (n=14), rVSV-F (n=10), or DSM plus rVSV-F (n=14) by hepatic arterial infusion, and followed for survival. Animals were monitored daily, and data was plotted as a Kaplan-Meier survival curve, and statistical significance was determined by log rank test.

2.2.4 Discussion

This work involved a novel treatment modality in which oncolytic VSV therapy was significantly enhanced by co-administration with a clinically approved embolization agent, which resulted in an impressive cure rate. For this purpose, we chose EmboCept®, a representative of the group of embolization agents known as DSM. DSM are manufactured from hydrolyzed potato starch, and provide relatively transient embolization before being degraded by serum amylases (Erichsen 1985). Although the physical presence of DSM within tumor vessels is temporary, the effect can be long-lasting due to the formation of emboli at the arterio-capillary level, as well as hypoxia and ischemic necrosis, which prevent reperfusion of the tumor, even after the DSM are degraded (Yoshikawa 1994; Wang 2006).

It is well documented that the peripheral border of HCC lesions close to the surrounding non-neoplastic liver tissue has a tendency to survive TAE treatment because this area is supplied by portal blood flow and collateral circulation. Therefore, we hypothesized that transient TAE therapy for HCC could be significantly enhanced via co-administration of oncolytic VSV. We envisioned that the remaining viable rim, which was unaffected by TAE, could instead be eradicated by VSV replication. Indeed, this is exactly what we observed through

immunohistochemical analysis of VSV/G, which did in fact co-localize to the viable peripheral tumor regions.

A comparison of the in vivo efficacy of transarterial viroembolization to each monotherapy revealed that, while VSV resulted in a modest effect, and embolization with DSM caused significantly enhanced tumor responses, the most striking results were achieved by viroembolization, which resulted in more than 90% tumor necrosis. Impressively, we were able to achieve 60% long-term tumor-free survival through transarterial viroembolization of multifocal HCC in our rat model. Statistical analysis indicated that a synergistic effect was derived through combination of each monotherapy. This data clearly illustrated a superior effect of the combination treatment; however, it left open questions regarding the mechanism of the additive response. We investigated the roles of apoptosis, anti-angiogenesis, and inflammation as potential players.

It is known that VSV causes lysis of infected tumor cells through activation of apoptotic pathways, induced by expression of the viral matrix (M) protein (Balachandran et al. 2001; Kopecky 2001). We hypothesized that VSV localized to the viable rim of tumors following embolization could induce apoptosis in the infected cells. TUNEL staining revealed large areas of apoptosis in tumors treated with rVSV-F, while there was significantly less evidence of apoptosis in the PBS and DSM groups. Furthermore, apoptosis secondary to viroembolization was, in fact, mostly confined to the outer borders of the lesions, while in tumors treated with VSV monotherapy, it appeared in seemingly random patches, mainly in the core.

In addition to direct tumor cell lysis, it has recently been shown that VSV is also responsible for indirect killing of uninfected tumor cells through inhibition of vascular perfusion within infected tumors induced by the rapid recruitment of inflammatory cells to the tumor bed (Breitbach 2007). While embolization is known to stimulate angiogenesis (Gupta 2006), in our model, we observed a clear reduction in CD31 staining within tumors treated in combination with VSV. The anti-angiogenic effect of VSV could provide a powerful tool for improving the efficacy of TAE by preventing new vessel formation feeding the remaining viable tumor cells.

Finally, in addition to the effect of inflammation on tumor blood flow, the infiltration of inflammatory cells in virus-infected tumor has the complimentary function of killing infected and surrounding tumor cells. The recruitment of NK cells to sites of VSV infected tumor has previously been demonstrated (Altomonte 2008), and we have reproduced this phenomenon here. NK cells represent a distinct population of cytotoxic lymphocytes that act as an integral component of the innate cellular immune response system to invading viruses, prior to the launch of the adaptive immune responses (Welsh 1986). These cells function by directly killing infected cells and inducing anti-viral cytokines, and can result in a bystander effect by killing neighboring uninfected cells. Interestingly, several groups have recently attempted to combine TAE with adoptive immunotherapy in the clinic, and have shown enhancement of

efficacy in patients (Takayama 2000; Nakamoto 2007). In addition, oncolytic virus therapy may also promote cross-presentation of released tumor antigens to CD8+ T cells, leading to a long-term antitumor effect long after the virus is cleared (Di Paolo et al. 2006; Diaz 2007). Therefore it is possible that long-term survival in the current study may be mediated by an immune response, which is elicited through viral infection and oncolysis of the HCC cells.

2.3 Engineered Newcastle Disease Virus as an improved oncolytic agent

Newcastle disease virus (NDV) is an intrinsically tumor specific virus which is currently under investigation as a clinical oncolytic agent. Several clinical trials have reported NDV to be a safe and effective agent for cancer therapy; however, there remains a clear need for improvement in therapeutic outcome. Here we employed the Newcastle disease virus, which attaches to susceptible cancer cells and subsequently initiates membrane fusion through processes directed by two genomic glycoproteins: the hemagglutinin-neuraminidase (HN) attachment protein and the fusion (F) protein. A recombinant NDV from the strain Hitchner B1 (NDV/B1), expressing a modified F protein with a multibasic cleavage and activation site (rNDV/F3aa), is reported to be highly fusogenic and efficient in tumor cell killing through formation of large multinucleated cells called syncytia (Bateman 2002; Vigil 2007). Though impressive, it has further been demonstrated that a single amino acid substitution from leucine to alanine at amino acid 289 (L289A) in the F protein, results in even greater syncytial formation (Sergel 2000). In addition to providing the ability to promote fusion in the absence of the viral HN protein, the L289A-modified F protein demonstrates 50-70% augmented fusogenicity in HN-dependent fusion over the wild-type F protein (Li 2004). However, these studies had only been performed using in vitro expression vectors, and never validated in the endogenous NDV vector. Employing site directed mutagenesis, as well as the newly established reverse-genetics system for rescuing recombinant NDV viruses, we introduced the L289A mutation into the recombinant NDV/F3aa vector to result in a novel hyperfusogenic vector termed rNDV/F3aa(L289A).

Here we demonstrate the superior ability of the F3aa(L289A)-modified virus to promote cell-cell fusion in human and rat HCC cell lines in vitro. In vivo administration of the recombinant vector in a pre-clinical, immune competent rat model of HCC, via intrahepatic arterial infusion resulted in tumor-specific syncytia formation and necrosis, in the absence of local or systemic toxicity. Furthermore, the improved oncolysis conferred by the L289A mutation translated to a significant prolongation of survival over buffer- and F3aa control virus-treated rats. Taken together, these results indicate that rNDV/F3aa(L289A) represents a safe, yet more effective vector than wild-type NDV for the treatment of HCC, making it an ideal candidate for clinical application in HCC patients.

2.3.1 Construction and molecular characterization of an engineered Newcastle Disease Virus vector

The NDV cDNA sequence was derived from the mesogenic Hitchner B1 strain engineered to express the modified F cleavage site (F3aa), as previously described (Park 2006). A plasmid expressing this full-length cDNA was used as a template for site-directed mutagenesis to introduce the L289A amino acid mutation in the F gene by PCR, and the modified sequence was cloned back into the full-length vector using unique restriction sites. The recombinant virus was rescued using an established method of reverse-genetics (Nakaya 2001).

To determine if the L289A mutation in the endogenous NDV/F3aa protein results in enhanced cell-cell fusion, we evaluated the recombinant virus in vitro. Human and rat HCC cells were infected with either rNDV/F3aa or rNDV/F3aa(L289A) and stained for β-galactosidase (β-gal) expression to compare the fusogenicity of each virus. While moderate β-gal expression and some evidence of fusion could be observed in cells infected with rNDV/F3aa, rNDV/F3aa(L289A) resulted in large syncytial formation which seemed to originate from infection of a single cell and spread outward as infected cells fused with neighboring cells (Fig. 9, left panel). To quantify the hyper-fusogenic potential of the modified virus, we counted the number of nuclei per syncytia, and expressed the value in terms of its syncytial index. In all HCC cell lines tested, the syncytial index of rNDV/F3aa(L289A) was significantly higher than that of rNDV/F3aa (Fig. 9, right panel).

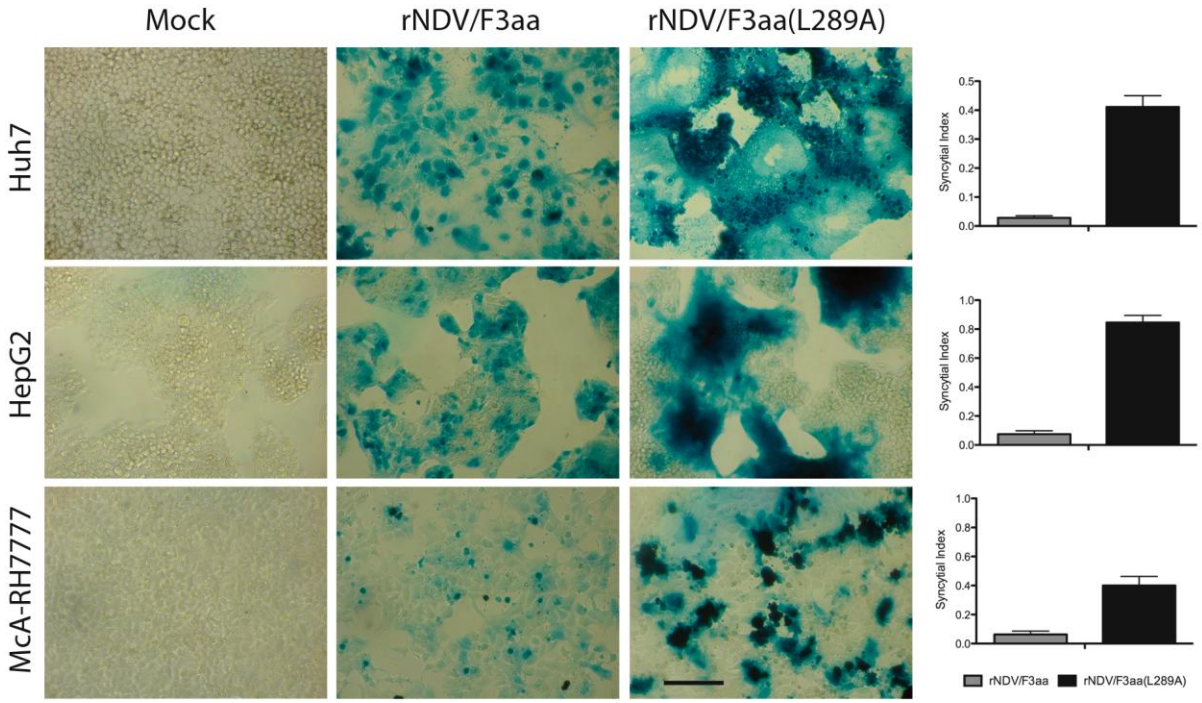

Figure 9. F(L289A) modification results in enhanced fusogenic activity of NDV. Human (Huh7 and HepG2) and rat (McA-RH7777) cells were mock infected or infected with rNDV/F3aa or rNDV/F3aa(L289A) at a multiplicity of infection of 0.1. 48 hours post-infection, cells were stained for β-gal expression (**left panel**) or analyzed for syncytial index (**right panel**). The syncytial index was calculated as the number of nuclei per syncytia divided by the number of nuclei per field of view. Each cell line was analyzed in triplicate, and data are expressed as the mean + standard deviation. Scale bar = 100μm.

2.3.2 Hyper-fusogenic NDV induces significant tumor necrosis in HCC tumors in rats due to tumor specific syncytia formation

To determine the oncolytic potential and tumor-specificity of rNDV/F3aa(L289A) in vivo, rats bearing multifocal HCC tumors in their livers were infused with 10^8 $TCID_{50}$ via the

hepatic artery. Animals were sacrificed at various time-points post-treatment for evaluation of tumor response to therapy. Morphometric analysis of necrotic areas revealed an increase in tumor necrosis, which peaked on day 5 after treatment (Fig. 10a). Syncytia, which are represented by giant multi-nucleated cells, were observed within necrotic areas and appeared exclusively in tumor tissue. Histological examination of the surrounding liver parenchyma revealed no signs of hepatotoxicity, and, in particular, there was no evidence of inflammatory cell infiltrates or syncytia formation.

To quantify the in vivo kinetics of rNDV replication in HCC and normal liver cells, multifocal HCC-bearing rats were infused with rNDV/F3aa(L289A) through the hepatic artery, and animals were euthanized at various time-points (30 minutes, 1, 3, 5, and 7 days post-treatment). Sections of liver and tumor were prepared for $TCID_{50}$ quantitation of viral contents. While NDV titers steadily increased within tumor tissue, with a peak in replication on day 5, the virus was rapidly cleared from the surrounding liver parenchyma to levels below detection by day 5 (Fig. 10b). Similarly, β-gal staining of liver and tumor sections revealed multiple foci of LacZ-postive cells within tumors, while no positive staining was observed in the surrounding liver.

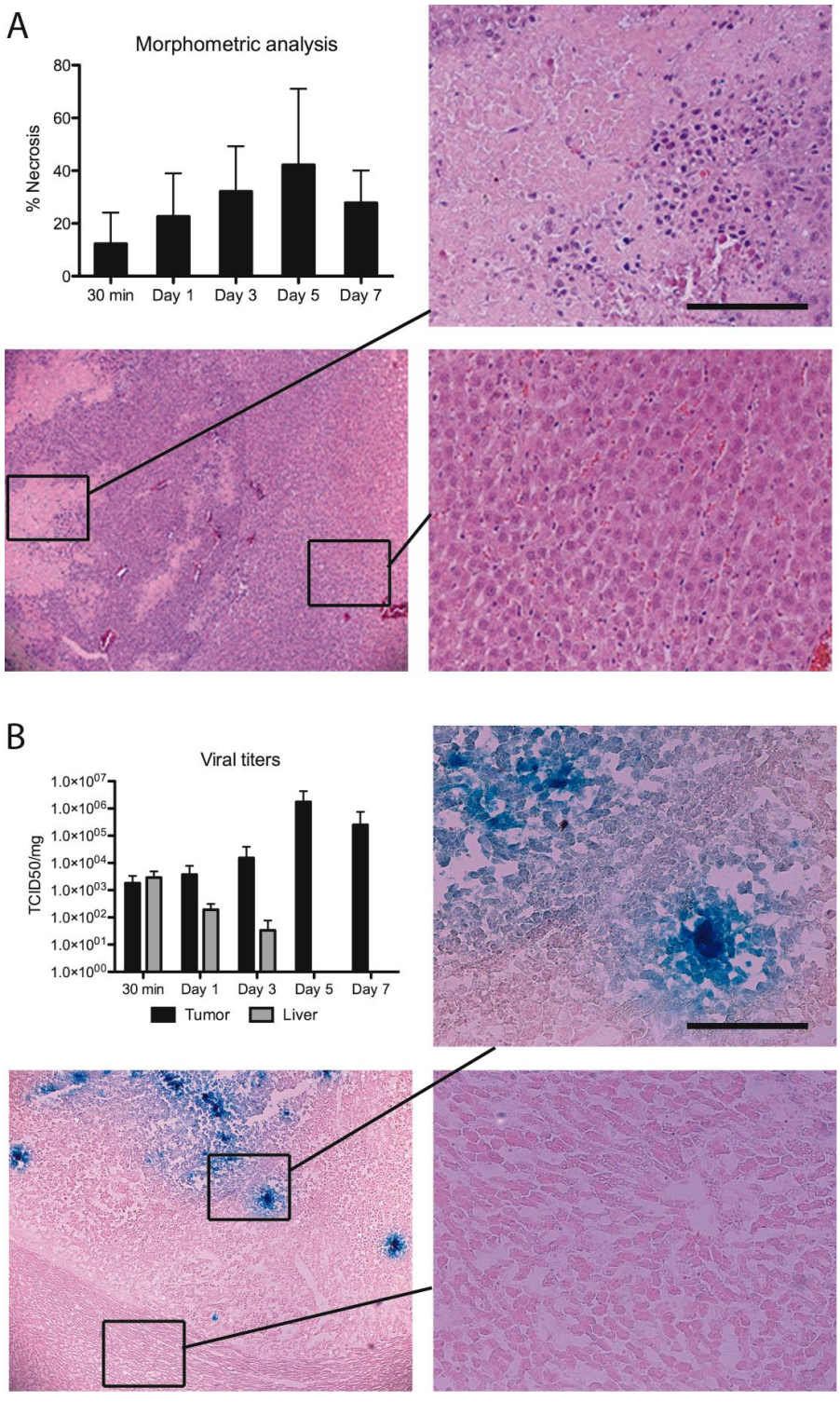

Figure 10. NDV/F3aa(L289A) treatment results in tumor-specific necrosis and virus replication in HCC-bearing rats. Male Buffalo rats bearing multifocal orthotopic HCC nodules were treated with rNDV/F3aa(L289A) (10^8 $TCID_{50}$) by hepatic arterial infusion, and sacrificed at the indicated time-points post-treatment (n=3). (**A**) Tumor-containing liver sections were subjected to H/E staining and analyzed for tumor necrosis and liver toxicity. Representative sections are shown at 5x (overview) and 20x (magnification of tumor and liver sections) magnification. Scale bar = 100µm. Morphometric analysis of tumor necrosis was performed using ImageJ software, and is shown as the mean + standard deviation at each time-point. (**B**) Tumor-containing liver sections were subjected to β-gal staining. Representative sections are shown at 5x (overview) and 20x (magnification of tumor and liver sections) magnification. Scale bar = 100µm. Viral titers were quantified by $TCID_{50}$ analysis of liver and tumor lysate, and are expressed as the mean + standard deviation.

2.3.3 Hyperfusogenic NDV results in a survival prolongation in multifocal HCC-bearing rats.

Although the short-term response to rNDV/F3aa(L289A) indicated an oncolytic effect in our HCC model, it remained to be seen whether or not this would translate to a prolongation in survival. To answer this question, rats harboring multifocal HCC lesions in their livers were randomly assigned to be treated with PBS, rNDV/F3aa, or rNDV/F3aa(L289A) by hepatic arterial infusion (Fig. 11). PBS-treated rats began to succumb to tumor progression at 22 days after treatment, and all had expired by day 37 (median survival, 32 days). In contrast, animals treated with rNDV/F3aa survived for up to 57 days, with a median survival of 36.5 days, which was a significant prolongation over PBS treatment ($p=0.0135$). However, rNDV/F3aa(L289A) treatment further extended the median survival time to 44 days, which represents a 20% prolongation compared with rNDV/F3aa treatment. Therein, superior oncolytic effects of the hyperfusogenic virus compared to the parental rNDV/F3aa vector translated into a significant survival advantage for rats bearing HCC ($p=0.0377$). Furthermore, two animals from the rNDV/F3aa(L289A) treatment group enjoyed long-term tumor-free survival. These rats were euthanized on day 150 for examination of liver pathology. Macroscopically, there was no visible indication of tumor within the liver or elsewhere, and no histological evidence of residual tumor cells or liver abnormality was observed. These results indicate that even large multi-focal lesions (up to 10mm in diameter at the time of treatment) had undergone complete remission in these animals, which translated into long-term and tumor-free survival.

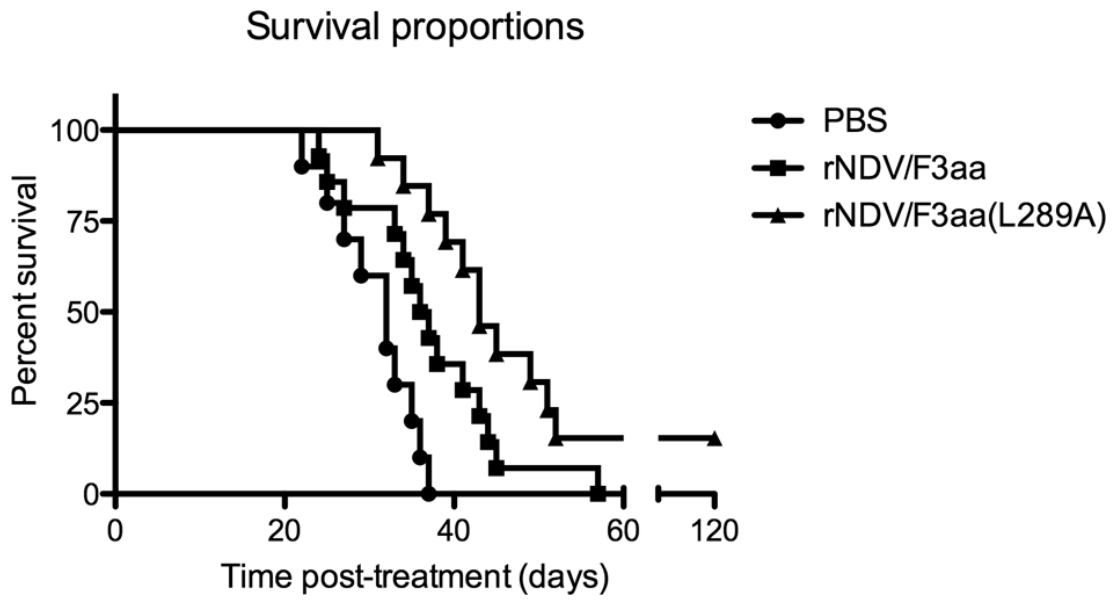

Figure 11. rNDV/F3aa(L289A) therapy results in significant survival prolongation HCC-bearing rats. Male Buffalo rats bearing multifocal HCC lesions were treated by hepatic arterial infusion of PBS (n=10), rNDV/F3aa (n=14), or rNDV/F3aa(L289A) (n=13) and followed for survival. Animals were monitored daily, and survival was plotted as a Kaplan-Meier survival curve. P values for PBS vs. rNDV/F3aa is < 0.02, for rNDV/F3aa vs. rNDV/F3aa(L289A) is < 0.04. Statistical significance was determined by log rank test.

2.3.4 Discussion

NDV represented an attractive vector because naturally occurring strains have been applied for clinical application as oncolytic agents for several decades, and the outcomes of phase I and II clinical trials have been positive. It had previously been demonstrated that the construction of a recombinant NDV vector based on the attenuated (lentogenic) Hitchner B1 strain, with a modified F protein (rNDV/F3aa), resulted in syncytia formation in tumor cells and an improved therapeutic response compared to that of rNDV/B1 in immunocompetent tumor-bearing mice (Vigil 2007). Importantly, although the cleavage site of the NDV F protein has been postulated to be a major determinant of virulence (de Leeuw 2003), the F3aa modification only moderately upgraded the virulence classification from lentogenic to intermediate (mesogenic) in embryonated chicken eggs, based on the mean death time assay (Park 2006). Because this F3aa-modified vector has already demonstrated anti-tumor efficacy in several cancer models (Vigil 2007; Zamarin et al. 2009), we chose the rNDV/F3aa vector as the basis for additional modifications to further enhance the oncolytic potential.

We hypothesized that the incorporation of the previously reported L289A mutation of the F protein into the rNDV/F3aa vector would result in an enhanced oncolytic agent, which could spread easily throughout the tumor mass via cell-cell fusion and result in significant tumor necrosis and survival prolongation in an animal model of cancer. Hepatic arterial infusion of rNDV/F3aa(L289A) at the highest obtainable dose yielded no appreciable signs of toxicity, and histological and immunohistochemical analyses revealed syncytial formation, necrosis, and NDV-mediated LacZ expression exclusively within tumors, while none could be detected in the surrounding liver. Quantification of infectious NDV particles within liver and tumor tissue demonstrated tumor-specific viral replication, with viral titers falling below the level of detection in normal liver by day 5 post-treatment. Finally, Kaplan-Meier survival curve analysis demonstrated a significant survival benefit conferred by rNDV/F3aa(L289A) treatment compared with rNDV/F3aa or PBS.

It is noteworthy to mention the potential safety concerns raised by the concept of uncontrolled viral-mediated syncytia induction (Fu 2003; Nakamori 2003). Although modifications to the F protein have been correlated to changes in virulence, a mean death time assay in embryonated chicken eggs demonstrated that the F(L289A) mutation did not alter the virulence classification from that of the parental mesogenic Hitchner B1/F3aa strain. Moreover, the F modification did not alter the ability of the virus to elicit an innate IFN response in normal cells, nor did it interfere with the intrinsic IFN sensitivity of NDV, which is important for maintenance of tumor specificity. Indeed, hepatic arterial infusion of rNDV/F3aa(L289A) resulted in tumor-specific syncytia formation and caused no observable damage to surrounding hepatocytes or signs of systemic toxicity.

Although much of our previous work has focused on the characterization and development of VSV vectors for the treatment of HCC, we were intrigued by the possibility of establishing a second oncolytic virus system in our model. The establishment of two independent oncolytic

viruses providing effective therapy to a single tumor model provides the unique opportunity to administer combination viral therapy for an additive, or potentially synergistic effect through a "prime-boost" approach for induction of a robust antitumor immune response. In addition, neutralizing antiviral antibodies begin circulating several days after viral administration, thereby significantly limiting the efficacy of readministration of the same virus. The potential to administer an adjuvant treatment at a later time-point using a heterologous virus would provide a novel strategy to circumvent this obstacle to in vivo viral therapy.

2.4 Elucidating the interferon defect responsible for the susceptibility of HCC cells to VSV infection

In contrast to primary human hepatocytes, which are refractory to VSV infection, human HCC cells support robust viral replication. It is generally accepted that defects in the type I interferon (IFN) pathway are responsible for the susceptibility of cancer cells to VSV infection (Stojdl et al. 2000); however, a clear elucidation of the impairment in IFN signaling in tumor cells was lacking. Our aim was to define the nature of the IFN defect in human HCC.

In this study, we characterized the defect in the IFN-induction associated with malignant transformation, tracing the deficit down to the level of the IRF3 protein. We demonstrate that expression of IRF3 could efficiently restore intracellular double-stranded RNA (dsRNA)-dependent IFN-signaling in HCC cells. Furthermore, we observed that the HCC cell lines, HepG2 and Huh-7, as well as primary HCC samples from various human donors, express impressively higher levels of splicing variant IRF3-nirs3 in comparison to primary human hepatocytes. By over-expressing the IRF3-nirs3 variant in IFN-competent cells, we were able to reverse the phenotype, and reproduce the scenario of poor IFN-induction and enhanced VSV replication observed in HCC cells. Therefore, we concluded that the impairment of IFN-β expression in HCC cells might be due to constitutive IRF3-nirs3 expression.

2.4.1 IRF3 and IRF3-nirs3 spliced variant are constitutively activated in HCC

Interferon regulatory factor 3 (IRF3) is a key player in the IFN signaling pathway, which acts by regulating the transcription of IFNs. It is constitutively expressed in most cells types, and contains a highly conserved DNA binding domain at its N-terminus, while the C-terminal region comprises a cluster of phosphoacceptor sites. Virus infection in a normal cell results in phosphorylation at the C-terminal domain, thereby activating dimerization and translocation of IRF3 to the nucleus, where in cooperation with AP-1 and NF-kB transcription factors, promotes the transcriptional activation of the IFN-β promoter (Servant et al. 2003; Sharma et al. 2003).

To determine whether or not the IRF3 promoter could be stimulated in HCC cells, we transfected a reporter plasmid driven by the IRF3 promoter, and observed an activation of the promoter by transfection of Poly (I:C) (Fig. 12A). Next, to determine if perhaps a defect occurs at the post-transcriptional level, we performed a Western blot to compare IRF3 protein concentrations in lysates of primary human hepatocytes to those in HCC cells. Although total protein levels of IRF3 were comparable in both cell types, a second, faster migrating band in the HCC cell lines was detected using an antibody specific to human IRF3. We therefore hypothesized that this smaller band might correspond to a spliced variant of IRF3. To assess whether this isoform is involved in the impairment of dsRNA-induced IFN-gene expression in HCC cells, we cloned IRF3 and the IRF3-spliced isoform expression vectors. Sequence

analysis revealed that the shorter form of IRF3 corresponded to the spliced variant IRF3-nirs3 (GenBank accession number: AB102887).

To examine IRF3 activation, we utilized a phospho-specific antibody that reacts only with the form of IRF3 that is phosphorylated at serine 396. As expected, no phosphorylated IRF3 was detected in the nuclei of un-stimulated primary human hepatocytes, while we found constitutively high levels of both phoshorylated IRF3 and IRF3-nirs3 in HCC cells (Fig. 12C). Importantly, clinical samples of primary human HCC from various donors (three representatives out of seven analyzed samples are shown) also revealed constitutive activation of IRF3 and IRF3-nirs3 by phosphorylation (Fig. 12D), indicating that our results in HCC cell lines are consistent with the scenario in primary HCC tissue.

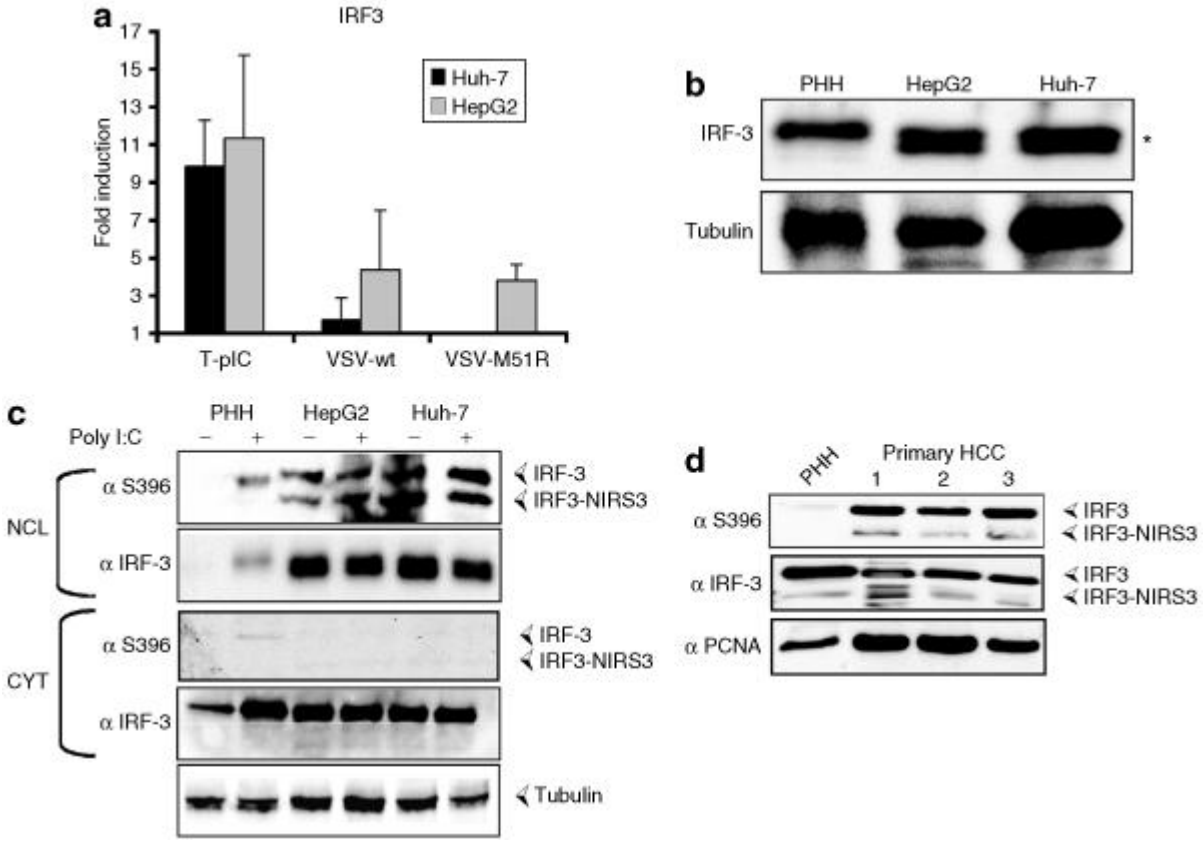

Figure 12. Constitutive expression of IRF3 and IRF3-nirs3 spliced variant in HCC cell lines and primary HCC samples from various donors. (**A**) IRF3 promoter activation in HCC cell lines by Poly (I:C) and virus infection. Luciferase activity notably increased after transfection of dsRNA and to much lower extent in response to viral infection. Experiments were performed in triplicate; each bar indicates mean + standard deviation (**B**) Western blot showing the basal expression of IRF3 and the alternative IRF3-nirs3 form (*) in HCC cells and primary human hepatocytes. Whole protein lysates of mock cultures were separated by SDS/PAGE followed by transfer to PVDF membrane. IRF3 was detected by using a rabbit polyclonal antibody raised against the full length human IRF3 (**C**) Phosphorylation of IRF3. Nuclear (NCL) and cytoplasmic (CT) extracts prepared from mock-transfected or Poly (I:C) transfected primary hepatocytes HepG2 and Huh-7 cells, were analysed by immunoblotting. The membrane was probed with antibody recognizing the total IRF3 and the IRF3 phosphorylated form (phospho-S396). Lysates were probed also with anti-PCNA and anti-tubulin antibodies, respectively. (**D**) Protein expression of IRF3 in the same primary HCC samples compared to un-stimulated PHH. Basal expression and phosphorylation state were analyzed as described previously. Western blots are representatives of two independent experiments.

2.4.2 IRF3-nirs3 impairs the IFN-β response and enhances viral replication in IFN-competent cells

While overexpression of IRF3 restored IFN-β promoter activation in response to intracellular Poly (I:C) in HepG2 and Huh-7 cells, this response was almost completely abrogated by co-transfection with IRF3-nirs3 (Fig. 13A). Similarly, when IRF3-nirs3 was expressed in IFN-competent A549 cells, a significantly impaired response ($p<0.05$) to VSV-M51R (a recombinant VSV vector which induces a strong IFN response in IFN-competent cells) was observed in comparison to mock-transfected cells (Fig. 13B). To support the hypothesis that IRF3-nirs3 might enhance viral replication due to perturbation of the IFN response, we performed multi-step growth analysis of the mutant virus VSV-M51R in A549 cells. Since A549 cells are able to respond to VSV-M51R infection by inducing IFN, we transfected cells with IRF3-nirs3 or an empty vector as a control and infected them. The altered growth kinetics in cells expressing IRF3-nirs3 reflected a significant increase in viral titers by approximately 2 logs at 24 hours post-infection (Fig. 13C).

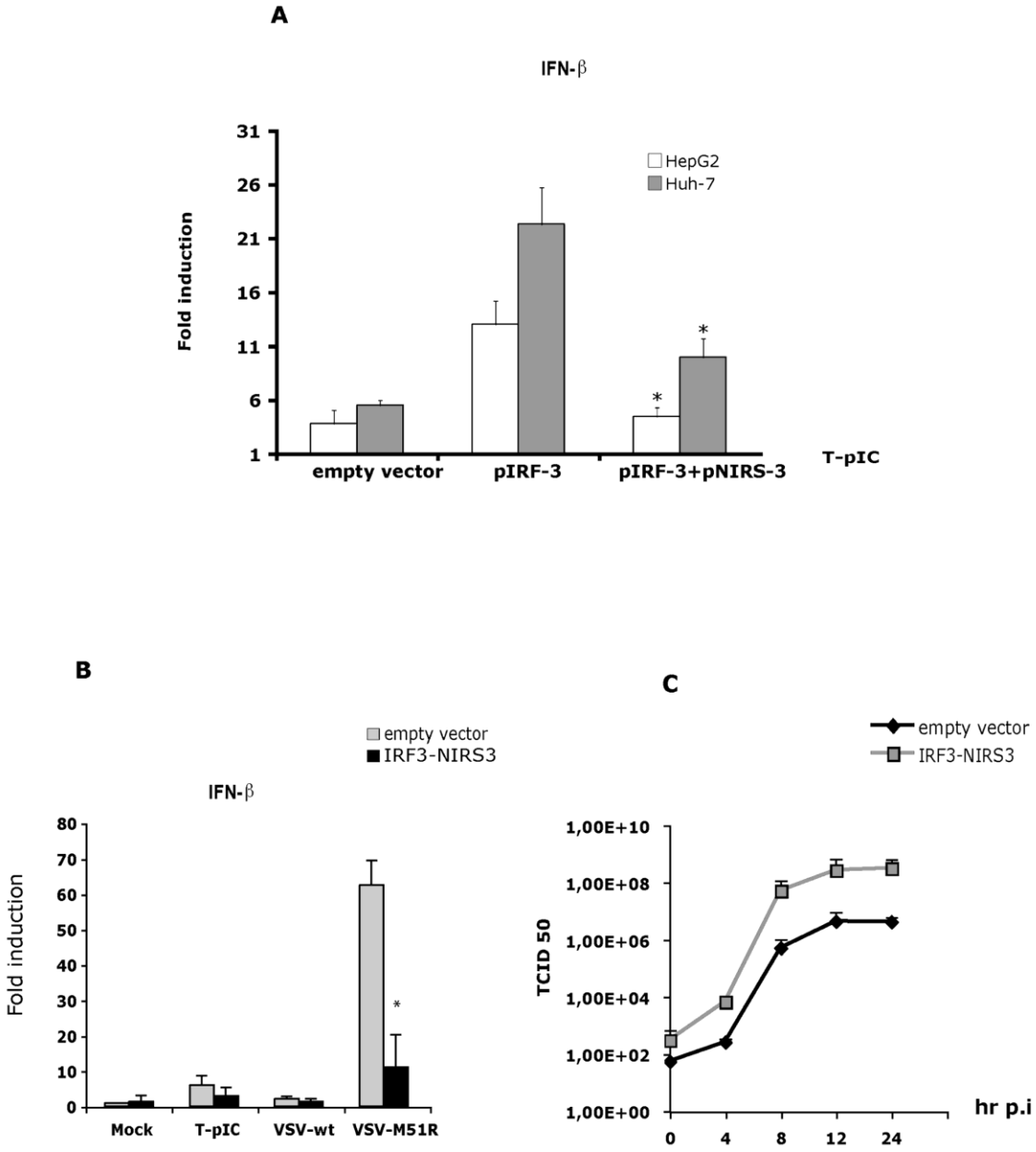

Figure 13. Restoration of IFN-β induction by expression of IRF3 in HCC cells is abrogated by IRF3nirs3. *(A)* HepG2 and Huh-7 cells ectopically expressing IRF3 alone or in combination with IRF3nirs3 were stimulated with Poly (I:C). Fold induction of the IFN-β promoter-dependent luciferase-activity calculated by normalizing with Renilla luciferase expression. * p≤ 0,05 *(B)* IRF3nirs3 expression in A549 inhibits activation of the IFN-β promoter by Poly (I:C) and VSV-M51R infection. A549 cells transfected with an empty vector or IRF3-nirs3 expression plasmid (100 ng) were stimulated with Poly (I:C) or infected. Luciferase-activity was calculated as mentioned above *(C)* A549 cells were either transfected with IRF3-nirs3 or an empty vector. 48 hours post-transfection, infection with VSV-M51R was performed at an MOI of 0,01 and viral titers were determined at 0,4, 8,12 and 24 hours post-infection.

2.4.3 Discussion

As previously described, HCC cells are defective in type I IFN signaling (Keskinen et al. 1999), while primary human hepatocytes possess a functional IFN pathway and can efficiently respond to stimulation by synthetic dsRNA and viral infection. IRF3 is a member of the IFN regulatory transcription factor family, which, upon stimulation, translocates to the nucleus and activates the transcription of IFN-α and -β, as well as other IFN-inducible genes (Hiscott et al. 1999). Therefore, due to the requirement of IRF3 signaling for successful induction of type I IFN gene expression, we investigated the possibility that the impairment in IFN expression in HCC cells could be attributed to a defect in IRF3.

Intrigued by our observation of a truncated isoform of IRF3 in the HCC cell lines and primary HCC tissue, we investigated the possibility of alternative splicing. Several alternative spliced variants of IRF3 have been recently reported in literature, and although their roles remain to be fully elucidated, some of these spliced isoforms seem to exert dominant-negative functions (Karpova et al. 2000; Karpova et al. 2001). We identified the truncated form of IRF3 found in HCC cells as a spliced form of IRF3, known as IRF3-nirs3. This variant lacks 127 amino acids included in the highly conserved β-sandwich core of the IRF3 regulatory-domain (Qin et al. 2003). Although the spliced-variant lacks the domain necessary for dimerization, the phosphorylation acceptors at its carboxyl terminus are conserved, which is consistent with our observation of a second IRF3 protein in the nuclei of HCC cells, also phosphorylated at its carboxy-terminus, corresponding to the predicted size of IRF3-nirs3. This demonstrates that the phosphorylation of these serine-residues is viable, allowing the translocation of IRF3-nirs3 to the nucleus. Furthermore, according to our ChIP assay data, both IRF3 and IRF3-nirs3 have comparable binding affinity to the IFN-β promoter sequence, suggesting that the interference in IRF3 signaling could be the result of competition with IRF3-nirs3 for limited binding sites. We speculate that the disruption of the regulatory-domain in the central portion of the protein might influence the relative conformation of the DNA binding domain and the C-terminal region crucial for its transcriptional activity, as is the case for IRF2 and IRF1.(Koenig Merediz et al. 2000; Lee et al. 2006) Taken together, our results indicate that competitive binding between functional full-length IRF3 and the defective IRF3-nirs3, could explain the malfunction in IRF3 signaling in HCC.

Due to the abnormally high levels of IRF3-nirs3 in HCC cell lines and primary HCC tissue, we postulated that this splicing variant might play a role in the permissiveness of HCC cells to virus infection. Expression of IRF3-nirs3 in A549 cells not only reduced luciferase activity of the IFN-β promoter upon infection with VSV-M51R, but also enhanced viral growth, presumably as a consequence of a delayed IFN response. These data verify our hypothesis, and collectively, this study demonstrates that the deregulation in IRF3 signaling caused by over-expression of IRF3-nirs3 contributes to the susceptibility of HCC cells to viral replication.

Although the reduced IFN-β expression in cancer cells may be attributable to multiple defects in the type I IFN-induction pathways, the impairment of IRF3 activity seems to play a major role in HCC cells. The identification of differential expression of IRF3 and IRF3-nirs3 in HCC cells represents a critical step forward in the understanding of the mechanism whereby oncolytic viruses exert their tumor-specificity. The expression profile of IRF3-nirs3 may represent a potential marker to predict the magnitude of transformation, as well as to screen candidate tumors for susceptibility to VSV oncolytic therapy in future clinical applications.

3. Final conclusions

Over the past century, considerable progress has been made in the field of oncolytic virus therapy for cancer. It is now generally accepted that viruses can be safely used to treat a variety of malignancies, and they can be further adapted or engineered to enhance safety, specificity, and efficacy. However, despite these advancements, a number of issues remain to be addressed.

One major issue is the debate over the use of human versus animal pathogens as oncolytic agents. Although there are indications that certain human pathogens are able to inflict far more significant damage to tumors than to normal host tissues, most human viruses cannot be considered suitable therapeutic agents due to their pathogenicity. A further obstacle is that humans have acquired antibodies to many human viruses, either through vaccination or exposure to the pathogen in the general population, thereby rendering the viruses ineffective in these individuals. On the other hand, several animal viruses have been shown to lack pathogenicity in humans, while being nevertheless capable of destroying human tumor tissue. However, the main impediment to using animal viruses for human cancer therapeutics is the ever-present risk of virus mutation giving rise to a new human pathogen capable of spreading from patient to the general population. Although this risk is not easy to accept, it is important to note that certain animal viruses (e.g. NDV) have been administered safely to humans for several years without any incidents of adverse consequences. These viruses are now generally considered to be safe platforms for the development of therapeutics (Murray et al. 1977; Cassel et al. 1992; Sinkovics et al. 2000).

A second area of controversy surrounds the issue of the importance of the host immune system in fighting cancer. One strategy involves the incorporation of various immune-stimulating genes into the viral vector. The rationale for such an approach is that by boosting the anti-tumor immune responses, one can achieve an additive or synergistic enhancement of tumor response as compared with wild-type viral therapy. After the initial de-bulking of the tumor mass through viral oncolysis, the immune-stimulating gene can promote anti-tumor immune responses to control the remaining viable tumor cells long after the virus has been cleared from the host. While this approach may be attractive to many investigators, the opposing line of thought argues that, due to the striking vulnerability of oncolytic viruses to anti-viral host defenses, any enhancement of host immune responses would be counter-productive to the cytopathic effect of the virus. Upon administration of an oncolytic virus, the host quickly launches a robust anti-viral response, including the release of interferons, activation of natural killer cells, amplification of antigen-specific cytotoxic T cells, and the secretion of virus-specific antibodies. Therefore, the host responses to virus invasion have been recognized as an obstacle to successful therapy, as the virus is often eliminated from the body before it has the opportunity to spread throughout the entire tumor mass and cause substantial destruction of the tumor cells. As a result, various strategies have emerged, which involve suppressing or circumventing the anti-viral host immune responses. This can be

achieved through co-administration with immuno-suppressive agents or through modifications to the viral genome to evade the host defense system.

Regardless of the ultimate strategy, most efforts to improve oncolytic viral therapy involve a mechanism for addressing tumor specificity, delivery, or efficacy. The work presented here represents three distinct, yet potentially complimentary approaches for the enhancement of oncolytic viruses for the treatment of hepatocellular carcinoma. We first demonstrated that combination therapy consisting of a potent oncolytic virus, together with a clinically approved embolization agent, produced a significant synergistic response, potentiating a dramatic prolongation of survival in immune-competent rats bearing multi-focal HCC nodules. We then went on to show that genetic engineering of the Newcastle disease virus genome to introduce a single amino acid modification in the fusion protein greatly improved the fusogenicity of the recombinant virus, thereby resulting in enhanced tumor cell killing through the formation of large multi-nucleated syncytia throughout the tumor mass. The final aim was to better elucidate the defect in interferon signaling in HCC cells, which determines the selective permissivity of these cells to vesicular stomatis virus infection. As a result of this work, we identified an alternative splice variant of IRF3, a key molecule in the interferon signaling pathway, which was present in the HCC cell lines and human primary HCC tissue. Because the expression of this splice variant proved to be a major determinant of virus replication, this could be a potential target for molecular screening of HCC patients for the future selection of candidates for VSV therapy.

While each of these three studies provided fundamental advancements in the field of oncolytic viral therapy, it is important to note that each strategy is not mutually exclusive. Rather, the ultimate goal would be to combine these approaches to produce an optimized protocol for eventual clinical application. For example, after engineering a superior viral vector with enhanced safety and/or efficacy features, this vector would be applied in combination with a previously approved drug or embolization agent for an additive or synergistic enhancement of each monotherapy. Furthermore, in order to identify candidate patients who would be most amenable to this therapy, we aim apply the knowledge derived from mechanistic studies to screen tumor cells for key mutations involved in virus permissiveness. Therefore, the work presented here represents a small portion of numerous ongoing investigations with the common goal of producing an ideal translational product for future clinical application in HCC patients, who are in urgent need of improved treatment options.

4. References

Ackerman, N., Lein, WM., Silverman, NA. (1972). "The blood supply of experimental liver metastases." Surgery **71**: 636-41.

Altomonte, J., R. Braren, S. Schulz, S. Marozin, E. J. Rummeny, et al. (2008). "Synergistic antitumor effects of transarterial viroembolization for multifocal hepatocellular carcinoma in rats." Hepatology **48**(6): 1864-73.

Altomonte, J., Wu, L., Chen, L., Meseck, M., Ebert, O., Garcia-Sastre, A., Fallon, J., and Woo, SLC. (2008). "Exponential enhancement of oncolytic vesicular stomatitis virus potency by vector-mediated suppression of inflammatory responses in vivo." Mol Ther **16**(1): 146-53.

Anderson, J., Gianturco, C., and Wallace, S. (1981). "Experimental transcatheter intraarterial infusion-occlusion chemotherapy." Invest Radiol **16**: 496-500.

Arii, S., Yamaoka, Y., Futagawa, S., et al (2000). "Results of surgical and nonsurgical treatment for small-sized hepatocellular carcinomas: a retrospective and nationwide survey in Japan." Hepatology **32**: 1224-9.

Balachandran, S., M. Porosnicu and G. N. Barber (2001). "Oncolytic activity of vesicular stomatitis virus is effective against tumors exhibiting aberrant p53, Ras, or myc function and involves the induction of apoptosis." J Virol **75**(7): 3474-9.

Balachandran, S. a. B., G.N. (2000). "Vesicular stomatitis virus (VSV) therapy of tumors." IUBMB Life **50**(2): 135-8.

Barker, D. D. a. B., A.J. (1987). "Adenovirus proteins from both E1B reading frames are required for transformation of rodent cells by viral infection and DNA transfection." Virology **156**(1): 107-21.

Bateman, A. R., Harrington, K.J., et al (2002). "Viral fusogenic membrane glycoproteins kill solid tumor cells by nonapoptotic mechanisms that promote cross presentation of tumor antigens by dendritic cells." Cancer Research **62**(22): 6566-78.

Bertolozzi, C., Lencioni, R., Caramella, D., Vignali, C., Cioni, R., Mazzeo, S., et al (1995). "Treatment of large HCC: transcatheter arterial chemoembolization combined with percutaneous ethanol injection versus repeated transcatheter arterial chemoembolization." Radiology **197**: 812-8.

Bierman, H. R., D. M. Crile, K. S. Dod, K. H. Kelly, N. L. Petrakis, et al. (1953). "Remissions in leukemia of childhood following acute infectious disease: staphylococcus and streptococcus, varicella, and feline panleukopenia." Cancer **6**(3): 591-605.

Bischoff, J. R., Kirn, D.H., Williams, A., Heise, C., Horn, S., Muna, M., Ng, L., Nye. J.A., Sampson-Johannes, A., Fattaey, A., and McCormick, F. (1996). "An adenovirus mutant that replicates selectively in p53-deficient human tumor cells." Science **274**(5286): 373-6.

Blank, S. V., Rubin, S.C., Coukos, G., Amin, K.M., Albelda, S.M., and Molnar-Kimber, K.L. (2002). "Replication-selective herpes simplex virus type 1 mutant therapy of cervical cancer is enhanced by low-dose radiation." Human Gene Therapy **13**(5): 627-39.

Blum, H. (2005). "Hepatocellular carcinoma: Therapy and prevention." World J Gastroenterol **11**(47): 7391-7400.

Breitbach, C. J., Paterson, J.M., Lemay, C.G., Falls, T.J., McGuire, A., Parato, K.A., Stojdl, D.F., Daneshmand, M., Speth, K., Kirn, D., McCart, J.A., Atkins, H., and Bell, J.C. (2007). "Targeted inflammation during oncolytic virus therapy severely compromises tumor blood flow." Mol Ther **15**(9): 1686-93.

Bruix, J., Castells, A., Bosch, J., et al (1996). "Surgical resection of hepatocellular carcinoma in cirrhotic patients: prognostic value of preoperative portal pressure." Gastroenterology **111**: 1018-22.

Bruix, J., Llovet, JM., Castells, A., Montaua, X., Bru, C., Ayuso, MC., et al (1998). "Transarterial embolization versus symptomatic treatment in patients with advanced hepatocellular carcinoma: results of a randomized controlled trial in a single institution." Hepatology **27**: 1578-83.

Bruix, J., Sala, M., and Llovet, JM (2004). "Chemoembolization for hepatocellular carcinoma." Gastroenterology **127**: S179-88.

Camma, C., Schepis, F., Orlando, A., Albanese, M., Shahied, L., Trevisani, F., et al (2002). "Transarterial chemoembolization for unresectable hepatocellular carcinoma: meta-analysis of randomized controlled trials." Radiology **224**: 47-54.

Cassel, W. A. and R. E. Garrett (1965). "Newcastle Disease Virus As An Antineoplastic Agent." Cancer **18**: 863-8.

Cassel, W. A. and D. R. Murray (1992). "A ten-year follow-up on stage II malignant melanoma patients treated postsurgically with Newcastle disease virus oncolysate." Med Oncol Tumor Pharmacother **9**(4): 169-71.

Chang, J., Tzeng, WS., Pan, HB, Yang, CF., and Lai, KH. (1994). "Transcatheter arterial embolization with or without cisplatin treatment of hepatocellular carcinoma: A randomized controlled study." Cancer **74**: 2449-53.

Chiocca, E. A., Abbed, K.M., Tatter, S., et al (2004). "A phase I open-label, dose-escalation, multi-institutional trial of injection with an E1B-attenuated adenovirus, ONYX-015, into the peritumoral region of recurrent malignant gliomas, in the adjuvant setting." Mol Ther **10**(5): 958-66.

Coffey, M. C., Strong, J.E., Forsyth, P.A., Lee, P.W. (1998). "Reovirus therapy of tumors with activated Ras pathway." Science **282**: 1332-4.

Conzelmann, K. K. (1998). "Nonsegmented negative-strand RNA viruses: genetics and manipulation of viral genomes." Annu Rev Genet **32**: 123-62.

Coukos, G., Makrigiannakis, A., Kang, E.H., Rubin, S.C., Albelda, S.M., and Molnar-Kimber, K.L. (2000). "Oncolytic herpes simplex virus-1 lacking ICP34.5 induces p53-independent death and is efficacious against chemotherapy-resistant ovarian cancer." Clin Cancer Res **6**(8): 3342-53.

Csatary, L. K., Gosztonyi, G., Szeberenyi, J., Fabian, Z., Liszka, V., Bodey, B., and Csarary, C.M. (2004). "MTH-68/H oncolytic viral treatment in human high-grade gliomas." J Neurooncol **67**: 83-93.

de Leeuw, O. S., Hartog, L., Koch, G., and Peeters, B.P. (2003). "Effect of fusion protein cleavage site mutations on virulence of Newcastle disease virus: nonvirulent cleavage site mutants revert to virulence after one passage in chicken brain." J Gen Virol **84**: 475-84.

DePace, N. (1912). "Sulla scomparsa di un enome canco vegetante del collo dell'utero senza cura chirurgica." Ginecologia **9**: 82-9.

Deuffic, S., Poynard, T., Buffat, L., Valleron, A-J (1998). "Trends in primary liver cancer." Lancet **351**: 214-5.

Di Paolo, N. C., S. Tuve, S. Ni, K. E. Hellstrom, I. Hellstrom, et al. (2006). "Effect of adenovirus-mediated heat shock protein expression and oncolysis in combination with low-dose cyclophosphamide treatment on antitumor immune responses." Cancer Res **66**(2): 960-9.

Diaz, R., Galivo, F., Kottke, T., Wongthida, P., Qiao, J., Thompson, J., Valdes, M., Barber, G., and Vile, RG. (2007). "Oncolytic immunovirotherapy for melanoma using vesicular stomatitis virus." Cancer Research **67**(7): 2840-8.

Dock, G. (1904). "The influence of complicating diseases upon leukemia." Am J Med Sci **127**: 563-92.

Dunn, G. P., C. M. Koebel and R. D. Schreiber (2006). "Interferons, immunity and cancer immunoediting." Nat Rev Immunol **6**(11): 836-48.

Dyer, Z., Peltekian, K., and van Zanten, S.V. (2005). "The changing epidemiology of hepatocellular carcinoma in Canada." Aliment Pharmacol Ther **22**(1): 17-22.

Ebert, O., Shinozaki, K., Kournioti, C., et al (2004). "Syncytia induction enhances the oncolytic potential of vesicular stomatitis virus in virotherapy for cancer." Cancer Research **64**: 3265-70.

El-Serag, H., Davila, JA., Petersen, NJ., McGlynn, KA. (2003). "The continuing increase in the incidence of hepatocellular carcinoma in the United States." Ann Intern Med **139**: 817-23.

El-Serag, H. B. a. M., A.C. (1999). "Rising incidence of hepatocellular carcinoma in the United States." N Engl J Med **340**(10): 745-50.

Erichsen, C., Bolmsjo, M., Hugander, A., and Jonsson, PE. (1985). "Blockage of the hepatic-artery blood flow by biodegradable microspheres (Spherex) combined with local hyperthermia in the treatment of experimental liver tumors in rats." Clin Oncol **109**: 38-41.

Fernandez, M., Porosnicu, M., Markovic, D., and Barber, G.N. (2002). "Genetically engineered vesicular stomatitis virus in gene therapy: application for treatment of malignant disease." J Virol **76**: 895-904.

Freeman, A. I., Zakay-Rones, Z., Gomori, J.M., Linetsky, E., Rasooly, L., Greenbaum, E., Rozenman, Yair, S., Panet, A., Libson, E., Irving, C.S., Galun, E., and Siegal, T. (2006). "Phase I/II trial of intravenous NDV-HUJ oncolytic virus in recurrent glioblastoma multiforme." Mol Ther **13**(1): 221-8.

Fu, X., Tao, L., et al (2003). "Expression of a fusogenic membrane glycoprotein by an oncolytic herpes simplex virus potentiates the viral antitumor effect." Mol Ther **7**(6): 748-54.

Fuerst, T. R., E. G. Niles, F. W. Studier and B. Moss (1986). "Eukaryotic transient-expression system based on recombinant vaccinia virus that synthesizes bacteriophage T7 RNA polymerase." Proc Natl Acad Sci U S A **83**(21): 8122-6.

Fueyo, J., Gomez-Manzano, C., Alemany, R., Lee, P.S., McDonnell, T.J., Mitlianga, P., Shi, Y.X., Levin, V.A., Yung, W.K. and Kyritsis, A.P. (2000). "A mutant oncolytic adenovirus targeting the Rb pathway produces anti-glioma effect in vivo." Oncogene **19**(1): 2-12.

Garber, K. (2006). "China approves world's first oncolytic virus therapy for cancer treatment." J Natl Cancer Inst **98**(5): 298-300.

Graziadei, I., Sandmueller, H., Waldenberger, P., Koenigsrainer, A., Nachbaur, K., Jaschke, W., Margreiter, R., and Vogel, W. (2003). "Chemoembolization followed by liver transplantation for hepatocellular carcinoma impedes tumor progression while on the waiting list and leads to excellent outcome." Liver Transpl **9**(557-563).

Gupta, S., Kobayashi, S., Phongkitkarun, S., Broemeling, L.D., and Kan, Z. (2006). "Effect of transcatheter hepatic arterial embolization on angiogenesis in an animal model." Invest Radiol **41**(6): 516-21.

Hallenbeck, P. L., Chang, Y.N., Hay, C., Golightly, D., Stewart, D., Lin, J., Phipps, S., and Chiang, Y.L. (1999). "A novel tumor-specific replication-restricted adenoviral vector for gene therapy of hepatocellular carcinoma." Hum Gene Ther **10**(10): 1721-33.

Heise, C., Sampson-Johannes, A., Williams, A., McCormick, F., Von Hoff, D.D., and Kirn, D.H. (1997). "ONYX-015, an E1B gene-attenuated adenovirus, causes tumor-specific

cytolysis and antitumoral efficacy that can be augmented by standard chemotherapeutic agents." Nat Med **3**(6): 639-45.

Hiscott, J., P. Pitha, P. Genin, H. Nguyen, C. Heylbroeck, et al. (1999). "Triggering the interferon response: the role of IRF-3 transcription factor." J Interferon Cytokine Res **19**(1): 1-13.

Hoster, H. A., R. P. Zanes, Jr. and E. Von Haam (1949). "Studies in Hodgkin's syndrome; the association of viral hepatitis and Hodgkin's disease; a preliminary report." Cancer Res **9**(8): 473-80.

Hotte, S. J., Lorence, R.M., Hirte, H.W., Polawski, S.R., Bamat, M.K., O'Neil, J.D., Roberts, M.S., Groene, W.S., and Major, P.P. (2007). "An optimized clinical regimen for the oncolytic virus PV701." Clin Cancer Res **13**(3): 977-85.

Huebner, R. J., W. P. Rowe, W. E. Schatten, R. R. Smith and L. B. Thomas (1956). "Studies on the use of viruses in the treatment of carcinoma of the cervix." Cancer **9**(6): 1211-8.

Ikeda, K., Wakimoto, H., Ichikawa, T., Jhung, S., Hochberg, F.H., Louis, D.N., and Chiocca, E.A. (2000). "Complement depletion facilitates the infection of multiple brain tumors by an intravascular, replication-conditional herpes simplex virus mutant." J Virol **74**(10): 4765-75.

Janke, M., Peeters, B., de Leeuw, O., Moorman, R., Arnold, A., Fournier, P., and Schirrmacher, V. (2007). "Recombinant Newcastle disease virus (NDV) with inserted gene for GM-CSF as a new vector for cancer immunogene therapy." Gene Therapy **14**(23): 1639-49.

Kambara, H., Okano, H, Chiocca, E.A., and Saeki, Y (2005). "An oncolytic HSV-1 mutant expressing ICP34.5 under control of a nesin promoter increases survival of animals even when symptomatic from brain cancer." Cancer Research **65**(7): 32-9.

Kan, Z., Ivancev, K., Lunderquist, A., et al (1983). "In vivo microscopy of hepatic tumors in animal models: a dynamic investigation of blood supply to hepatic metastases." Radiology **187**: 621-626.

Karpova, A. Y., P. M. Howley and L. V. Ronco (2000). "Dual utilization of an acceptor/donor splice site governs the alternative splicing of the IRF-3 gene." Genes Dev **14**(22): 2813-8.

Karpova, A. Y., L. V. Ronco and P. M. Howley (2001). "Functional characterization of interferon regulatory factor 3a (IRF-3a), an alternative splice isoform of IRF-3." Mol Cell Biol **21**(13): 4169-76.

Kato, T., Nemoto, R., Mori, H., Takahashi, M., Tamakawa, Y. (1981). "Transcatheter arterial chemoembolization of renal cell carcinoma with microencapsulated mitomycin C on dog kidney." J Urol **125**: 19-24.

Keeffe, E. (1998). "Summary of guidelines on organ allocation and patient listing for liver transplantation." Liver Transpl **4**: S108-14.

Kenji, J., Hyodo, I., Tanimizu, M., Tanada, M., Nishikawa, Y., Hosokawa, Y., Mandai, K., and Moriwaki, S. (1997). "Total necrosis of hepatocellular carcinoma with a combination therapy of arterial infusion of chemotherapeutic lipiodol and transcatheter arterial embolization: report of 14 cases." Semin Oncol **24**: S6-71-S6-80.

Keskinen, P., M. Nyqvist, T. Sareneva, J. Pirhonen, K. Melen, et al. (1999). "Impaired antiviral response in human hepatoma cells." Virology **263**(2): 364-75.

Kirn, D., Martuza, R.L., and Zwiebel, J. (2001). "Replication-selective virotherapy for cancer: biological principles, risk management, and future directions." Nat Med **7**: 781-7.

Koenig Merediz, S. A., M. Schmidt, G. J. Hoppe, J. Alfken, D. Meraro, et al. (2000). "Cloning of an interferon regulatory factor 2 isoform with different regulatory ability." Nucleic Acids Res **28**(21): 4219-24.

Kopecky, S. A., Willingham, M.C., and Lyles, D.S. (2001). "Matrix protein and another viral component contribute to induction of apoptosis in cells infected with vesicular stomatitis virus." J Virol **75**(24): 12169-81.

Lawson, N. D., E. A. Stillman, M. A. Whitt and J. K. Rose (1995). "Recombinant vesicular stomatitis viruses from DNA." Proc Natl Acad Sci U S A **92**(10): 4477-81.

Lee, E. J., M. Jo, J. Park, W. Zhang and J. H. Lee (2006). "Alternative splicing variants of IRF-1 lacking exons 7, 8, and 9 in cervical cancer." Biochem Biophys Res Commun **347**(4): 882-8.

Lein, W., and Ackerman, NB. (1970). "The blood supply of experimental liver metastases." Surgery **68**: 334-40.

Letchworth, G. J., L. L. Rodriguez and J. Del C. Barrera (1999). "Vesicular stomatitis." Vet J **157**(3): 239-60.

Li, J., Melanson, V.R., Mirza, A.M., and Iorio, R.M. (2004). "Decreased dependence on receptor recognition for the fusion promotion activity of L289A-mutated Newcastle disease virus fusion protein correlates with a monoclonal antibody-detected conformational change." J Virol **79**(2): 1180-90.

Liau, K. H., Rou, L., Shia, J., et al (2005). "Outcome of partial hepatectomy for large (>10cm) hepatocellular carcinoma." Cancer.

Livraghi, T., Bolondi, L., Lazzaroni, S., Marin, G., Morabito, A., Rapaccini, G.L., Salmi, A, and Torzilli, G. (1992). "Percutaneous ethanol injection in the treatment of hepatocellular carcinoma in cirrhosis. A study on 207 patients." Cancer **69**(4): 925-9.

Llovet, J., and Bruix, J. (2003). "Systematic review of randomized trials for unresectable hepatocellular carcinoma: Chemoembolization improves survival." Hepatology **37**: 429-42.

Llovet, J., Burroughs, A., Bruix, J (2003). "Hepatocellular carcinoma." Lancet **362**: 1907-17.

Llovet, J., Fuster, J., Bruix, J. (1999). "Intention-to-treat analysis of surgical treatment for early hepatocellular carcinoma: resection versus transplantation." Hepatology **39**: 1434-40.

Llovet, J. M., S. Ricci, V. Mazzaferro, P. Hilgard, E. Gane, et al. (2008). "Sorafenib in advanced hepatocellular carcinoma." N Engl J Med **359**(4): 378-90.

Lorence, R. M., Katubig, B.B., Reichard, K.W., et al (1994). "Complete regression of human fibrosarcoma xenografts after local Newcastle disease virus therapy." Cancer Research **54**: 6017-21.

Martuza, R. L., Malick, A., Markert, J.M., Ruffner, K.L. and Coen, D.M. (1991). "Experimental therapy of human glioma by means of a genetically engineered virus mutant." Science **252**(5007): 854-6.

Mathurin, P., Rixe, O., Carbonell, N., Bernard, B., Cluzel, P., Bellin, MF., at al (1998). "Overview of medical treatments in unresectable hepatocellular carcinoma--an impossible meta-analysis?" Aliment Pharmacol Ther **12**: 111-26.

Merli, M., Nicolini, G., Gentili, F., et al (2005). "Predictive factors of outcome after liver transplantation in patients with cirrhosis and hepatocellular carcinoma." Transplant Proc **37**(6): 2535-40.

Mineta, T., Rabkin, S.D., Yazaki, T., Hunter, W.D. and Martuza, R.L. (1995). "Attenuated multi-mutated herpes simplex virus-1 for the treatment of malignant gliomas." Nat Med **1**(9): 938-43.

Miraglia, R., Pietrosi, G., Maruzzelli, L., Petridis, I., Caruso, S., Marrone, G., Mamone, G., Vizzini, G., Luca, A., and Gridelli, B. (2007). "Efficacy of transcatheter embolization/chemoembolization (TAE/TACE) for the treatment of single hepatocellular carcinoma." World J Gastroenterol **13**(21): 2952-5.

Miyatake, S. I., Tani, S., Feigenbaum, F., Sundaresan, P., Toda, H., Narumi, O., Kikuchi, H., Hashimoto, N., Hangai, M., Martuza, R.L., and Rabkin, S.D. (1999). "Hepatoma-specific antitumor activity of an albumin enhancer/promoter regulated herpes simplex virus in vivo." Gen Ther **6**(4): 564-72.

Mohr, L., Geissler, M., et al (2002). "Gene therapy for malignant liver disease." Expert Opin Biol Ther **2**(2): 163-75.

Murray, D. R., W. A. Cassel, A. H. Torbin, Z. L. Olkowski and M. E. Moore (1977). "Viral oncolysate in the management of malignant melanoma. II. Clinical studies." Cancer **40**(2): 680-6.

Nakamori, M., Fu, X., Meng, F., Jin, A., Tao, L., Bast, R.C. Jr., and Zhang, X. (2003). "Effective therapy of metastatic ovarian cancer with an oncolytic herpes simplex virus encorporating two membrane fusion mechanisms." Clin Cancer Res **9**(7): 2727-33.

Nakamoto, Y., Mizukoshi, E., Tsuji, H., Sakai, Y., Kitahara, M., Arai, K., Yamashita, T., Yokoyama, K., Mukaida, N., Matsushima, K., Matsui, O., and Kaneko, S. (2007). "Combined therapy of transcatheter hepatic arterial embolization with intratumoral dendritic cell infusion for hepatocellular carcinoma: clinical safety." Clinical and Experimental Immunology **147**: 296-305.

Nakaya, T., Cros, J., Park, M.S., Nakaya, Y., Zheng, H., Sagrera, A., Villar, E., Garcia-Sastre, A., and Palese, P. (2001). "Recombinant Newcastle disease virus as a vaccine vector." J Virol **75**(23): 11868-11873.

Nemunaitis, J. (2002). "Live viruses in cancer treatment." Oncology **16**: 1483-92.

Nemunaitis, J., Ganly, I., Khuri, F., Arseneau, J., Kuhn, J., McCarty, T., Landers, S., Maples, P., Romel, L., Randlev, B., Reid, T., Kaye, S., and Kirn, D. (2000). "Selective replication and oncolysis in p53 mutant tumors with ONYX-015, an e1B-55kD gene-deleted adenovirus, in patients with advanced head and neck cancer: a phase II trial." Cancer Res **60**(22): 6359-66.

Pack, G. T. (1950). "Note on the experimental use of rabies vaccine for melanomatosis." AMA Arch Derm Syphilol **62**(5): 694-5.

Park, M. S., A. Garcia-Sastre, J. F. Cros, C. F. Basler and P. Palese (2003). "Newcastle disease virus V protein is a determinant of host range restriction." J Virol **77**(17): 9522-32.

Park, M. S., Steel, J., Garcia-Sastre, A., Swayne, D., and Palese, P. (2006). "Engineered viral vaccine constructs with dual specificity: Avain influenza and Newcastle disease." Proc. Natl. Acad. Sci. **103**(21): 8203-8208.

Parkin, D. M., Bray, F., Ferlay, J., and Pisani, P. (2001). "Estimating the world cancer burden: Globocan 2000." Int J Cancer **94**: 153-6.

Pasquinucci, G. (1971). "Possible effect of measles on leukaemia." Lancet **1**(7690): 136.

Peng, K. W., Ahmann, G.J., Pham, L, et al (2001). "Systemic therapy of myeloma xenografts by an attenuated measles virus." Blood **98**: 2002-7.

Popescu, I., Sirbu-Boeti, M.P., Tomulescu, V., et al (2005). "Therapy of malignant liver tumors using microwave and radiofrequency ablation." Chirurgia(Bucur) **100**(2): 111-20.

Qin, B. Y., C. Liu, S. S. Lam, H. Srinath, R. Delston, et al. (2003). "Crystal structure of IRF-3 reveals mechanism of autoinhibition and virus-induced phosphoactivation." Nat Struct Biol **10**(11): 913-21.

Randall, R. E. and S. Goodbourn (2008). "Interferons and viruses: an interplay between induction, signalling, antiviral responses and virus countermeasures." J Gen Virol **89**(Pt 1): 1-47.

Reichard, K. W., Lorence, R.M., Cascino, C.J., Peeples, M.E., Walter, R.J., Fernando, M.B., Reyes, H.M., and Greager, J.A. (1992). "Newcastle disease virus selectively kills human tumor cells." J Surg Res **52**(5): 448-453.

Rose, J. K. and M. A. Whitt (2001). Rhabdoviridae: the viruses and their replication. Fields Virology. D. M. Knipe and P. M. Howley. Philadelphia, Lippincott Williams & Wilkins**:** 1221-1242.

Schnell, M. J., L. Buonocore, E. Kretzschmar, E. Johnson and J. K. Rose (1996). "Foreign glycoproteins expressed from recombinant vesicular stomatitis viruses are incorporated efficiently into virus particles." Proc Natl Acad Sci U S A **93**(21): 11359-65.

Schnell, M. J., L. Buonocore, M. A. Whitt and J. K. Rose (1996). "The minimal conserved transcription stop-start signal promotes stable expression of a foreign gene in vesicular stomatitis virus." J Virol **70**(4): 2318-23.

Schwartz, M., Roayaie, S., and Uva, P (2007). "Treatment of HCC in patients awaiting liver transplantation." American Journal of Transplantation **7**: 1875-81.

Sergel, T. A., McGinnes, L.W., and Morrison, T.G. (2000). "A single amino acid change in the Newcastle disease virus fusion protein alters the requirement for HN protein in fusion." J Virol **74**(11): 5101-7.

Servant, M. J., N. Grandvaux, B. R. tenOever, D. Duguay, R. Lin, et al. (2003). "Identification of the minimal phosphoacceptor site required for in vivo activation of interferon regulatory factor 3 in response to virus and double-stranded RNA." J Biol Chem **278**(11): 9441-7.

Sharma, S., B. R. tenOever, N. Grandvaux, G. P. Zhou, R. Lin, et al. (2003). "Triggering the interferon antiviral response through an IKK-related pathway." Science **300**(5622): 1148-51.

Shinozaki, K., Ebert, O., Kournioti, C., et al (2004). "Oncolysis of multifocal hepatocellular carcinoma in the rat liver by hepatic artery infusion of vesicular stomatitis virus." Mol Ther **9**: 368-376.

Simonetti, R. G., Liberati, A., Angiolini, C., and Pagliaro, L. (1997). "Treatment of hepatocellular carcinoma: a systemic review of randomized controlled trials." Ann Oncol **8**(2): 117-36.

Sinkovics, J. G. and J. C. Horvath (2000). "Newcastle disease virus (NDV): brief history of its oncolytic strains." J Clin Virol **16**(1): 1-15.

Stetson, D. B. and R. Medzhitov (2006). "Type I interferons in host defense." Immunity **25**(3): 373-81.

Stojdl, D. F., N. Abraham, S. Knowles, R. Marius, A. Brasey, et al. (2000). "The murine double-stranded RNA-dependent protein kinase PKR is required for resistance to vesicular stomatitis virus." J Virol **74**(20): 9580-5.

Stojdl, D. F., B. Lichty, S. Knowles, R. Marius, H. Atkins, et al. (2000). "Exploiting tumor-specific defects in the interferon pathway with a previously unknown oncolytic virus." Nat Med **6**(7): 821-5.

Stojdl, D. F., Lichty, B.D., tenOever, B.R., et al (2003). "VSV strains with defects in their ability to shutdown innate immunity are potent systemic anti-cancer agents." Cancer Cell **4**(4): 263-75.

Takayama, T., Sekine, T., Makuuchi, M., Yamasaki, S., Kosuge, T., Yamamoto, J., Shimada, K., Sakamoto, M., Hirohashi, S., Ohashi, Y., and Kakizoe, T. (2000). "Adoptive immunotherapy to lower postsurgical recurrence rates of hepatocellular carcinoma: a randomized trial." Lancet **356**: 802-7.

Tancredi, T., McCuskey, PA., Kan, Z., and Wallace, S. (1999). "Changes in rat liver microcirculation after experimental hepatic arterial embolization: comparison of different embolic agents." Radiology **211**: 177-81.

Taqi, A. M., M. B. Abdurrahman, A. M. Yakubu and A. F. Fleming (1981). "Regression of Hodgkin's disease after measles." Lancet **1**(8229): 1112.

Taylor-Robinson, S., Foster, GR., Arora, S., Hargreaves, S., and Thomas HC (1997). "Increase in primary liver cancer in the UK." Lancet **350**: 1142-3.

Varela, M., M. I. Real, M. Burrel, A. Forner, M. Sala, et al. (2007). "Chemoembolization of hepatocellular carcinoma with drug eluting beads: efficacy and doxorubicin pharmacokinetics." J Hepatol **46**(3): 474-81.

Vigil, A., Park, M.S., Martinez, O., Chua, M.A., Xiao, S., Cros, J.F., Martinez-Sobrido, L., Woo, S.L.C., and Garcia-Sastre, A. (2007). "Use of reverse genetics o enhance the oncolytic properties of newcastle disease virus." Cancer Research **67**(7): 8285-92.

Wang, J., Murata, S., and Kumazaki, T. (2006). "Liver microcirculation after hepatic artery embolization with degradable starch microspheres." World J Gastroenterol **12**(26): 4214-8.

Welsh, R. M. (1986). "Regulation of virus infections by natural killer cells." Nat Immun Cell Growth Reg **5**: 169-99.

Whelan, S. P., L. A. Ball, J. N. Barr and G. T. Wertz (1995). "Efficient recovery of infectious vesicular stomatitis virus entirely from cDNA clones." Proc Natl Acad Sci U S A **92**(18): 8388-92.

Wickham, T. J., Tzeng, E., Shears, L.L., 2nd, Roelvink, P.W., Li, Y., Lee, G.M., Brough, D.E., Lizonova, A., and Kovesdi, I. (1997). "Increased in vitro and in vivo gene transfer by adenovirus vectors containing chimeric fiber proteins." J Virol **71**(11): 8221-9.

Yao, F., Bass, NM., Nikolai, B., et al (2002). "Liver transplantation for hepatocellular carcinoma: analysis of survival according to the intention-to-treat principle and dropout from the waiting list." Liver Transpl **8**: 873-83.

Yeung, Y. P., Lo, C.M., Liu, C.L., et al (2005). "Natural history of untreated nonsurgical hepatocellular carcinoma." Am J Gastroenterol **100**(9): 1995-2004.

Yoneyama, M., M. Kikuchi, T. Natsukawa, N. Shinobu, T. Imaizumi, et al. (2004). "The RNA helicase RIG-I has an essential function in double-stranded RNA-induced innate antiviral responses." Nat Immunol **5**(7): 730-7.

Yoshikawa, T., Kokura, S., Oyamada, H., Iinuma, S., Nishimura, S., Kaneko, T., Naito, Y., and Kondo, M. (1994). "Antitumor effect of ischemia-reperfusion injury induced by transient embolization." Cancer Research **54**: 5033-5.

Yusoff, K. and W. S. Tan (2001). "Newcastle disease virus: macromolecules and opportunities." Avian Pathol **30**(5): 439-55.

Zamarin, D., Martinez-Sobrido, L., Kelly, K., Mansour, M., Sheng, G., Vigil, A., Garcia-Sastre, A., Palese, P., and Fong, Y. (2009). "Enhancement of oncolytic properties of recombinant Newcastle disease virus through antagonism of cellular innate immune responses." Mol Ther **17**(4): 697-706.

Zamarin, D., A. Vigil, K. Kelly, A. Garcia-Sastre and Y. Fong (2009). "Genetically engineered Newcastle disease virus for malignant melanoma therapy." Gene Ther.

Zhao, H., M. Janke, P. Fournier and V. Schirrmacher (2008). "Recombinant Newcastle disease virus expressing human interleukin-2 serves as a potential candidate for tumor therapy." Virus Res **136**(1-2): 75-80.

Zygiert, Z. (1971). "Hodgkin's disease: remissions after measles." Lancet **1**(7699): 593.

5. Acknowledgements

I would first like to thank Dr. Oliver Ebert for inviting me to come to Germany for my PhD. It has been a great experience and has changed my life forever.

I am extremely grateful to my Doktorvater, Prof. Dieter Langosch, for all of his help and guidance through the process. I would also like to thank Prof. Arne Skerra for agreeing to chair my exam on such short notice.

To my wonderful colleagues, Dr. Sabrina Marozin, Sybille Apfel, Barbara Lindner, and Sabrina Goldman, I am especially thankful. They provided much-needed assistance, support, humor, and especially chocolate and Schnapps, when I needed them most.

Finally I would like to express my special gratitude to my beloved husband, Dr. Johannes Schwarz, for his patience, encouragement, and never-ending support. This work would not have been possible without him.

Synergistic Antitumor Effects of Transarterial Viroembolization for Multifocal Hepatocellular Carcinoma in Rats

Jennifer Altomonte,[1] Rickmer Braren,[2] Stephan Schulz,[3] Sabrina Marozin,[1] Ernst J. Rummeny,[2] Roland M. Schmid,[1] and Oliver Ebert[1]

Oncolytic virotherapy is a promising strategy for safe and effective treatment of malignancy. We have reported previously that recombinant vesicular stomatitis virus (VSV) vectors are effective oncolytic agents that can be safely administered via the hepatic artery in immunocompetent rats to treat multifocal hepatocellular carcinoma (HCC), resulting in tumor necrosis and prolonged survival. Though the results were encouraging, complete tumor regression was not observed, which led us to explore alternative approaches to further enhance the efficacy of VSV treatment. Transarterial embolization techniques have been shown to improve the efficiency and tumor selectivity of anticancer treatments. Degradable starch microspheres (DSM) are one such embolic agent that provides transient embolization of the therapeautic agent before being degraded by serum amylases. Here we demonstrate via dynamic contrast-enhanced magnetic resonance imaging that in our rat model of multifocal HCC, DSM injection into the hepatic artery results in a substantial reduction in tumor perfusion of systemically applied contrast agent. VSV, when administered in combination with DSM, results in enhanced tumor necrosis and synergistically prolongs survival when compared with VSV or DSM monotherapy. *Conclusion:* This regimen of viroembolization represents an innovative therapeutic modality that can augment the future development of transarterial oncolytic virus therapy for patients with advanced HCC. (HEPATOLOGY 2008;48: 1864-1873.)

Hepatocellular carcinoma (HCC) represents a major worldwide health concern, ranking among the top five most prevalent malignancies.[1] The incidence of HCC has more than doubled over the last two decades,[2] and now accounts for over 500,000 new cases annually.[3-5] Recent reports suggest that the rate of HCC diagnoses will continue to rise, presumably as a consequence of an ever-increasing prevalence of hepatitis C virus infection and increased alcohol consumption observed in most industrialized countries.[6,7]

Whereas the incidence of HCC has been increasing steadily, the emergence of new and effective therapeutic agents remains relatively stagnant. The majority of HCC cases are detected at an advanced stage, at which time the treatment options are even further limited.[5] Surgical resection and liver transplantation are considered curative; however, the majority of patients do not meet the strict criteria designated by such treatments. In general, surgical therapy is indicated only in patients with limited HCC progression (1 to 3 nodules), without portal hypertension or advanced underlying liver disease.[8,9] The feasibility of liver transplantation is further limited by a shortage of donor livers, resulting in waiting times in excess of 12 months in some Western countries.[10]

For patients with nonresectable HCC or patients on the waiting list for liver transplantation, local regional therapy using transarterial embolization (TAE) or transarterial chemoembolization (TACE) are considered stan-

Abbreviations: DCE-MRI, dynamic contrast-enhanced magnetic resonance imaging; DSM, degradable starch microspheres; HCC, hepatocellular carcinoma; MTS, 3-(4,5-dimethylthiazol-2-yl)-5-(3-carboxymethoxyphenyl)-2-(4-sulfophenyl)-2H-tetrazolium; NK, natural killer; PBS, phosphate-buffered saline; pfu, plaque-forming units; TACE, transarterial chemoembolization; TAE, transarterial embolization; TCID50, tissue culture infectious dose 50; VSV, vesicular stomatitis virus.

From [1]II. Medical Clinic, [2]Institute for Radiology, and [3]Institute for Pathology, Technical University of Munich, Munich, Germany.

Received March 7, 2008; accepted July 20, 2008.

Supported in part by the German Research Aid (Max-Eder Research Program) and the Federal Ministry of Education and Research (Grant 01GU0505).

Address reprint requests to: Oliver Ebert, II Medizinische Klinik und Poliklinik, Klinikum rechts der Isar, Technical University of Munich, Trogerstr. 32, 81675 Munich, Germany. Email: oliver.ebert@lrz.tum.de; fax: (49)-89-41402258.

Published online in Wiley InterScience (www.interscience.wiley.com).

DOI 10.1002/hep.22546

Potential conflict of interest: Nothing to report.

dard palliative treatment.[11-13] The rationale for such therapies lies in the dual blood supply feeding the liver. Whereas normal hepatocytes receive the majority of their blood flow from the portal vein, with only about 25% being supplied by the hepatic artery, tumors receive their blood almost exclusively from the hepatic artery.[14] TAE and TACE therapies exploit this unique feature by blocking the arterial blood flow in the liver, thereby delivering a concentrated dose of a chemotherapeutic drug and/or embolizing agent selectively to the tumor, resulting in ischemia-induced necrosis and enhanced oncolysis due to a prolonged exposure time of the tumor cells to the chemotherapeutic agent.[15,16] Although it is generally accepted that TAE and TACE techniques result in substantial tumor response after treatment,[17,18] several trials have produced controversial data regarding a resulting prolongation of survival.[19-21] Furthermore, it is not yet clear whether the incorporation of chemotherapy provides an additional survival benefit over TAE alone.

Due to the overwhelming deficit in effective treatment options for HCC, several alternative approaches have emerged. Oncolytic viruses are a promising option due to their intrinsic ability to selectively replicate and kill tumor cells while sparing the surrounding normal tissue.[22-24] Vesicular stomatitis virus (VSV), a negative-strand RNA virus of the *Rhabdoviridae* family, is a particularly appealing oncolytic vector because of its wide host range, short replication cycle, and ability to reach high titers in many rodent and human tumor cell lines. VSV is nonpathogenic in humans and derives its tumor selective replication through its extreme sensitivity to the antiviral effects of type I interferon responses in normal cells, which are defective in most tumor cells.[25] Furthermore, because the general population has never been exposed to VSV, it is presumed that there will be no issue of pre-existing immunity, which would interfere with its future potential for clinical application.[26]

We have previously described the efficacy of recombinant VSV vectors as oncolytic agents for treatment of orthotopic HCC in immunocompetent rats.[27] We demonstrated that, by vector infusion through the hepatic artery, VSV could effectively gain access and selectively replicate in multifocal HCC tumors of various sizes, resulting in tumor necrosis and prolongation of survival.[28-30] Though these results are encouraging, complete tumor regression was not achieved, and the remaining viable tumor eventually relapsed, preventing the possibility of long-term survival. Based on these observations, we sought an alternate strategy to improve upon the outcome of VSV therapy for HCC.

We present a therapeutic approach for the treatment of multifocal HCC, involving recombinant VSV administered in combination with an embolization agent, and infused through the hepatic artery in tumor-bearing rats. In this study, we used degradable starch microspheres (DSM), an embolic agent currently being used clinically for TAE of HCC and metastatic liver tumors, injected as a mixture with a low dose of our previously reported rVSV-F vector. This strategy, which we have termed viroembolization, resulted in massive tumor necrosis and translated to substantial prolongation of survival in comparison to monotherapy with either VSV or DSM alone.

Materials and Methods

Cell Lines. The rat HCC cell line McA-RH7777 was purchased from the American Type Culture Collection (Manassas, VA) and maintained in Dulbecco's modified Eagle's medium adjusted to contain 1.5 g/L sodium bicarbonate and 4.5 g/L glucose (American Type Culture Collection). BHK-21 cells purchased from the American Type Culture Collection were maintained in Glasgow minimum essential medium (GIBCO, Carlsbad, CA). All culture media were supplemented with 10% heat-inactivated fetal bovine serum (Biochrome, Berlin, Germany), and all cells were cultured in a humidified atmosphere at 5% CO_2 and 37°C.

Recombinant Virus. The construction and rescue of the rVSV vector expressing a mutant (L289A) NDV fusion protein (rVSV-F) has been described.[28] The virus was amplified on BHK-21 cells, and the supernatant was purified with a sucrose gradient. Briefly, the cells were infected at a multiplicity of infection of 0.0001, and 48 hours later, the supernatant was collected and centrifuged to clear floating cells. The supernatant was then subjected to ultra-centrifugation at 24,000 rpm for 1 hour. The pellet was resuspended in phosphate-buffered saline (PBS) and layered on top of a sucrose gradient ranging from 60% to 10%, and ultra-centrifuged for 1 hour at 24,000 rpm. The band containing the virus was carefully collected with a syringe and 20-gauge needle, aliquoted, and stored at −80°C.

Growth Curves. Viral growth in the presence and absence of degradable starch microspheres (EmboCept, PharmaCept, Berlin, Germany) was compared in McA-RH7777 cells. The cells were plated in 6-well dishes at 1×10^6 cells per well, and infected with rVSV-F at a multiplicity of infection of 10, mixed with an equal volume of either DSM or PBS in triplicate. After infection at room temperature for 30 minutes, cells were washed three times with PBS, and fresh complete medium was added. Aliquots of supernatant were collected at 0, 8, 16, and 24 hours postinfection, and assayed for viral titer via tissue culture infectious dose 50 (TCID50) analysis.

Cell Proliferation Assay. McA-RH7777 cells were seeded overnight in 24-well dishes at 2×10^5 cells per well and infected the following day with rVSV-F at a multiplicity of infection of 10, mixed with an equal volume of either DSM or PBS. Cell viability was measured at 0, 6, 12, 24, 48, and 72 hours after infection using the 3-(4,5-dimethylthiazol-2-yl)-5-(3-carboxymethoxyphenyl)-2-(4-sulfophenyl)-2H-tetrazolium (MTS) tetrazolium compound (CellTiter96 AQ_{ueous} One Solution Cell Proliferation Assay, Promega, Madison, WI). All cell viability data are expressed as a percentage of viable cells compared withmock-infected controls at each time point.

Animal Studies. All procedures involving animals were approved and performed according to the guidelines of the institution's animal care and use committee and the government of Bavaria, Germany. Six-week-old male Buffalo rats were purchased from Harlan Winkelmann (Borchen, Germany), and housed under standard conditions. To establish multifocal HCC lesions within the liver, 10^7 syngeneic McA-RH7777 rat HCC cells were infused as a 1-mL suspension in serum-free Dulbecco's modified Eagle's medium through the portal vein. A second laparotomy was performed 21 days after tumor cell implantation, and animals with visible tumors within the range of 1 to 10 mm in diameter were randomly assigned to the following treatment groups: PBS, DSM, rVSV-F, or combination treatment of rVSV-F plus DSM. All treatments were administered as a 1-mL solution injected via the hepatic artery. A dose of 1×10^6 plaque-forming units (pfu) of VSV was used in the monotherapy and combination group. 500 μL of DSM was diluted 1:1 with either PBS or rVSV-F, depending on the treatment group. Representative animals from each group were sacrificed on day 1 and day 3 for histology and immunohistochemical analysis of tumor and liver sections. In addition, TCID50 analysis of extracts from snap-frozen tumor samples was performed for quantification of VSV yield on day 1. Finally, animals were followed for survival to compare the therapeutic outcome of each treatment. The animals were monitored daily and euthanized at humane endpoints.

Magnetic Resonance Imaging Acquisition and Image Analysis. Magnetic resonance images were acquired on a 1.5-T whole-body magnetic resonance imaging scanner (Philips, Achieva, Netherlands). Buffalo rats bearing multifocal McA-RH7777 HCC tumors, either untreated or treated with transarterial injection of DSM, were subjected to dynamic contrast-enhanced magnetic resonance imaging (DCE-MRI) approximately 30 minutes after infusion of the embolization agent. Rat livers were imaged individually using a 47-mm surface coil (Philips). Axial images were obtained for tumor localization using a T1-weighed three-dimensional gradient echo sequence (Repetition Time [TR] = 20 ms, Echo Time [TE] = 4.6 ms, flip angle = 30°, Field of View [FOV] = 6.4 × 4.0 cm, imaging matrix = 224 × 179, slice thickness = 1 mm). Contrast dynamics with three baseline scans and 27 postcontrast scans were then visualized using an axial T1-weighted three-dimensional gradient echo sequence (TR = 20 ms, TE = 2.9 ms, flip angle = 45° slice thickness = 2 mm) with a time resolution of 28 seonds/dynamic. Bolus injection via the tail vein of 0.2 mmol/kg GdDTPA (Magnevist, Bayer HealthCare Pharmaceuticals) was performed manually within 2 seconds. Data were quantitatively analyzed using View Forum software (Philips, Netherlands) by measuring gray-scale signal intensities in equally sized regions of interest within tumor nodules and adjacent normal liver tissue.

Histology and Immunohistochemistry. Liver sections containing tumor were fixed overnight in 4% paraformaldehyde and paraffin-embedded. Three-micrometer-thin sections were subjected to either hematoxylin-eosin staining for histological analysis or immunohistochemical staining using monoclonal antibodies against VSV/G protein (Alpha Diagnostic, San Antonio, TX), CD31 (Santa Cruz Biotechnology, Santa Cruz, CA), and natural killer (NK) cell marker ANK61 (Santa Cruz Biotechnology). Terminal deoxynucleotidyl transferase-mediated dUTP nick-end labeling was performed using the *In Situ* Cell Death Detection Kit, Flourescein (Roche, Indianapolis, IN) according to the manufacturer's protocol. ImageJ software (National Institutes of Health, Bethesda, MD) was used for morphometric analysis of tumors, and necrotic areas were measured and expressed as a percentage of the entire tumor area.

Statistical Analyses. For comparison of individual data points, a two-sided Student *t* test was applied to determine statistical significance. Survival curves were plotted according to the Kaplan-Meier method, and statistical significance between different treatment groups was determined using the log-rank test. Statistical data were obtained using GraphPad Prism 5.0 (GraphPad Software, San Diego, CA). *P* values of less than 0.05 were considered statistically significant.

Results

In Vitro *Characterization of DSM Treatment on HCC Cells.* To rule out an inhibitory effect of the embolization agent on viral replication, rVSV titers in McA-RH7777 cells were monitored in the presence versus absence of DSM. Aliquots of the supernatants were harvested at the indicated time points and subjected to TCID50 analysis, and the growth curves were plotted

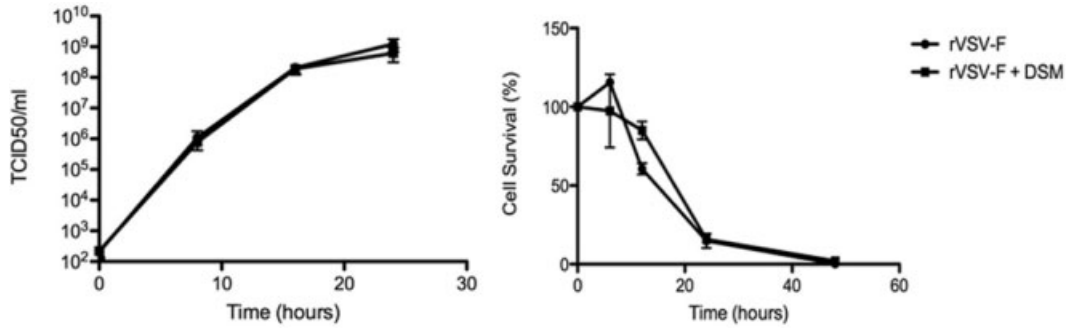

Fig. 1. DSM does not alter viral replication and cell killing of rVSV-F in McA-RH7777 rat HCC cells in vitro. Rat McA-RH7777 cells were infected at a multiplicity of infection of 10 in the presence or absence of degradable starch microspheres (DSM). Left: TCID50 assays were performed on conditioned media at 0, 8, 16, and 26 hours after infection. Right: MTS assays for cell viability were performed at 0, 6, 12, 24, 48, and 72 hours after infection. Triplicate samples were analyzed at each time point. Data are expressed as the mean ± standard deviation.

(Fig. 1). The virus replicated to similar titers at all time points tested, regardless of the presence of DSM during infection. Furthermore, to determine a cytotoxic effect incurred by DSM on VSV-infected McA-RH7777 cells, MTS assays were performed at various time points after treatment with rVSV alone or with rVSV plus DSM. The kinetics of cell killing in each group was nearly identical.

In Vivo Imaging of Embolized Tumors. To monitor the effectiveness of transarterial infusion of DSM in HCC tumor-bearing rats, animals were randomly assigned as untreated controls or treated with DSM via the hepatic artery. Approximately 30 minutes after embolization, the animals were subjected to DCE-MRI. Perfusion of the gadolinium contrast agent within the tumors and normal surrounding liver was analyzed (Fig. 2). The resulting intensity plots revealed perfusion of tumor and liver tissue with a prolonged washout phase in the tumor tissue compared with the normal liver tissue, while in the embolized animals only the normal liver tissue is perfused with contrast agent. These data indicate that hepatic arterial infusion of DSM results in nearly complete embolization of tumors, while having little effect on normal liver perfusion at early time points.

VSV/G Expression Within Tumors Treated by Viroembolization. To assess the in vivo effect of VSV administered in combination with an embolization agent, animals were randomly assigned to receive rVSV-F monotherapy or combination therapy of rVSV-F plus DSM. To compare the contents of VSV within tumor and normal liver tissues administered in the presence versus absence of embolization agent, three animals per group were sacrificed on day 1 after treatment for histo-

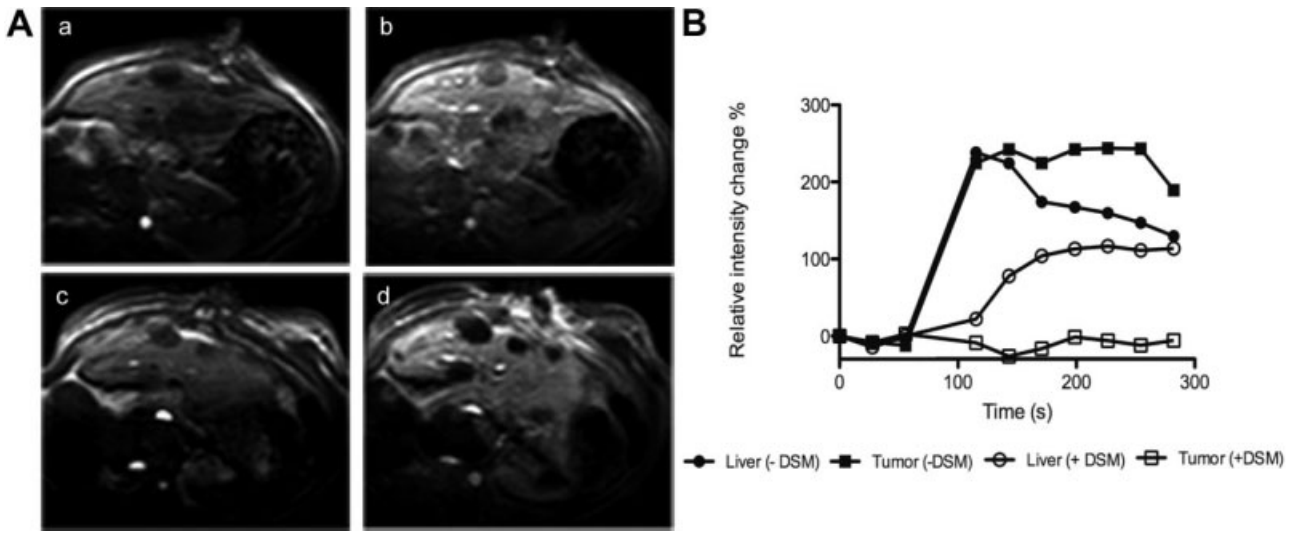

Fig. 2. Dynamic contrast-enhanced magnetic resonance imaging. McA-RH7777 tumor-bearing rats, either nonembolized or 30 minutes after hepatic arterial embolization with DSM, were imaged with DCE-MRI. (A) Axial T1-weighed precontrast (a, c) and postcontrast (b, d) images show lack of contrast in embolized tumor nodules (d). (B) Data were quantitatively analyzed by measuring gray-scale signal intensities in equal-sized regions of interest of tumor nodules and adjacent normal liver tissue. One representative data set is shown.

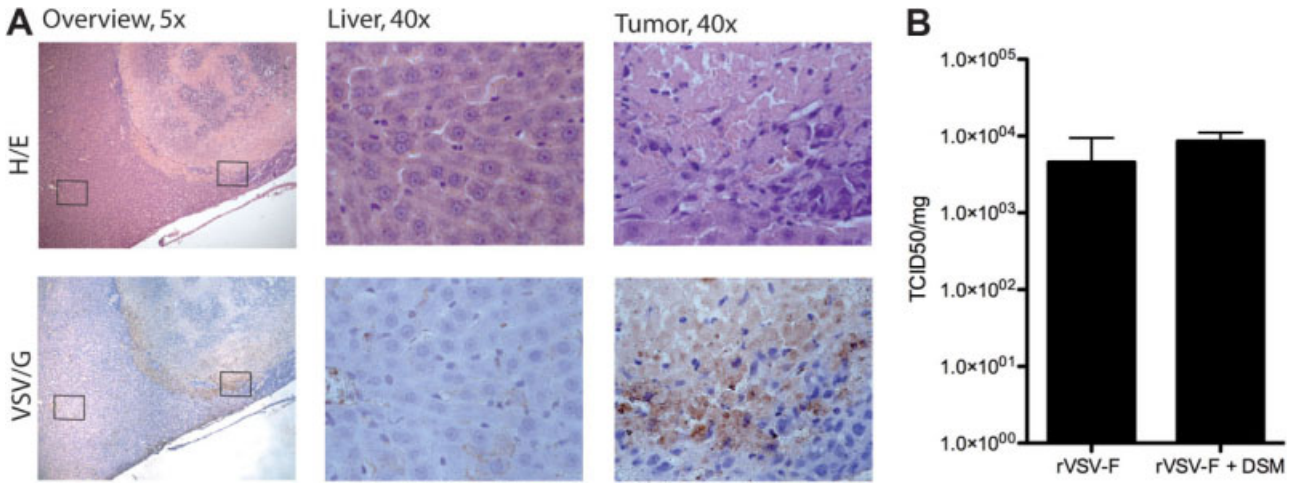

Fig. 3. Tumor-specific VSV/G expression localized in viable border region of HCC after treatment with rVSV-F and DSM. Tumor-bearing rats were treated via hepatic arterial infusion with PBS, DSM, rVSV-F, or DSM plus rVSV-F with a viral dose of 1×10^6 pfu/animal. Tumor samples were obtained on day 1 after treatment. (A) Three-micrometer-thin paraffin sections were stained with hematoxylin-eosin (upper panel) and a monoclonal anti-VSV/G antibody counterstained with hematoxylin (lower panel). Representative sections of liver and tumor are shown at low (×5) and high (×40) power. (B) Tumor samples were snap frozen, and lysates were subjected to TCID50 analysis to compare intratumoral virus titers in rVSV-F versus rVSV-F and DSM-treated rats. Results are expressed as the mean + standard deviation.

logical and immunohistochemical staining, as well as quantification of viral titers via TCID50 analysis (Fig. 3). Immunohistochemical staining using a monoclonal antibody against VSV/G revealed VSV/G protein localized within the viable tumor rim of viroembolized animals. Importantly, the histology of neighboring hepatic parenchyma in both treatment groups was completely normal, and in consecutive sections there was no evidence for VSV/G expression via immunohistochemistry (Fig. 3A). TCID50 analyses of snap-frozen tumor lysates demonstrated similar viral titers in the two groups (Fig. 3B). Infectious VSV particles within the normal liver were below the level of detection (10 pfu/mg wet weight) and subsequently could not be determined.

Enhanced Tumor Response in Viroembolized HCC Tumor-Bearing Rats. To determine the impact of transarterial viroembolization on tumor viability, multifocal HCC-bearing rats were treated with PBS, DSM, rVSV-F, or rVSV-F plus DSM and were euthanized on day 3 after treatment. Liver sections containing tumor were prepared for hematoxylin-eosin staining and analyzed morphometrically for quantification of necrotic areas (Fig. 4). ImageJ software was employed to measure necrotic areas, which were then calculated as a percentage of the entire tumor area. In the PBS control group, less than 15% necrosis was observed, which can be attributed to spontaneous necrosis that occurs naturally in most tumors. Whereas VSV treatment alone resulted in less than 30% necrosis, DSM treatment caused nearly 60% necrosis, and combination treatment resulted in more than 90% tumor necrosis. The morphometric analysis data are statistically significant for each group compared with every other group (that is, PBS versus rVSV-F, $P < 0.05$; DSM versus rVSV-F plus DSM, $P < 0.0001$).

Enhanced Apoptosis Observed in HCC Tumors Treated with rVSV-F. To identify a potential mechanism for the additive effect of rVSV-F plus DSM on tumor response, we compared the degree of apoptosis

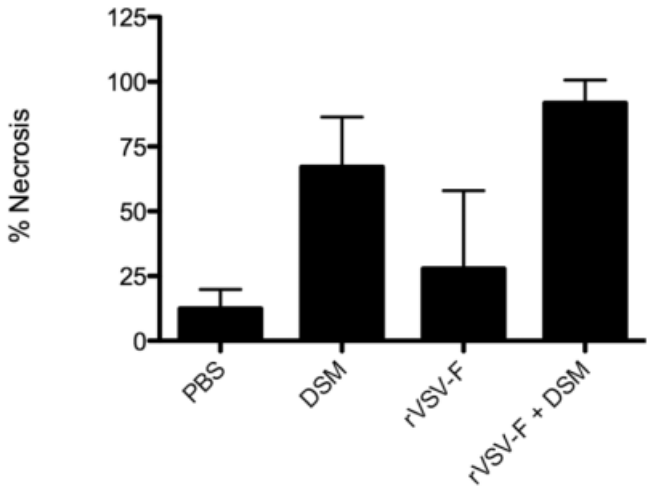

Fig. 4. Enhanced tumor response in multifocal HCC-bearing rats treated with rVSV-F and DSM. Rats bearing multifocal HCC tumors were infused via the hepatic artery with PBS, DSM, rVSV-F, or DSM plus rVSV-F with a viral dose of 1×10^6 pfu/animal, and sacrificed 3 days after treatment. Three-micrometer-thin tumor sections were stained with hematoxylin-eosin and analyzed. The percentage of necrotic area within each tumor was measured morphometrically using ImageJ software. Data are expressed as the mean + standard deviation, and the results were analyzed statistically via two-sided Student *t* test. All data were statistically significant compared with all other treatment groups ($P < 0.05$).

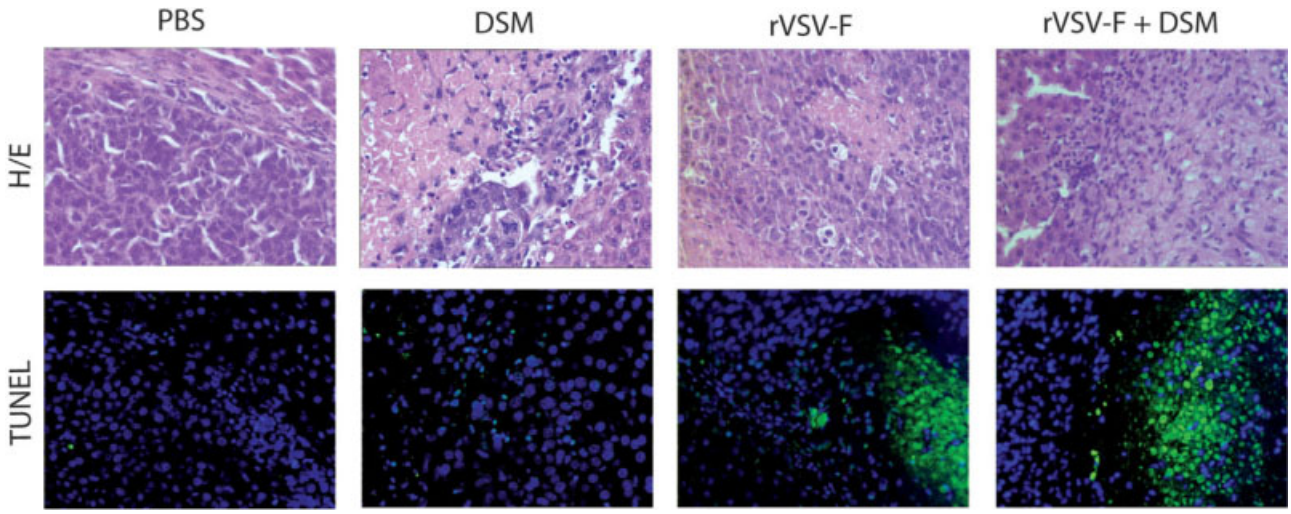

Fig. 5. Treatment with rVSV-F or viroembolization results in enhanced apoptosis in HCC tumors. Rats bearing multifocal HCC were treated via hepatic arterial infusion of PBS, DSM, rVSV-F, or DSM plus rVSV-F with a viral dose of 1×10^6 pfu/animal, and sacrificed 3 days after treatment. Three-micrometer-thin paraffin sections containing liver and tumor were subjected to hematoxylin-eosin analysis (top) or fluorescein-conjugated terminal deoxynucleotidyl transferase-mediated dUTP nick-end labeling and counterstained with 4',6-diamidino-2-phenylindole for localization of nuclei (bottom). Representative sections are shown (original magnification ×20).

among treatment groups. Although on day 1 there were no remarkable differences (data not shown), on day 3 we observed patches of apoptosis in tumors treated with rVSV-F alone, and significantly enhanced apoptosis in the outer borders of those tumors subjected to transarterial viroembolization (Fig. 5) compared with those treated with either monotherapy or PBS.

Attenuated CD31 Expression Following Treatment with rVSV-F. To investigate a possible anti-angiogenic effect of rVSV-F in HCC, we performed immunohistochemical analysis of CD31 in tumor sections on day 3 after treatment (Fig. 6, upper panel). Whereas normal vasculature with CD31+ endothelial staining was observed in tumors treated with PBS, rVSV-F and viroembolization resulted in almost complete loss of positive staining on vessel walls. In the DSM monotherapy group, we observed CD31 staining localized mainly to the border regions of tumors, indicating that the vasculature in this

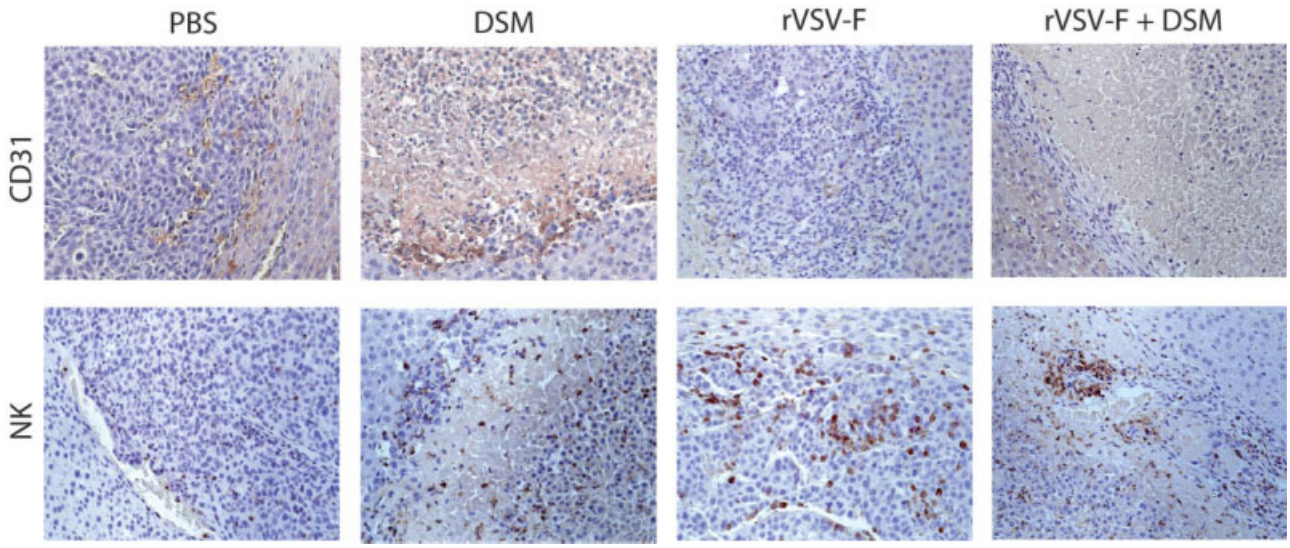

Fig. 6. rVSV-F causes reduction in CD31+ endothelial cells and stimulation of NK cell infiltration within tumors. Rats bearing multifocal HCC were treated via hepatic arterial infusion of PBS, DSM, rVSV-F, or DSM plus rVSV-F with a viral dose of 1×10^6 pfu/animal and sacrificed on day 3 after treatment. Three-micrometer-thin paraffin sections containing liver and tumor were analyzed via immunohistochemistry using a polyclonal antibody against CD31 (top) or NK cell marker ANK61 (bottom). Sections were counterstained with hematoxylin. Representative sections are shown (original magnification ×20).

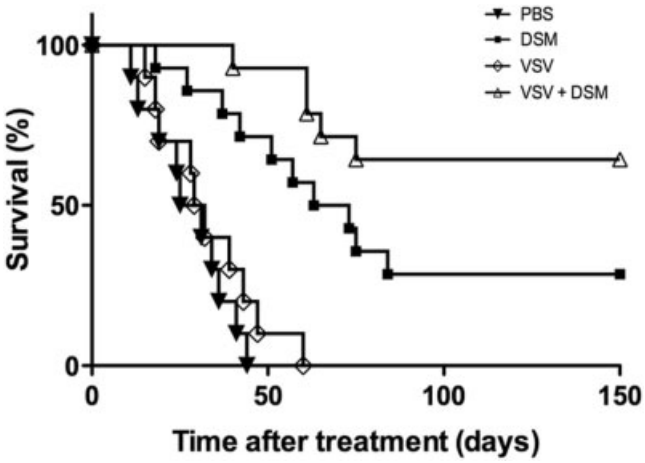

Fig. 7. DSM combined with rVSV-F results in significant survival prolongation in HCC-bearing rats. Multifocal hepatocellular carcinoma-bearing rats were treated with PBS (n = 10), DSM (n = 14), rVSV-F (n = 10), or DSM plus rVSV-F (n = 14) via hepatic arterial infusion and were followed for survival. Animals were monitored daily, and data were plotted as a Kaplan-Meier survival curve. Statistical significance was determined via log rank test.

area is still viable, and new angiogenesis has possibly been initiated.

Enhanced Infiltration of Inflammatory Cells in rVSV-F Infected Tumors. Because we postulated an inflammatory response conferred by the virus, we performed immunohistochmical staining of various immune cell markers on tumor tissue following treatment with PBS, DSM, rVSV-F, or rVSV-F plus DSM. Although we observed no significant differences in the numbers of macrophages and neutrophils among treatment groups (data not shown), we observed a significant infiltration of NK cells in tumors treated with virus, either alone or in combination with DSM (Fig. 6, bottom panel). To a lesser degree, DSM monotherapy also appeared to stimulate NK cell accumulation within tumors.

Significant Prolongation of Survival After Transarterial Viroembolization in Multifocal HCC-Bearing Rats. To assess the potential long-term benefit of the combination treatment modality for multifocal HCC tumor-bearing rats, a survival experiment was conducted. Tumor-bearing rats were randomly assigned to receive one of the following treatments via the hepatic artery: PBS (n = 10), DSM (n = 14), rVSV-F (n = 10), or DSM combined with rVSV-F (n = 14). Animals were monitored daily for survival, and the data were plotted as a Kaplan-Meier survival curve (Fig. 7). Although monotherapy with rVSV-F at this low dose did not significantly alter survival compared with PBS treatment, DSM treatment resulted in statistically significant survival benefit ($P < 0.0001$), both alone and in combination with rVSV-F. Furthermore, combination therapy with rVSV-F and DSM significantly prolonged survival compared with DSM treatment alone, resulting in more than 60% of viroembolized animals experiencing complete tumor regression. As dictated by Kaplan-Meier analysis, these data indicate a synergistic effect of the combination therapy. Furthermore, the long-term surviving rats were sacrificed after 150 days and evaluated for signs of residual malignancy. Macroscopically, there was no visible tumor within the liver or elsewhere, and there was no histological evidence of residual tumor cells or liver toxicity.

Discussion

Although oncolytic virus therapy represents a promising approach for treatment of multifocal cancers, it has several limitations. In our previous studies, we reported that VSV administration via the hepatic artery in HCC tumor-bearing rats results in tumor-selective viral replication and oncolysis[27-30]; however, intratumoral virus spread and treatment efficacy is limited, highlighting the need for an improved strategy. We report a treatment modality in which oncolytic VSV therapy was significantly enhanced by coadministration with a clinically approved embolization agent, which resulted in an impressive cure rate.

In this study, we used EmboCept, a representative of the group of embolization agents known as DSM. DSM are manufactured from hydrolyzed potato starch and provide relatively transient embolization before being degraded by serum amylases.[31] Although the physical presence of DSM within tumor vessels is temporary, the effect can be long-lasting due to the formation of emboli at the arterio-capillary level, as well as hypoxia and ischemic necrosis, which prevent reperfusion of the tumor.[32,33] After first confirming in vitro that DSM do not interfere or alter the ability of VSV to replicate in or kill tumor cells, our next major concern was the ability of DSM, when administered via the hepatic artery, to effectively embolize multifocal HCC lesions in our rat model. By performing DCE-MRI with embolized and nonembolized tumor-bearing rats, we were able to confirm that DSM resulted in complete embolization of all tumors analyzed, regardless of size. Furthermore, although there was a slight delay in gadolinium uptake in the livers of embolized animals, the peak was equivalent to that in the control animals, indicating that the embolic effect was tumor-specific.

It is well documented that the peripheral border of HCC lesions close to the surrounding nonneoplastic liver tissue has a tendency to survive TAE treatment, because this area is supplied by portal blood flow and collateral

circulation. Therefore, we hypothesized that transient TAE therapy for HCC could be significantly enhanced via coadministration of oncolytic VSV. We envisioned that extensive tumor necrosis could be induced through hypoxia and ischemia–reperfusion injury secondary to transient embolization, and the remaining viable rim could then be eradicated via VSV replication. Indeed, this is exactly what we observed through immunohistochemical analysis of VSV/G, which did in fact colocalize to the viable peripheral tumor regions. Although the number of recovered infectious viral particles, as determined by TCID50 analysis, was not significantly higher in the viroembolization group compared with VSV monotherapy, we speculated that this was due to the extent of tumor necrosis, which limited the areas where the virus could replicate to the border regions where viable tumor remained.

A comparison of the in vivo efficacy of transarterial viroembolization to each monotherapy revealed that, while VSV resulted in a modest effect, and embolization with DSM caused significantly enhanced tumor response, the most striking results were achieved by viroembolization, which resulted in more than 90% tumor necrosis. Impressively, we were able to achieve 60% long-term tumor-free survival through transarterial viroembolization of multifocal HCC in our rat model. Statistical analysis indicated that a synergistic effect was derived through combination of each monotherapy. These data clearly illustrated a superior effect of the combination treatment; however, it left open questions regarding the mechanism of the additive response. Because the effects of transarterial embolization in HCC have been fairly well characterized, we chose to focus on the contribution of VSV therapy to elucidate the mechanism whereby combination therapy confers its enhanced therapeutic outcome. In particular, we investigated the roles of apoptosis, antiangiogenesis, and inflammation as potential players.

VSV causes lysis of infected tumor cells through activation of apoptotic pathways, induced by expression of the viral matrix protein.[34,35] We hypothesized that VSV localized to the viable rim of tumors following embolization could induce apoptosis in the infected cells. Terminal deoxynucleotidyl transferase-mediated dUTP nick-end labeling revealed large areas of apoptosis in tumors treated with rVSV-F, whereas there was significantly less evidence of apoptosis in the PBS and DSM groups. Furthermore, apoptosis secondary to viroembolization was, in fact, mostly confined to the outer borders of the lesions, while in tumors treated with VSV monotherapy, it appeared in seemingly random patches, mainly in the core. Together, this implicated VSV induced-apoptosis as a contributing factor in eliminating the viable tumor rim, which survived embolization.

In addition to direct tumor cell lysis, it has been shown that VSV is also responsible for indirect killing of uninfected tumor cells through inhibition of vascular perfusion within infected tumors induced by the rapid recruitment of inflammatory cells to the tumor bed.[36] Furthermore, it was demonstrated that in situ expression of the VSV M protein resulted in decreased tumor vasculature in implanted glioma tumors in a rat model.[37] While embolization is known to stimulate angiogenesis,[38] in our model, we observed a clear reduction in CD31 staining within tumors treated in combination with VSV. The anti-angiogenic effect of VSV could provide a powerful tool for improving the efficacy of TAE by preventing new vessel formation feeding the remaining viable tumor cells.

In addition to the effect of inflammation on tumor blood flow, the infiltration of inflammatory cells in virus-infected tumor has the complimentary function of killing infected and surrounding tumor cells. The recruitment of NK cells to sites of VSV-infected tumor has been demonstrated,[39] and we have reproduced this phenomenon here. NK cells represent a distinct population of cytotoxic lymphocytes that act as an integral component of the innate cellular immune response system to invading viruses, prior to the launch of the adaptive immune responses.[40] These cells function by directly killing infected cells and inducing antiviral cytokines, and can result in a bystander effect by killing neighboring uninfected cells. Interestingly, several groups have recently attempted to combine TAE with adoptive immunotherapy in the clinic, and have shown enhancement of efficacy in patients.[41,42] In addition, oncolytic virus therapy may also promote cross-presentation of released tumor antigens to CD8+ T cells, leading to a long-term antitumor effect long after the virus is cleared.[43,44] Therefore, it is possible that long-term survival in the current study may be mediated by a tumor immune response, which is elicited through viral infection and oncolysis of the HCC cells.

Although we have not yet performed a direct comparison between TACE and viroembolization, several key factors indicate that viroembolization with VSV vectors might be the more effective therapy. Whereas a recent clinical report confirmed that TACE prolongs survival,[45] a comparison of TACE versus TAE alone demonstrated no survival difference.[46] This phenomenon can be explained by the well-documented fact that many HCCs are resistant to chemotherapeutic drugs,[47,48] which would support the concept that embolization is the more important component of TACE than chemotherapy. In addition, it has also been shown that hypoxia can further contribute to drug-resistance of cancer cells.[49] Because

TAE blocks arterial blood flow to the tumor, and subsequently results in hypoxia, it would follow that the efficacy of a chemotherapeutic drug might be further limited in this scenerio. In contrast, VSV has an inherent capacity for infecting and killing hypoxic cancer cells.[50] This ability could represent a critical advantage over existing therapies in treating established tumors.

In conclusion, this study has provided conclusive data to support the concept of viroembolization therapy for multifocal HCC. This is an innovative and effective treatment modality that results in massive tumor necrosis and extensive prolongation of survival compared with VSV or DSM monotherapy. Furthermore, through combination of VSV with a transient embolization agent, we were able to achieve enhanced efficacy despite administration of virus at 10-fold lower than the maximum tolerated dose, thereby improving the therapeutic index of viral therapy. Thus, viral therapy in combination with clinically approved embolization agents has the potential for providing potent oncolytic therapy for HCC and, potentially, metastatic liver tumors in cancer patients.

Acknowledgment: We thank PharmaCept GmbH (Berlin, Germany) for generously providing the EmboCept used in the study. In addition, we thank Barbara Lindner and Marcel Lee for excellent technical support.

References

1. Parkin DM, Bray F, Ferlay J.,Pisani, P. Estimating the world cancer burden: Globocan 2000. Int J Cancer 2001;94:153-156.
2. El-Serag HB, Mason AC. Rising incidence of hepatocellular carcinoma in the United States. N Engl J Med 1999;340:745-750.
3. Befeler A, Di Bisceglie AM. Hepatocellular carcinoma: diagnosis and treatment. Gastroenterology 2002;122:1609-1619.
4. Schafer DF, Sorrell MF. Hepatocellular carcinoma. Lancet 1999;353: 1253-1257.
5. Llovet J, Burroughs A, Bruix J. Hepatocellular carcinoma. Lancet 2003; 362:1907-1917.
6. Deuffic S, Poynard T, Buffat L, Valleron A-J. Trends in primary liver cancer. Lancet 1998;351:214-215.
7. Taylor-Robinson S, Foster GR, Arora S, Hargreaves S, Thomas HC. Increase in primary liver cancer in the UK. Lancet 1997;350:1142-1143.
8. Llovet J, Fuster J, Bruix J. Intention-to-treat analysis of surgical treatment for early hepatocellular carcinoma: resection versus transplantation. HEPATOLOGY 1999;39:1434-1440.
9. Bruix J, Castells A, Bosch J, Feu F, Fuster J, Garcia-Pagan JC, et al. Surgical resection of hepatocellular carcinoma in cirrhotic patients: prognostic value of preoperative portal pressure. Gastroenterology 1996;111:1018-1022.
10. Yao F, Bass NM, Nikolai B, Davern TJ, Kerlan R, Wu V, et al. Liver transplantation for hepatocellular carcinoma: analysis of survival according to the intention-to-treat principle and dropout from the waiting list. Liver Transpl 2002;8:873-883.
11. Blum H. Hepatocellular carcinoma: therapy and prevention. World J Gastroenterol 2005;11:7391-7400.
12. Bruix J, Sala M, Llovet JM. Chemoembolization for hepatocellular carcinoma. Gastroenterology 2004;127:S179-S188.
13. Miraglia R, Pietrosi G, Maruzzelli L, Petridis I, Caruso S, Marrone G, et al. Efficacy of transcatheter embolization/chemoembolization (TAE/TACE) for the treatment of single hepatocellular carcinoma. World J Gastroenterol 2007;13:2952-2955.
14. Lein W, Ackerman NB. The blood supply of experimental liver metastases. Surgery 1970;68:334-340.
15. Anderson J, Gianturco C, Wallace S. Experimental transcatheter intraarterial infusion-occlusion chemotherapy. Invest Radiol 1981;16:496-500.
16. Tancredi T, McCuskey PA, Kan Z, Wallace S. Changes in rat liver microcirculation after experimental hepatic arterial embolization: comparison of different embolic agents. Radiology 1999;211:177-181.
17. Llovet J, Bruix J. Systematic review of randomized trials for unresectable hepatocellular carcinoma: chemoembolization improves survival. HEPATOLOGY 2003;37:429-442.
18. Chang J, Tzeng WS, Pan HB, Yang CF, Lai KH. Transcatheter arterial embolization with or without cisplatin treatment of hepatocellular carcinoma: a randomized controlled study. Cancer 1994;74:2449-2453.
19. Bruix J, Llovet JM, Castells A, Montaua X, Bru C, Ayuso MC, et al. Transarterial embolization versus symptomatic treatment in patients with advanced hepatocellular carcinoma: results of a randomized controlled trial in a single institution. HEPATOLOGY 1998;27:1578-1583.
20. Pelletier G, Ducreux M, Gay F, Luboinski M, Hagege M, Dao T, et al. Treatment of unresectable hepatocellular carcinoma with lipiodol chemoembolization: a multicenter randomized trial. J Hepatol 1998;29:129-134.
21. Camma C, Schepis F, Orlando A, Albanese M, Shahied L, Trevisani F, et al. Transarterial chemoembolization for unresectable hepatocellular carcinoma: meta-analysis of randomized controlled trials. Radiology 2002;224: 47-54.
22. Kirn D, Martuza RL, Zwiebel J. Replication-selective virotherapy for cancer: biological principles, risk management, and future directions. Nat Med 2001;7:781-787.
23. Lorence RM, Katubig BB, Reichard KW, Reyes HM, Phuangsab A, Sassetti MD, et al. Complete regression of human fibrosarcoma xenografts after local Newcastle disease virus therapy. Cancer Research 1994;54: 6017-6021.
24. Peng KW, Ahmann GJ, Pham L, Greipp PR, Cattaneo R, Russell SJ, et al. Systemic therapy of myeloma xenografts by an attenuated measles virus. Blood 2001;98:2002-2007.
25. Stojdl DF, Lichty B, Knowles S, Marius R, Atkins H, Sonenberg N, Bell, JC. Exploiting tumor-specific defects in the interferon pathway with a previously unknown oncolytic virus. Nat Med 2000;6:821-825.
26. Rose JK, Whitt MA. Rhabdoviridae: the viruses and their replication. In: Knipe DM, Howley PM, eds. Fields Virology. 4th ed. Philadelphia: Lippincott Williams & Wilkins, 2001:1221-1242.
27. Ebert O, Shinozaki K, Huang TG, Savontaus MJ, Garcia-Sastre A, Woo SLC. Oncolytic vesicular stomatitis virus for treatment of orthotopic hepatocellular carcinoma in immune-competent rats. Cancer Res 2003;63: 611-613.
28. Ebert O, Shinozaki K, Kournioti C, Park MS, Garcia-Sastre A, Woo SL, et al. Syncytia induction enhances the oncolytic potential of vesicular stomatitis virus in virotherapy for cancer. Cancer Res 2004;64:3265-3270.
29. Shinozaki K, Ebert O, Kournioti C, Tai YS, Woo SL. Oncolysis of multifocal hepatocellular carcinoma in the rat liver by hepatic artery infusion of vesicular stomatitis virus. Mol Ther 2004;9:368-376.
30. Shinozaki K, Ebert O, Woo SL. Eradication of advanced hepatocellular carcinoma in rats via repeated hepatic arterial infusions of recombinant VSV. HEPATOLOGY 2005;41:196-203.
31. Erichsen C, Bolmsjo M, Hugander A, Jonsson PE. Blockage of the hepatic-artery blood flow by biodegradable microspheres (Spherex) combined with local hyperthermia in the treatment of experimental liver tumors in rats. Clin Oncol 1985;109:38-41.
32. Wang J, Murata S, Kumazaki T. Liver microcirculation after hepatic artery embolization with degradable starch microspheres. World J Gastroenterol 2006;12:4214-4218.
33. Yoshikawa T, Kokura S, Oyamada H, Iinuma S, Nishimura S, Kaneko T, et al. Antitumor effect of ischemia-reperfusion injury induced by transient embolization. Cancer Res 1994;54:5033-5035.

34. Balachandran S, Porosnicu M, Barber GN. Oncolytic activity of vesicular stomatitis virus is effective against tumors exhibiting aberrant p53, Ras, or myc function and involves the induction of apoptosis. J Virol 2001;75: 3474-3479.
35. Kopecky SA, Willingham MC, Lyles DS. Matrix protein and another viral component contribute to induction of apoptosis in cells infected with vesicular stomatitis virus. J Virol 2001;75:12169-12181.
36. Breitbach CJ, Paterson JM, Lemay CG, Falls TJ, McGuire A, Parato KA, et al. Targeted inflammation during oncolytic virus therapy severely compromises tumor blood flow. Mol Ther 2007;15:1686-1693.
37. Zhang H, Wen YJ, Mao BY, Gong QY, Qian ZY, Wei YQ. Plasmid encoding matrix protein of vesicular stomatitis viruses as an antitumor agent inhibiting rat glioma growth in situ. Exp Oncol 2007;29:85-93.
38. Gupta S, Kobayashi S, Phongkitkarun S, Broemeling LD, Kan Z. Effect of transcatheter hepatic arterial embolization on angiogenesis in an animal model. Invest Radiol 2006;41:516-521.
39. Altomonte J, Wu L, Chen L, Meseck M, Ebert O, Garcia-Sastre A, et al. Exponential enhancement of oncolytic vesicular stomatitis virus potency by vector-mediated suppression of inflammatory responses in vivo. Mol Ther 2008;16:146-153.
40. Welsh RM. Regulation of virus infections by natural killer cells. Nat Immun Cell Growth Reg 1986;5:169-199.
41. Nakamoto Y, Mizukoshi E, Tsuji H, Sakai Y, Kitahara M, Arai K, et al. Combined therapy of transcatheter hepatic arterial embolization with intratumoral dendritic cell infusion for hepatocellular carcinoma: clinical safety. Clin Exp Immunol 2007;147:296-305.
42. Takayama T, Sekine T, Makuuchi M, Yamasaki S, Kosuge T, Yamamoto J, et al. Adoptive immunotherapy to lower postsurgical recurrence rates of hepatocellular carcinoma: a randomized trial. Lancet 2000;356:802-807.
43. Diaz R, Galivo F, Kottke T, Wongthida P, Qiao J, Thompson J, et al. Oncolytic immunovirotherapy for melanoma using vesicular stomatitis virus. Cancer Res 2007;67:2840-2848.
44. Di Paolo NC, Tuve S, Ni S, Hellstrom KE, Hellstrom I, Lieber A. Effect of adenovirus-mediated heat shock protein expression and oncolysis in combination with low-dose cyclophosphamide treatment on antitumor immune responses. Cancer Res 2006;66:960-969.
45. Llovet JM, Real MI, Montana X, Planas R, Coll S, Aponte J, et al. Barcelona Liver Cancer Group. Arterial embolisation or chemoembolisation versus symptomatic treatment in patients with unresectable hepatocellular carcinoma: a randomized controlled trial. Lancet 2002; 38:1734-1739.
46. Marelli L, Stigliano R, Triantos C, Senzolo M, Cholongitas E, Davies N, et al. Transarterial therapy for hepatocellular carcinoma: which technique is more effective? A systematic review of cohort and randomized studies. Cardiovasc Intervent Radiol 2006;30:6-25.
47. Petraccia L, Onori P, Sferra R, Lucchetta MC, Liberati G, Grassi M, et al. MDR (multidrug resistance) in hepatocarcinoma clinical-therapeutic implications. Clin Ter 2003;154:325-335.
48. Nies AT, Konig J, Pfannschmidt M, Klar E, Hofmann WJ, Keppler D. Expression of the multidrug resistance proteins MRP2 and MRP3 in human hepatocellular carcinoma. Int J Cancer 2001;94:492-499.
49. Wu XZ, Xie GR, Chen D. Hypoxia and hepatocellular carcinoma: the therapeutic target for hepatocellular carcinoma. J Gastroenterol Hepatol 2007;22:1178-1182.
50. Connor JH, Naczki, Koumenis C, Lyles DS. Replication and cytopathic effect of oncolytic vesicular stomatitis virus in hypoxic tumor cells in vitro and in vivo. J Virol 2004;78:8960-8970.

Engineered Newcastle Disease Virus as an Improved Oncolytic Agent Against Hepatocellular Carcinoma

Jennifer Altomonte[1], Sabrina Marozin[1], Roland M Schmid[1] and Oliver Ebert[1]

[1]*II. Medizinische Klinik und Poliklinik, Klinikum rechts der Isar, Technical University of Munich, Munich, Germany*

Newcastle disease virus (NDV) is an intrinsically tumor-specific virus, which is currently under investigation as a clinical oncolytic agent. Several clinical trials have reported NDV to be a safe and effective agent for cancer therapy; however, there remains a clear need for improvement in therapeutic outcome. The endogenous NDV fusion (F) protein directs membrane fusion, which is required for virus entry and cell–cell fusion. Here, we report a novel NDV vector harboring an L289A mutation within the *F* gene, which resulted in enhanced fusion and cytotoxicity of hepatocellular carcinoma (HCC) cells *in vitro*, as compared with the rNDV/F3aa control virus. *In vivo* administration of the recombinant vector, termed rNDV/F3aa(L289A), via hepatic arterial infusion in immune-competent Buffalo rats bearing multifocal, orthotopic liver tumors resulted in tumor-specific syncytia formation and necrosis, with no evidence of toxicity to the neighboring hepatic parenchyma. Furthermore, the improved oncolysis conferred by the L289A mutation translated to significantly prolonged survival compared with control NDV. Taken together, rNDV/F(L289A) represents a safe, yet more effective vector than wild-type NDV for the treatment of HCC, making it an ideal candidate for clinical application in HCC patients.

Received 28 April 2009; accepted 9 September 2009; published online 6 October 2009. doi:10.1038/mt.2009.231

INTRODUCTION

Hepatocellular carcinoma (HCC) represents a major worldwide health concern, ranking among the top five most prevalent malignancies.[1] The incidence of HCC has more than doubled over the past two decades,[2,3] and epidemiological trends suggest that the rate of HCC diagnoses will continue to rise, presumably as a consequence of an ever-increasing prevalence of hepatitis B and C virus infection and increased alcohol consumption in most industrialized countries.[4,5] However, despite incremental advances in treatment, the outcome for HCC patients has not changed significantly. Although surgical resection and liver transplantation are considered to be curative, the majority of HCC cases are detected at an advanced stage, at which time the treatment options are extremely limited.[6,7]

Oncolytic viruses, which inherently replicate selectively within tumor cells, provide an attractive new tool for cancer therapy. A number of RNA viruses, including reovirus, Newcastle disease virus (NDV), measles virus, and vesicular stomatitis virus (VSV), are members of this novel class of viruses currently being exploited as potential oncolytic agents.[8–10] NDV is a nonsegmented, negative-strand RNA virus of the *Paramyxoviridae* family, whose natural host range is limited to avian species; however, it is known to enter cells by binding to sialic acid residues present on a wide range of human and rodent cancer cells.[11] NDV has been shown to selectively replicate in and destroy tumor cells, while sparing normal cells, a property believed to stem from the defective antiviral responses in tumor cells.[12,13] Normal cells, which are competent in launching an efficient antiviral response quickly after infection, are able to inhibit viral replication before cell damage can be initiated. The sensitivity of NDV to interferon (IFN), coupled with the defective IFN signaling pathways in tumor cells, provides a mechanism whereby NDV can replicate exclusively within neoplastic tissue.[14]

Due to compelling preclinical data implicating NDV as an ideal candidate for cancer therapy, phase I and II clinical trials have been initiated.[15–17] Several have successfully demonstrated that NDV is a safe and effective therapeutic agent, with no reports of pathologic effects in patients beyond conjunctivitis or mild flu-like symptoms.[18] Although the results of ongoing clinical trials are encouraging, strategies for improving the therapeutic potential of this virus are warranted, and the established system for generating modified NDV vectors through reverse-genetics has provided a unique opportunity to achieve this aim. To this end, recent reports have demonstrated the successful use of recombinant NDV vectors engineered to express various transgenes to provide improved oncolytic efficacy.[19,20]

As NDV is an enveloped virus, it initiates infection through attachment to susceptible cells and subsequent membrane fusion, processes directed by two genomic glycoproteins: the hemagglutinin-neuraminidase (HN) attachment protein and the fusion (F) protein.[21] A recombinant NDV from the strain Hitchner B1 (NDV/B1), expressing a modified F protein with a multibasic cleavage and activation site (rNDV/F3aa), is reported to be highly fusogenic and efficient in tumor-cell killing through formation of large multinucleated cells called syncytia.[19,22] Though impressive, it has further been demonstrated that a single amino acid substitution from alanine to leucine at amino acid 289 (L289A) in the F protein, results in even greater syncytial formation.[23] In addition to providing the ability to promote fusion in the absence of the viral HN protein, the L289A-modified F protein demonstrates 50–70% augmented fusogenicity in HN-dependent fusion

Correspondence: *Oliver Ebert, II. Medizinische Klinik und Poliklinik, Klinikum rechts der Isar, Technical University of Munich, Trogerstrasse 32, 81675 Munich, Germany. E-mail: oliver.ebert@lrz.tum.de*

over wild-type F protein.[24] We have previously demonstrated that a recombinant VSV vector expressing the NDV/F(L289A) protein successfully promotes syncytial formation, both *in vitro* and *in vivo*, and results in enhanced intratumoral viral spread and oncolysis;[25,26] however, to date, a recombinant NDV vector harboring the F(L289A) mutation has not been reported.

We hypothesized that we could enhance the promising oncolytic potential of rNDV/F3aa by engineering the F3aa protein to further maximize it fusogenic abilities. Here, we report the cloning and rescue of the modified vector, rNDV/F3aa(L289A). We demonstrate *in vitro* the superior ability of the F3aa(L289A)-modified virus to promote cell–cell fusion in human and rat HCC cell lines. We then applied the new vector *in vivo* in a preclinical rat model for HCC, by intrahepatic arterial administration in immunecompetent rats bearing multifocal HCC nodules in their livers. We report tumor-specific syncytia formation, in the absence of local or systemic toxicity, which translated to a significant prolongation of survival over buffer- and F3aa control virus-treated rats. These results indicate that rNDV/F3aa(L289A) represents an enhanced oncolytic virus, which could potentially be applied for clinical application for HCC in patients.

RESULTS

L289A modification does not interfere with the sensitivity of NDV to type I IFN

To determine whether the L289A modification to the fusion protein would alter the relative sensitivity of NDV/F3aa to the inhibitory effects of type I IFN, viral titers of the F3aa and F3aa(L289A) vectors were measured after pretreatment with escalating doses of universal type I IFN and compared with those of rVSV. VSV was chosen as a control for comparison purposes, due to its well-characterized sensitivity to IFN. In primary human hepatocytes (PHHs), both rVSV and the rNDV vectors demonstrated severe growth inhibition in the presence of IFN, even at the lowest dose (10 IU). Although rVSV replication was reduced by 3 logs in the presence of 1,000 IU of IFN, rNDV/F3aa and rNDV/F3aa(L289A) titers dropped 4 logs to a level below detection, and their growth patterns in the presence of each dose of IFN were nearly identical (**Figure 1**). As predicted, the inhibitory effects of IFN on viral growth were almost negligible in HCC cells, which are known to harbor defects in their IFN signaling pathways.

rNDV/F3aa(L289A) effectively induces IFN signaling in PHHs

To determine the ability of rNDV/F3aa(L289A) to induce IFN signaling, PHHs, as well as human and rat HCC cells, were subjected to reporter assays in which the firefly-luciferase reporter was driven by either the IFN-β or the IFN-stimulated response element (ISRE) promoter. Transfected cells were then stimulated with either rVSV, rNDV/F3aa, or rNDV/F3aa(L289A) or the positive controls, polyinosinic:polycytidylic acid or IFN. Although neither promoter was susceptible to viral stimulation in HCC cells, rNDV proved to be an efficient stimulator of IFN-β and ISRE promoter activity in PHHs (**Figure 2**). Importantly, the L289A-modified vector behaved similarly to the parental NDV/F3aa vector in its IFN signaling properties. In comparison, rVSV resulted in only minimal promoter induction in PHHs.

Modified F protein results in enhanced fusion of HCC cells *in vitro*

To determine whether the L289A mutation in the endogenous NDV/F3aa protein results in enhanced cell–cell fusion, we

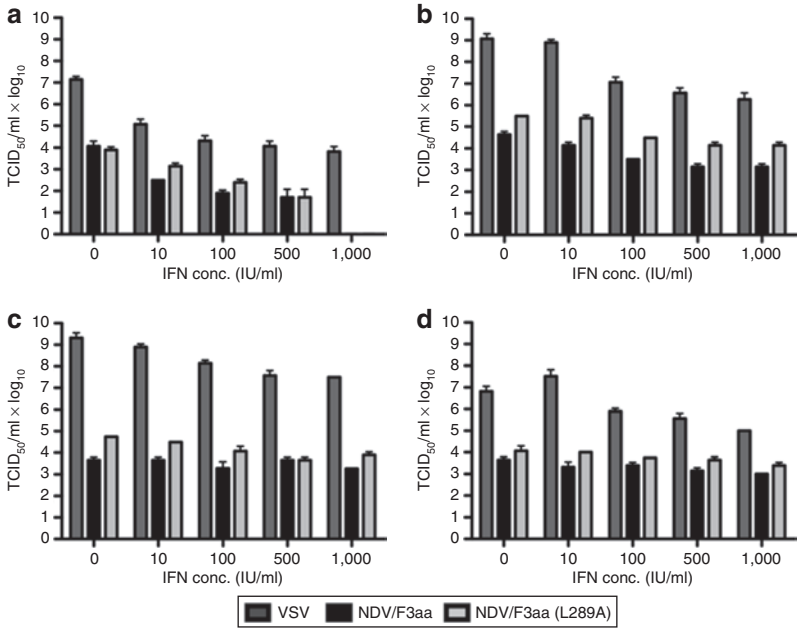

Figure 1 rNDV/F3aa(L289A) is sensitive to the inhibitory effects of interferon (IFN). (**a**) Primary human hepatocytes (PHHs), two human hepatocellular carcinoma (HCC) cell lines [(**b**) Huh7 and (**c**) HepG2], and (**d**) a rat HCC cell line (McA-RH7777) were untreated or treated overnight with increasing concentrations of universal type I interferon (IFN) (10–1,000 IU/ml) in 24-well dishes. Triplicate wells were infected with rVSV-LacZ, rNDV/F3aa, or rNDV/F3aa(L289A) at a multiplicity of infection of 1. Viral titers were determined by $TCID_{50}$ of conditioned media harvested 24 hours postinfection. Values represent the mean ± SD. NDV, Newcastle disease virus; $TCID_{50}$, 50% tissue culture infectious dose; VSV, vesicular stomatitis virus.

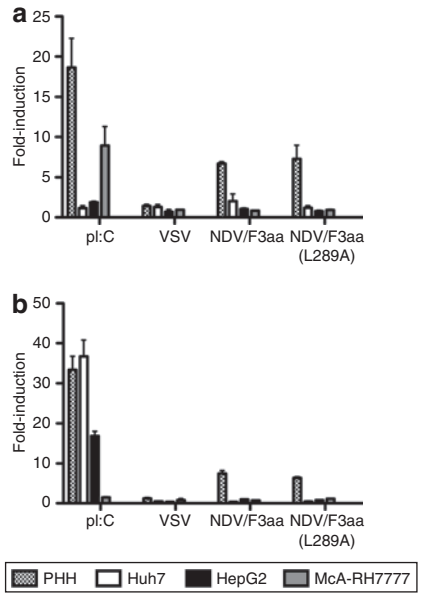

Figure 2 rNDV/F3aa(L289A) induces interferon (IFN) signaling in primary human hepatocytes (PHHs). PHHs, two human hepatocellular carcinoma (HCC) cell lines (Huh7 and HepG2), and a rat HCC cell line (McA-RH7777) were co-transfected with (**a**) pIFN-β-Luciferase or (**b**) pISRE-Luciferase and pRL-Luciferase in 24-well dishes. At 24 hours post-transfection, cells were mock-treated, stimulated with polyinosinic:polycytidylic acid (pI:C) (2.5 mg/ml) or IFN (1,000 IU/ml), or infected with rVSV-LacZ, rNDV/F3aa, or rNDV/F3aa(L289A) at a multiplicity of infection of 1.0 and incubated overnight. Firefly-luciferase activity was normalized to renilla activity to control for transfection efficiency. Fold-induction of the promoters was calculated as a function of luciferase activity in stimulated versus mock-treated cells. Data are presented as the mean ± SD of triplicate measurements. NDV, Newcastle disease virus; VSV, vesicular stomatitis virus.

evaluated the recombinant virus *in vitro*. Human and rat HCC cells were infected with either rNDV/F3aa or rNDV/F3aa(L289A) and stained for β-galactosidase (β-gal) expression to compare the fusogenicity of each virus. Although moderate β-gal expression and some evidence of fusion could be observed in cells infected with rNDV/F3aa, rNDV/F3aa(L289A) resulted in large syncytial formation, which seemed to originate from infection of a single cell and spread outward as infected cells fused with neighboring cells (**Figure 3a**). To quantify the hyperfusogenic potential of the modified virus, we counted the number of nuclei per syncytia, and expressed the value in terms of its syncytial index. In all HCC cell lines tested, the syncytial index of rNDV/F3aa(L289A) was significantly higher than that of rNDV/F3aa (**Figure 3b**).

Hyperfusogenicity does not affect virulence of NDV in chicken embryos

NDV can be classified as highly virulent (velogenic), intermediate (mesogenic), or nonvirulent (lentogenic) based on its pathogenicity in chickens. Because modified F proteins with enhanced fusogenic features are considered to be virulence factors, it was important to determine whether the L289A mutation affected the pathogenicity classification of the virus. For this purpose, we performed a mean death time (MDT) assay in embryonated chicken eggs. Lentogenic strains, which cause asymptomatic infection in birds, are characterized by MDTs of >90 hours; mesogenic strains, causing respiratory disease in birds, have MDTs between 60 and 90 hours; and velogenic strains, which cause severe disease in birds, have MDTs <60 hours. The MDTs of rNDV/F3aa and rNDV/F3aa(L289A) were both ~80 hours (81 and 79.2 hours, respectively), indicating that they are both mesogenic strains, and

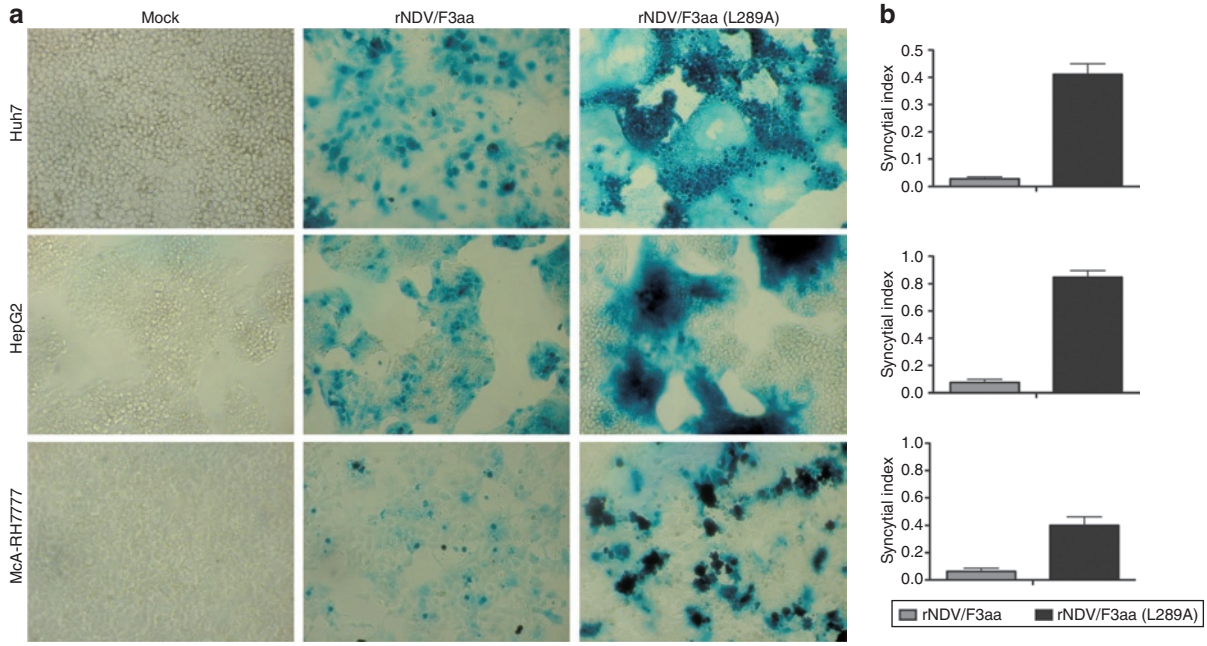

Figure 3 F(L289A) modification results in enhanced fusogenic activity of Newcastle disease virus (NDV). Human (Huh7 and HepG2) and rat (McA-RH7777) cells were mock infected or infected with rNDV/F3aa or rNDV/F3aa(L289A) at a multiplicity of infection of 0.1. At 48 hours postinfection, cells (**a**) were stained for β-gal expression or (**b**) analyzed for syncytial index. The syncytial index was calculated as the number of nuclei per syncytia divided by the number of nuclei per field of view. Each cell line was analyzed in triplicate, and data are expressed as the mean ± SD.

the F(L289A) mutation did not alter the pathogenicity status from that of the parental strain.

In vivo administration of rNDV results in mild and transient systemic effects

In order to assess potential toxicities associated with high-dose vector administration *in vivo*, a toxicity study was performed in Buffalo rats. Phosphate-buffered saline (PBS), rNDV/F3aa, or rNDV/F3aa(L289A) was injected by hepatic arterial infusion at a dose of 10^8 $TCID_{50}$ (50% tissue culture infectious dose), the highest dose achievable due to production limitations. For all animals, minor weight loss and dehydration were observed during the first 4 days following the surgical procedure, but these effects were quickly reversed, and body weights returned to normal by the end of the study (**Figure 4a**). Serum chemistries revealed insignificant changes in blood urea nitrogen and creatinine levels, and transient elevation of the liver enzymes, glutamic oxaloacetic transaminase and glutamic pyruvic transaminase, on day 1 after surgery; however, liver enzyme levels returned to normal by day 3 (**Figure 4b**). Taken together, we concluded that the local and systemic effects of rNDV treatment at 10^8 $TCID_{50}$/rat were similar to those resulting from PBS treatment by the same route, and therefore, this represented a safe dose.

Hyperfusogenic NDV induces significant tumor necrosis in HCC tumors in rats

To determine the oncolytic potential and tumor specificity of rNDV/F3aa(L289A) *in vivo*, rats bearing multifocal HCC tumors in their livers were infused with 10^8 $TCID_{50}$ via the hepatic artery. Animals were killed at various time points post-treatment for evaluation of tumor response to therapy. Morphometric analysis of necrotic areas revealed an increase in tumor necrosis, which peaked on day 5 after treatment (**Figure 5**). Syncytia, which are represented by giant multinucleated cells, were observed within necrotic areas and appeared exclusively in tumor tissue. Histological examination of the surrounding liver parenchyma revealed no signs of hepatotoxicity, and, in particular, there was no evidence of inflammatory cell infiltrates or syncytia formation.

Hyperfusogenic NDV replicates specifically within HCC tumors in rats

To quantify the *in vivo* replication kinetics of rNDV replication in HCC and normal liver cells, multifocal HCC-bearing rats were infused with rNDV/F3aa(L289A) through the hepatic artery, and animals were killed at various time points (30 min, 1, 3, 5, and 7 days post-treatment). Sections of liver and tumor were prepared for $TCID_{50}$ quantitation of viral contents.

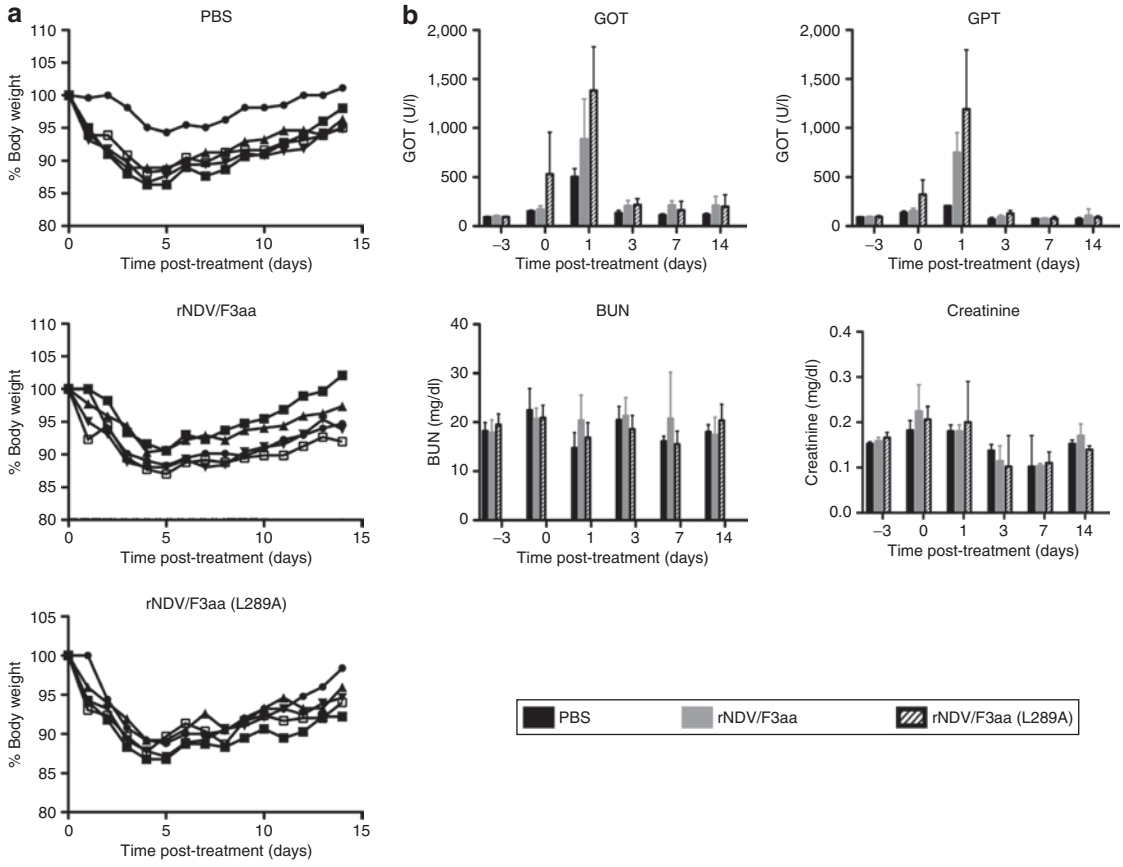

Figure 4 NDV causes transient body weight loss and elevation of liver enzymes in rats. Male non-tumor-bearing Buffalo rats were treated with PBS, or 10^8 $TCID_{50}$ of rNDV/F3aa or rNDV/F3aa(L289A) by hepatic arterial infusion ($N = 5$). (**a**) Body weight was recorded daily, and (**b**) blood was drawn at the indicated time points for measurement of serum chemistries (right panel). Values are expressed as mean ± SD. BUN, blood urea nitrogen; GOT, glutamic oxaloacetic transaminase; GPT, glutamic pyruvic transaminase; NDV, Newcastle disease virus; PBS, phosphate-buffered saline; $TCID_{50}$, 50% tissue culture infectious dose.

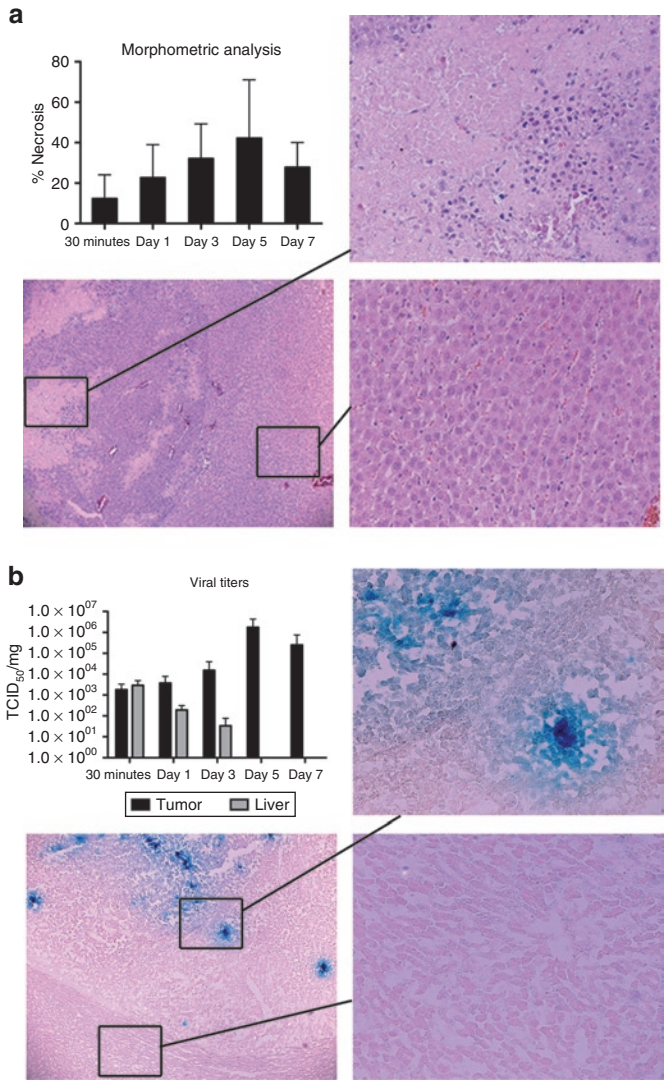

Figure 5 NDV/F3aa(L289A) treatment results in tumor-specific necrosis and virus replication in hepatocellular carcinoma (HCC)–bearing rats. Male Buffalo rats bearing multifocal orthotopic HCC nodules were treated with rNDV/F3aa(L289A) (10^8 $TCID_{50}$) by hepatic arterial infusion, and killed at the indicated time points post-treatment ($n = 3$). (**a**) Tumor-containing liver sections were subjected to hematoxylin and eosin staining and analyzed for tumor necrosis and liver toxicity. Representative sections are shown at ×5 (overview) and ×20 (magnification of tumor and liver sections) magnification. Morphometric analysis of tumor necrosis was performed using ImageJ software (National Institutes of Health), and is shown as the mean ± standard deviation at each time point. (**b**) Tumor-containing liver sections were subjected to β-gal staining. Representative sections are shown at ×5 (overview) and ×20 (magnification of tumor and liver sections) magnification. Viral titers were quantified by $TCID_{50}$ analysis of liver and tumor lysate, and are expressed as the mean ± SD. NDV, Newcastle disease virus; $TCID_{50}$, 50% tissue culture infectious dose.

Although NDV titers steadily increased within tumor tissue, with a peak in replication on day 5, the virus was rapidly cleared from the surrounding liver parenchyma to levels below detection by day 5 (**Figure 5b**). Similarly, β-gal staining of liver and tumor sections revealed multiple foci of LacZ-postive cells within tumors, whereas no positive staining was observed in the surrounding liver.

Transarterial infusion of rNDV/F3aa(L289A) results in immune cell accumulation in HCC tumors

To determine the immune cell response to NDV therapy of HCC, tumor and liver sections from multifocal tumor-bearing rats were treated with rNDV/F3aa(L289A), and killed at various time points post-treatment. Tumor-containing liver sections were prepared for immunohistochemical staining of various immune cell types. Sections were stained for natural killer (NK) cells with anti-ANK61, neutrophils by antimyeloperoxidase, pan-T cells by anti-OX-52, and macrophages by anti-ED1. Although no significant changes in pan-T cell and macrophage infiltration was observed (data not shown), quantification of marker-positive cells using ImageJ software (NIH, Bethesda, MD) revealed a significant accumulation of NK ($P < 0.0001$) and myeloperoxidase positive cells ($P = 0.04$), which peaked on days 5 and 7, respectively, post-treatment (**Figure 6**).

Hyperfusogenic NDV results in a survival prolongation in multifocal HCC-bearing rats

Although the short-term effects of rNDV/F3aa(L289A) indicated an oncolytic effect in our HCC model, it remained to be seen whether or not this would translate to a prolongation in survival. To answer this question, rats harboring multifocal HCC lesions in their livers were randomly assigned to be treated with PBS, rNDV/F3aa, or rNDV/F3aa(L289A) by hepatic arterial infusion (**Figure 7**). PBS-treated rats began to succumb to tumor progression at 22 days after treatment, and all had expired by day 37 (median survival: 32 days). In contrast, animals treated with rNDV/F3aa survived for up to 57 days, with a median survival of 36.5 days, which was a significant prolongation over PBS treatment ($P = 0.0135$). However, rNDV/F3aa(L289A) treatment further extended the median survival time to 44 days, which represents a 20% prolongation compared with rNDV/F3aa treatment. Therein, superior oncolytic effects of the hyperfusogenic virus compared to the parental rNDV/F3aa vector translated into a significant survival advantage for rats bearing HCC ($P = 0.0377$). Furthermore, two animals from the rNDV/F3aa(L289A) treatment group enjoyed long-term tumor-free survival. These rats were killed on day 150 for examination of liver pathology. Macroscopically, there was no visible indication of tumor within the liver or elsewhere, and no histological evidence of residual tumor cells or liver abnormality was observed. These results indicate that even large multifocal lesions (up to 10 mm in diameter at the time of treatment) had undergone complete remission in these animals, which translated into long-term and tumor-free survival.

DISCUSSION

Our previous work has focused on the characterization and development of VSV vectors for the treatment of HCC in an orthotopic, immune-competent rat model. Although these studies produced encouraging results, we were intrigued by the possibility of establishing a second oncolytic virus system in our model. NDV represented an attractive vector because naturally occurring strains have been applied for clinical application as oncolytic agents for several decades, and the outcomes of phase I and II clinical trials have been positive. Despite this fact, further development of NDV vectors is necessary for optimal antitumor efficacy, affording us

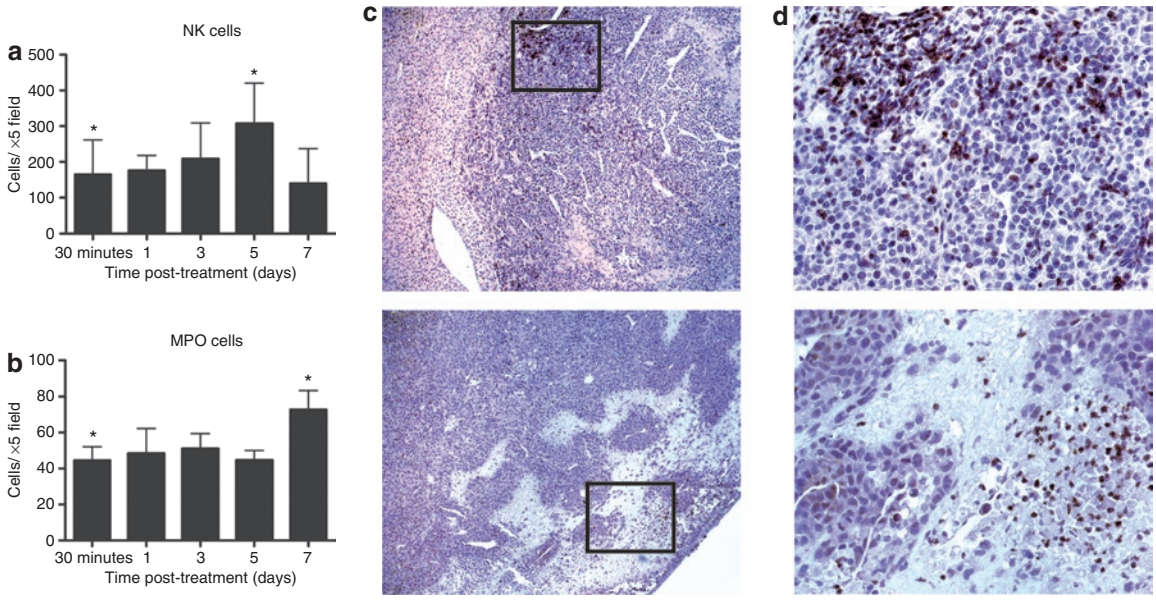

Figure 6 Infiltration of natural killer (NK) and myeloperoxidase (MPO) cells to NDV/F3aa(L289A) infected hepatocellular carcinoma (HCC) tumors. Rats bearing multifocal HCC lesions were treated by transarterial infusion of NDV/F3aa(L289A) and killed at 30 minutes, and day 1, 3, 5, and 7 after treatment. Tumor-containing liver sections were processed for immunohistochemical staining for (**a**) NK cell marker and (**b**) MPO. Positive stained cells were quantified using ImageJ software (NIH), and the mean ± SD are shown. Representative immunohistochemical sections are presented in (**c**) ×5 and (**d**) ×20 magnification. NDV, Newcastle disease virus.

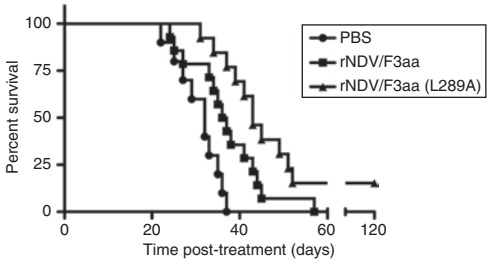

Figure 7 rNDV/F3aa(L289A) therapy results in significant survival prolongation hepatocellular carcinoma (HCC)–bearing rats. Male Buffalo rats bearing multifocal HCC lesions were treated by hepatic arterial infusion of phosphate-buffered saline (PBS) (n = 10), rNDV/F3aa (n = 14), or rNDV/F3aa(L289A) (n = 13) and followed for survival. Animals were monitored daily, and survival was plotted as a Kaplan–Meier survival curve. P values for PBS versus rNDV/F3aa is <0.02, for rNDV/F3aa versus rNDV/F3aa(L289A) is <0.04. Statistical significance was determined by log-rank test. NDV, Newcastle disease virus.

the opportunity to define the oncolytic potential of NDV in our model, while simultaneously enhancing it.

It has previously been demonstrated that the construction of a recombinant NDV vector based on the attenuated (lentogenic) Hitchner B1 strain, with a modified F protein (rNDV/F3aa), resulted in syncytia formation in tumor cells and an improved therapeutic response compared to that of rNDV/B1 in immunocompetent tumor-bearing mice.[19] The F protein is formed from a precursor, F_0, which is not capable of fusogenic activity before cleavage into functional disulfide-linked F1 and F2 polypeptides. The F protein cleavage sequences are recognized by distinct cellular proteases, and the F_0 proteins from lentogenic viruses can only be cleaved by trypsin-like proteases found in the respiratory and intestinal tracts of birds.[27] In contrast, the F3aa modification of the cleavage site into a polybasic amino acid sequence allows the protein to be cleaved by intracellular proteases, thereby permitting the virus to enter a wide range of cells more effectively and form syncytia in the absence of exogenous proteases.[28] Importantly, although the cleavage site of the NDV F protein has been postulated to be a major determinant of virulence,[29] the F3aa modification only moderately upgraded the virulence classification from lentogenic to intermediate (mesogenic) in embryonated chicken eggs, based on the MDT assay.[30] Because this F3aa-modified vector has already demonstrated antitumor efficacy in several cancer models,[19,31] we chose the rNDV/F3aa vector as the basis for additional modifications to further enhance the oncolytic potential.

It has previously been demonstrated that a single amino acid substitution in the F protein (L289A) alters the requirement for NDV HN in the promotion of fusion.[23] NDV F carrying this substitution is capable of promoting a significant level of syncytial formation in some cell types in the absence of HN. In addition, when F(L289A) is expressed in the presence of HN protein, syncytial formation is greatly enhanced compared to that observed when the wild-type F is applied.[24] We have previously exploited the unique features of the F(L289A) mutation to create a fusogenic rVSV expressing the exogenous NDV/F(L289) gene. We demonstrated that this novel vector was competent in forming syncytia in tumor cells *in vitro* and enhanced the spread and oncolysis of VSV in an immune-competent rat model of HCC, while maintaining its tumor specificity and introducing no indication of additional toxicity.[25] Although the superior fusogenic features of NDV/F(L289A) had been well characterized through the use of expression vectors and an exogenous virus (VSV), to date there have been no published reports of an rNDV vector engineered to encode the L289A mutation in its endogenous F protein.

We hypothesized that the incorporation of the L289A mutation into the rNDV/F3aa vector would result in an enhanced

oncolytic agent, which could spread easily throughout the tumor mass via cell–cell fusion and result in significant tumor necrosis and survival prolongation in an animal model of cancer. To this end, we cloned and rescued the recombinant vector, rNDV/F3aa(L289A).

The acute sensitivity of NDV to the antiviral effects of IFN has been proposed as the potential mechanism underlying the tumor selectivity of NDV replication,[32] as multiple defects in IFN signaling are known to be manifest in malignant transformation.[33] In particular, primary HCC and HCC cell lines are known to harbor defects in their IFN induction[33] and response pathways.[34] Therefore, it was critical to rule out the possibility that the L289A modification could inadvertently alter IFN signaling in infected cells or inhibit the intrinsic sensitivity of NDV to IFN-mediated protection of nontumor cells. Indeed, pretreatment of PHH resulted in a striking reduction in NDV/F3aa(L289A) titers. These results were comparable to those observed with NDV/F3aa and VSV, whose marked sensitivity to IFN has been extensively characterized by us and others.[10,34] Using luciferase reporter genes driven by the IFN-β and ISRE promoters, we similarly demonstrated that NDV/F3aa(L289A) is a competent stimulator of IFN induction and response, respectively, in PHH, while causing no appreciable induction in HCC cells. In contrast, VSV resulted in a quite modest induction of IFN signaling, indicating that NDV could potentially possess a more powerful mechanism for tumor specificity, thereby providing a benefit over VSV as the optimal oncolytic agent.

Based on *in vitro* characterization of syncytial formation, which demonstrated a striking enhancement of fusion promoted by the F(L289A)-modified vector compared to the wild-type F vector, we were encouraged to compare the two vectors *in vivo* to determine whether or not these results would translate into a difference in therapeutic outcome. Because we have extensively characterized the effects of oncolytic VSV therapy in our preclinical rat model of HCC, we chose to utilize the same model in our NDV studies to allow an indirect comparison of the two vector systems.

Hepatic arterial infusion of rNDV/F3aa(L289A) at the highest obtainable dose yielded no appreciable signs of toxicity, and histological and immunohistochemical analyses revealed syncytial formation, necrosis, and NDV-mediated LacZ expression exclusively within tumors, whereas none could be detected in the surrounding liver. Quantification of infectious NDV particles within liver and tumor tissue demonstrated tumor-specific viral replication, with viral titers falling below the level of detection in normal liver by day 5 post-treatment. Finally, Kaplan–Meier survival curve analysis demonstrated a significant survival benefit conferred by rNDV/F3aa(L289A) treatment compared with rNDV/F3aa or PBS. These results are comparable to the survival prolongation we achieved through VSV treatment in this HCC model,[25,35] and it will be interesting to compare these two vector systems side by side in future studies.

The establishment of two independent oncolytic viruses providing effective therapy to a single tumor model provides the unique opportunity to administer combination viral therapy for an additive, or potentially synergistic effect through a "prime-boost" approach for induction of a robust antitumor immune response. In addition, neutralizing antiviral antibodies begin circulating several days after viral administration, thereby significantly limiting the efficacy of readministration of the same virus. The potential to administer an adjuvant treatment at a later time point using a heterologous virus would provide a novel strategy to circumvent this obstacle to *in vivo* viral therapy.

The significant survival benefit of the hyperfusogenic NDV vector may be attributable to several factors. The process of syncytial formation is known to enhance oncolysis through a phenomenon known as the "bystander effect".[36] This effect involves the recruitment of adjacent nontransduced cells into the growing syncytium, thereby amplifying the degree of cell killing exponentially compared to that achieved by nonfusogenic viruses. In this regard, enhancement of the fusogenic capacity of a virus would provide an enormous oncolytic advantage in spread throughout the tumor mass, which is a major obstacle limiting the effectiveness of conventional oncolytic viral therapy *in vivo*.[37,38] Furthermore, cancer cell death through viral-mediated syncytia formation results in tumor necrosis, a process believed to lead to highly efficient immune activation and potentially potent antitumor responses.[39] In fact, we observed a statistically significant accumulation of NK cells and neutrophils following local transarterial infusion of rNDV/F3aa(L289A) to HCC. Natural killer cells are a major component of the innate immune system, and act as a first line of defense against invading pathogens and viruses before the launch of the adaptive immune responses.[40,41] NK cells represent a distinct population of cytotoxic lymphocytes characterized by the $CD16^+$ and/or $CD56^+$ phenotype, and they mediate direct lysis of target cells by releasing cytotoxic granules containing lytic enzymes, or by binding to apoptosis-inducing receptors on the target cell.[42] Furthermore, NK cells play an important role in adaptive antitumor immunity by mediating tumor antigen-specific crosspriming of T cells by plasmacytoid dendritic cells.[43] Our observation of NK cell accumulation following NDV infection is in line with published data describing the direct activation of NK cells by NDV-infected tumor cells, and the subsequent induction of the effector lymphokines, γ-IFN and tumor necrosis factor α.[44] Therefore, the superior oncolytic effect of hypofusogenic rNDV/F(L289A) may be the combined result of enhanced killing of bystander cell coupled with augmented antitumor immunity.

It is noteworthy to mention the potential safety concerns raised by the concept of uncontrolled viral-mediated syncytia induction. Although modifications to the F protein have been correlated to changes in virulence, a MDT assay in embryonated chicken eggs demonstrated that the F(L289A) mutation did not alter the virulence classification from that of the parental mesogenic Hitchner B1/F3aa strain. Moreover, the F modification did not alter the ability of the virus to elicit an innate IFN response in normal cells, nor did it interfere with the intrinsic IFN sensitivity of NDV, which is important for maintenance of tumor specificity. Indeed, hepatic arterial infusion of rNDV/F3aa(L289A) resulted in tumor-specific syncytia formation and caused no observable damage to surrounding hepatocytes or signs of systemic toxicity.

Despite the significant survival prolongation conferred by the modified F virus, most animals succumbed to relapse, indicating that additional enhancements to the treatment regimen are warranted. We previously demonstrated that VSV therapy for HCC

could be significantly improved via repeated hepatic arterial administration of the vector[45] and through coadministration with a clinically available embolization agent.[46] Therefore, it is anticipated that similar strategies applied to NDV could result in comparable benefits in therapeutic outcome. Furthermore, recent reports have described the efficacy of foreign gene insertion into the NDV genome for enhanced oncolytic response,[19,20] and the integration of therapeutic genes into the hyperfusogenic vector could exponentially improve the oncolytic potential of NDV therapy. Although it will be interesting to investigate each of these strategies, as well as to perform more detailed mechanistic studies to elucidate the means by which hyperfusogenic NDV exerts its therapeutic effects, these experiments are beyond the scope of this study. This report focuses on the preclinical characterization of rNDV/F3aa(L289A) as a safe and effective oncolytic agent for the treatment of HCC.

In conclusion, we have investigated the potential to enhance the inherent oncolytic efficacy of NDV by augmenting syncytia formation through a single amino acid substitution in the endogenous F gene. Using an orthotopic preclinical model of HCC, we determined that hepatic arterial delivery of rNDV/F3aa(L289A) results in significantly enhanced efficacy over the previously reported NDV/F3aa vector, while maintaining tumor specificity. Although naturally occurring strains of NDV have been employed in encouraging clinical studies for several decades,[47] the development of the reverse-genetics system for creating genetically engineered vectors has opened new doors for the optimization of viral agents. It remains to be seen how these modified vectors will translate into clinical application. Based on the data presented here, the F3aa(L289A)-modified NDV virus represents an attractive new vector for future clinical trials for HCC and, presumably, other types of cancer in the future.

MATERIALS AND METHODS

Cell lines. HepG2 and Huh7 cells were a kind gift from Ulrich Lauer (University Hospital of Tübingen). The DF1 chicken fibroblast cell line was provided by Roger Vogelmann (Klinikum rechts der Isar, Munich, Germany), and primary chicken embryo fibroblasts were obtained from Ingo Drexler (Klinikum rechts der Isar). A549, McA-RH7777, and BHK-21 cells were purchased from ATCC (Rockville, MD). HepG2, Huh7, and A549 cells were maintained in Dulbecco's modified Eagle's medium supplemented with 10% fetal bovine serum, 1% L-glutamine (200 mmol/l), 1% penicillin/streptomycin, 1% nonessential amino acids, and 1% sodium pyruvate. McA-RH7777, DF1, and chicken embryo fibroblast cells were maintained in Dulbecco's modified Eagle's medium (ATCC) supplemented with 10% fetal bovine serum and 1% penicillin/streptomycin. BHK-21 cells were cultured in Glasgow MEM BHK-21 medium (GIBCO-Invitrogen, Karlsruhe, Germany) supplemented with 10% fetal bovine serum and 1% tryptose phosphate broth. DF1 cells were maintained in a 39 °C incubator with 5% CO_2; all other cell lines were grown at 37 °C under 5% CO_2. All cell cultures were regularly tested for mycoplasma contamination.

PHHs were isolated from patients (negative for hepatitis B virus, hepatitis C virus, and human immunodeficiency virus) who underwent surgical resections of liver tumors, in accordance with the guidelines of the charitable state controlled foundation of Human Tissue and Cell Research (Regensburg, Germany).[48] PHHs were isolated from the resected nontumorous margin and maintained in culture with HepatoZYME-SFM medium (GIBCO) containing 1% L-glutamine.

Viruses. The NDV complementary DNA sequence was derived from the mesogenic Hitchner B1 strain engineered to express the modified F cleavage site (F3aa), as previously described.[30] The *LacZ* gene was inserted as an additional transcription unit into the unique *Xba*I restriction site between the *P* and *M* genes in the full-length plasmid, pT7NDV/F3aa (a kind gift from Adolfo Garcia-Sastre; Mount Sinai School of Medicine, New York, NY). To generate the recombinant NDV vector expressing the mutant F3aa(L289A) F protein, the pT7NDV/F3aa plasmid was modified by site-directed PCR mutagenesis. To this end, a long forward primer (5′-GGCTTAATCACCGGTAACCCTATTCTATACGACTCACAGACT CAA CTCTTGGGTATACAGGTAACT**GCA**CCTTCAGTCGGGAAC -3′) was designed to span amino acid 289, as well as the upstream *Age*I restriction site. The reverse primer (5′- GTCATCTACAACCGGTAGTTTTTTC TTAACTCTCCG -3′) corresponded to the noncoding region between the *F* and *HN* genes, including a second *Age*I restriction site. The nucleotides substituted in the primers to mutate the amino acid at position 289 from Leu to Ala appear in boldface, while sequences corresponding to the restriction sites are underlined. The resulting PCR fragment was then purified and digested with *Age*I, and inserted back into the full-length pT7NDV/F3aa plasmid, thereby replacing the corresponding segment of the endogenous *F* gene. Sequences of all modified plasmids were confirmed by DNA sequencing (Eurofins MWG, Ebersberg, Germany). Viruses were rescued using an established method of reverse-genetics.[49] For simplicity, the rNDV/F3aa-LacZ and rNDV/F3aa(L289A)-LacZ vectors will be referred to as rNDV/F3aa and rNDV/F3aa(L289A). The rVSV-LacZ control virus was generated as previously described.[35]

To amplify NDV stocks, 10 day-old embryonated pathogen-free chicken eggs were inoculated with 100 plaque-forming units of virus, and the allantoic fluid was harvested 48 hours later and pooled. The fluid was cleared by centrifugation at 1,800 *g* for 30 minutes, and then subjected to ultracentrifugation at 24,000 r.p.m. for 24 hours. The pellet was resuspended in Hanks' balanced salt solution and layered on top of a sucrose gradient ranging from 60 to 10%, and ultracentrifuged for 1 hour at 24,000 r.p.m. The band containing the virus was carefully collected with a syringe and 20 G needle, and ultracentrifuged for another hour at 24,000 r.p.m. to remove the sucrose. The pellet was resuspended in 3 ml of Hanks' balanced salt solution and aliquoted and stored at −80 °C until use. Titers were determined by $TCID_{50}$ analysis in DF1 cells.

IFN sensitivity assay. PHH and HCC cell lines (HepG2, Huh7, and McA-RH7777) were seeded in 24-well dishes at a density of 5×10^5 cells/well. Monolayers were mock-treated or treated overnight with Universal type I IFN (PBL Interferon Source, Piscataway, NJ) at concentrations of 10, 100, 500, and 1,000 IU/ml. Following the pretreatment, the cells were infected with either rVSV-LacZ, rNDV/F3aa, or rNDV/F3aa(L289A) at a multiplicity of infection of 1. At 24 hours postinfection, aliquots of the conditioned media were harvested and subjected to $TCID_{50}$ determination of viral titers.

IFN-β and ISRE promoter induction assays. PHH, Huh7, HepG2, and McA-RH7777 cells were seeded in 24-well dishes at a density of 5×10^5 cells/well. Cells were transfected with a firefly-luciferase reporter plasmid driven by either the IFN-β or ISRE promoter, using Lipofectamine 2000 (Invitrogen, Carlsbad, CA) according to the manufacturer's instructions. In addition, to control for transfection efficiency, cells were co-transfected with the *Renilla reniformis* plasmid. At 24 hours post-transfection, the cells were either mock-treated, or stimulated with poly I:C (2.5 µg), universal type I IFN (500 IU), or rVSV-LacZ, rNDV/F3aa, or rNDV/F3aa(L289A) at an multiplicity of infection of 1. Following overnight incubation, cell lysates were prepared, and the luciferase activities were quantified using the Dual-Luciferase Assay system (Promega, Mannheim, Germany) with a standard luminometer (Turner Designs, Sunnyvale, CA). The relative light units of firefly-luciferase activity were normalized to the constitutively active Renilla luciferase, and presented as the fold-induction of stimulated, compared to mock-treated cells.

Quantitation of syncytium formation. Huh7, HepG2, and McA-RH7777 cells were seeded at a density of 10^6 cells/well in 6-well dishes. Upon

attachment, they were infected with rNDV/F3aa or rNDV/F3aa(L289A) at an multiplicity of infection of 0.1 in triplicate. At 48 hours postinfection, the cells were stained using the β-gal staining set (Roche, Mannheim, Germany) according to the manufacturers instructions. For a quantitative assessment, the nuclei were labeled with propidium iodide and counted. The syncytial index was calculated as the number of nuclei per syncytia divided by the otal number of nuclei per field of view.

MDT assay. The 10-day-old embryonated chicken eggs were infected with serial tenfold dilutions of viruses, with five eggs per virus dose. The eggs were incubated at 37 °C and monitored twice daily for 7 days, and the time at which the embryos were found dead was recorded. The highest dilution that killed all embryos was considered to be the minimum lethal dose. The MDT was then calculated as the mean time required for the embryos to be killed at the minimum lethal dose.

Animal studies. All procedures involving animals were approved and performed according to the guidelines of the institution's animal care and use committee, and the government of Bavaria, Germany. Six-week-old male Buffalo rats were purchased from Harlan Winkelmann (Borchen, Germany), and housed under standard conditions.

To assess the potential toxicity of rNDV vectors when administered at 10^8 $TCID_{50}$/rat, non-tumor-bearing Buffalo rats were subjected to laparotomy for preparation of the hepatic artery, whereby a 1 ml suspension of PBS, rNDV/F3aa, or rNDV/F3aa(L289A) was slowly infused. Body weights were monitored daily from 0 to 14 days post-treatment. In addition, serum was prepared from whole blood drawn on days −3, 0, 1, 3, 7, and 14 for determination of serum concentrations of glutamic oxaloacetic transaminase, glutamic pyruvic transaminase, blood urea nitrogen, and creatinine. All serum chemistry measurements were performed by the Institute for Clinical Chemistry and Pathobiochemistry (Klinikum rechts der Isar).

To establish multifocal HCC lesions within the liver, 10^7 syngeneic McA-RH7777 rat HCC cells were infused as a 1 ml suspension in serum-free Dulbecco's modified Eagle's medium through the portal vein. A second laparotomy was performed 21 days after tumor-cell implantation to screen for the development of multifocal hepatic tumors of 1–10 mm in diameter. To determine *in vivo* oncolysis, as well as the intratumoral kinetics of NDV spread, rats bearing multifocal HCC were treated with 10^8 $TCID_{50}$ rNDV/F3aa(L289A) via the hepatic artery. Five animals were randomly chosen for killing at each of the following time points: 30 min, day 1, 3, or 7. Upon killing, sections of liver and tumor were snap frozen for $TCID_{50}$ determination of intratumoral and intrahepatic viral titers or prepared for histological and immunohistochemical analyses. An additional set of tumor-bearing rats was treated with PBS ($n = 10$), rNDV/F3aa ($n = 13$), or rNDV/F3aa(L289A) ($n = 14$) and followed for survival to compare the therapeutic outcome of each treatment. The animals were monitored daily and killed at humane end points, and data were plotted as a Kaplan–Meier survival curve.

Histology and immunohistochemistry. Tissue sections containing both liver and tumor were fixed overnight in 4% paraformaldehyde and paraffin embedded. Sections of 3 µm thickness were subjected to hematoxylin–eosin staining for histological analysis, or immunohistochemically stained for myeloperoxidase (Abcam, Cambridge, UK) or the NK cell marker, ANK61 (Santa Cruz Biotechnology, Santa Cruz, CA). Positive cells were detected using the ImPRESS Universal Reagent Kit (Vector Laboratories, Burlingame, CA) and quantified using ImageJ software (NIH). Additional sections were fixed in 1% paraformaldehyde for 4 hours followed by overnight incubation in 18% sucrose. The tissue was then embedded in Tissue-Tek O.C.T. compound (Sakura Finetek USA, Torrance, CA) and frozen on dry ice. Cryostat sections of 10 µm in thickness were stained using the β-gal Staining Set (Roche) for 16 hours at 37 °C, and counterstained with eosin.

Statistical analyses. For comparison of individual data points, a two-sided Student *t*-test was applied to determine statistical significance. Survival curves were plotted according to the Kaplan–Meier method, and statistical significance between different treatment groups was determined using the log-rank test. Statistical data were obtained using GraphPad Prism 5.0 (GraphPad Software, San Diego, CA). *P* values of <0.05 were considered statistically significant.

ACKNOWLEDGMENTS

We thank Barbara Lindner for excellent technical assistance. We express our appreciation to Human Tissue and Cell Research (HTCR, Regensburg) for providing human primary hepatocytes. This work was supported in part by the German Research Aid (Max-Eder Research Program) and the Federal Ministry of Education and Research (Grant 01GU0505).

REFERENCES

1. Parkin, DM, Bray, F, Ferlay, J and Pisani, P (2001). Estimating the world cancer burden: Globocan 2000. *Int J Cancer* **94**: 153–156.
2. El-Serag, HB, Mason, AC. Rising incidence of hepatocellular carcinoma in the United States. *N Engl J Med* 1999; **340**: 745–750.
3. Dyer, Z, Peltekian, K and van Zanten, SV (2005). Review article: the changing epidemiology of hepatocellular carcinoma in Canada. *Aliment Pharmacol Ther* **22**: 17–22.
4. El-Serag, HB, Davila, JA, Petersen, NJ and McGlynn, KA (2003). The continuing increase in the incidence of hepatocellular carcinoma in the United States: an update. *Ann Intern Med* **139**: 817–823.
5. Deuffic, S, Poynard, T, Buffat, L and Valleron, AJ (1998). Trends in primary liver cancer. *Lancet* **351**: 214–215.
6. Mathurin, P, Rixe, O, Carbonell, N, Bernard, B, Cluzel, P, Bellin, MF *et al.* (1998). Review article: overview of medical treatments in unresectable hepatocellular carcinoma—an impossible meta-analysis? *Aliment Pharmacol Ther* **12**: 111–126.
7. Llovet, JM, Burroughs, A and Bruix, J (2003). Hepatocellular carcinoma. *Lancet* **362**: 1907–1917.
8. Lorence, RM, Katubig, BB, Reichard, KW, Reyes, HM, Phuangsab, A, Sassetti, MD *et al.* (1994). Complete regression of human fibrosarcoma xenografts after local Newcastle disease virus therapy. *Cancer Res* **54**: 6017–6021.
9. Peng, KW, Ahmann, GJ, Pham, L, Greipp, PR, Cattaneo, R and Russell, SJ (2001). Systemic therapy of myeloma xenografts by an attenuated measles virus. *Blood* **98**: 2002–2007.
10. Stojdl, DF, Lichty, B, Knowles, S, Marius, R, Atkins, H, Sonenberg, N *et al.* (2000). Exploiting tumor-specific defects in the interferon pathway with a previously unknown oncolytic virus. *Nat Med* **6**: 821–825.
11. Reichard, KW, Lorence, RM, Cascino, CJ, Peeples, ME, Walter, RJ, Fernando, MB *et al.* (1992). Newcastle disease virus selectively kills human tumor cells. *J Surg Res* **52**: 448–453.
12. Balachandran, S, Barber, GN. Vesicular stomatitis virus (VSV) therapy of tumors. *IUBMB Life* 2000;**50**: 135–138.
13. Stojdl, DF, Lichty, BD, tenOever, BR, Paterson, JM, Power, AT, Knowles, S *et al.* (2003). VSV strains with defects in their ability to shutdown innate immunity are potent systemic anti-cancer agents. *Cancer Cell* **4**: 263–275.
14. Park, MS, García-Sastre, A, Cros, JF, Basler, CF and Palese, P (2003). Newcastle disease virus V protein is a determinant of host range restriction. *J Virol* **77**: 9522–9532.
15. Hotte, SJ, Lorence, RM, Hirte, HW, Polawski, SR, Bamat, MK, O'Neil, JD *et al.* (2007). An optimized clinical regimen for the oncolytic virus PV701. *Clin Cancer Res* **13**: 977–985.
16. Freeman, AI, Zakay-Rones, Z, Gomori, JM, Linetsky, E, Rasooly, L, Greenbaum, E *et al.* (2006). Phase I/II trial of intravenous NDV-HUJ oncolytic virus in recurrent glioblastoma multiforme. *Mol Ther* **13**: 221–228.
17. Csatary, LK, Gosztonyi, G, Szeberenyi, J, Fabian, Z, Liszka, V, Bodey, B *et al.* (2004). MTH-68/H oncolytic viral treatment in human high-grade gliomas. *J Neurooncol* **67**: 83–93.
18. Nemunaitis, J (2002). Live viruses in cancer treatment. *Oncology (Williston Park, NY)* **16**: 1483–1492; discussion 1495.
19. Vigil, A, Park, MS, Martinez, O, Chua, MA, Xiao, S, Cros, JF *et al.* (2007). Use of reverse genetics to enhance the oncolytic properties of Newcastle disease virus. *Cancer Res* **67**: 8285–8292.
20. Janke, M, Peeters, B, de Leeuw, O, Moorman, R, Arnold, A, Fournier, P *et al.* (2007). Recombinant Newcastle disease virus (NDV) with inserted gene coding for GM-CSF as a new vector for cancer immunogene therapy. *Gene Ther* **14**: 1639–1649.
21. Lamb, RA (1993). Paramyxovirus fusion: a hypothesis for changes. *Virology* **197**: 1–11.
22. Bateman, AR, Harrington, KJ, Kottke, T, Ahmed, A, Melcher, AA, Gough, MJ *et al.* (2002). Viral fusogenic membrane glycoproteins kill solid tumor cells by nonapoptotic mechanisms that promote cross presentation of tumor antigens by dendritic cells. *Cancer Res* **62**: 6566–6578.
23. Sergel, TA, McGinnes, LW and Morrison, TG (2000). A single amino acid change in the Newcastle disease virus fusion protein alters the requirement for HN protein in fusion. *J Virol* **74**: 5101–5107.
24. Li, J, Melanson, VR, Mirza, AM and Iorio, RM (2005). Decreased dependence on receptor recognition for the fusion promotion activity of L289A-mutated Newcastle disease virus fusion protein correlates with a monoclonal antibody-detected conformational change. *J Virol* **79**: 1180–1190.
25. Ebert, O, Shinozaki, K, Kournioti, C, Park, MS, García-Sastre, A and Woo, SL (2004). Syncytia induction enhances the oncolytic potential of vesicular stomatitis virus in virotherapy for cancer. *Cancer Res* **64**: 3265–3270.

26. Shin, EJ, Chang, JI, Choi, B, Wanna, G, Ebert, O, Genden, EM *et al.* (2007). Fusogenic vesicular stomatitis virus for the treatment of head and neck squamous carcinomas. *Otolaryngol Head Neck Surg* **136**: 811–817.
27. Sakaguchi, T, Matsuda, Y, Kiyokage, R, Kawahara, N, Kiyotani, K, Katunuma, N *et al.* (1991). Identification of endoprotease activity in the trans Golgi membranes of rat liver cells that specifically processes *in vitro* the fusion glycoprotein precursor of virulent Newcastle disease virus. *Virology* **184**: 504–512.
28. Peeters, BP, de Leeuw, OS, Koch, G and Gielkens, AL (1999). Rescue of Newcastle disease virus from cloned cDNA: evidence that cleavability of the fusion protein is a major determinant for virulence. *J Virol* **73**: 5001–5009.
29. de Leeuw, OS, Hartog, L, Koch, G and Peeters, BP (2003). Effect of fusion protein cleavage site mutations on virulence of Newcastle disease virus: non-virulent cleavage site mutants revert to virulence after one passage in chicken brain. *J Gen Virol* **84**: 475–484.
30. Park, MS, Steel, J, García-Sastre, A, Swayne, D and Palese, P (2006). Engineered viral vaccine constructs with dual specificity: avian influenza and Newcastle disease. *Proc Natl Acad Sci USA* **103**: 8203–8208.
31. Zamarin, D, Vigil, A, Kelly, K, García-Sastre, A and Fong, Y (2009). Genetically engineered Newcastle disease virus for malignant melanoma therapy. *Gene Ther* **16**: 796–804.
32. Krishnamurthy, S, Takimoto, T, Scroggs, RA and Portner, A (2006). Differentially regulated interferon response determines the outcome of Newcastle disease virus infection in normal and tumor cell lines. *J Virol* **80**: 5145–5155.
33. Keskinen, P, Nyqvist, M, Sareneva, T, Pirhonen, J, Melén, K and Julkunen, I (1999). Impaired antiviral response in human hepatoma cells. *Virology* **263**: 364–375.
34. Marozin, S, Altomonte, J, Stadler, F, Thasler, WE, Schmid, RM and Ebert, O (2008). Inhibition of the IFN-beta response in hepatocellular carcinoma by alternative spliced isoform of IFN regulatory factor-3. *Mol Ther* **16**: 1789–1797.
35. Shinozaki, K, Ebert, O, Kournioti, C, Tai, YS and Woo, SL (2004). Oncolysis of multifocal hepatocellular carcinoma in the rat liver by hepatic artery infusion of vesicular stomatitis virus. *Mol Ther* **9**: 368–376.
36. Bateman, A, Bullough, F, Murphy, S, Emiliusen, L, Lavillette, D, Cosset, FL *et al.* (2000). Fusogenic membrane glycoproteins as a novel class of genes for the local and immune-mediated control of tumor growth. *Cancer Res* **60**: 1492–1497.
37. Yun, CO (2008). Overcoming the extracellular matrix barrier to improve intratumoral spread and therapeutic potential of oncolytic virotherapy. *Curr Opin Mol Ther* **10**: 356–361.
38. Heise, CC, Williams, A, Olesch, J and Kirn, DH (1999). Efficacy of a replication-competent adenovirus (ONYX-015) following intratumoral injection: intratumoral spread and distribution effects. *Cancer Gene Ther* **6**: 499–504.
39. Melcher, A, Todryk, S, Hardwick, N, Ford, M, Jacobson, M and Vile, RG (1998). Tumor immunogenicity is determined by the mechanism of cell death via induction of heat shock protein expression. *Nat Med* **4**: 581–587.
40. Welsh, RM (1986). Regulation of virus infections by natural killer cells. A review. *Nat Immun Cell Growth Regul* **5**: 169–199.
41. Brutkiewicz, RR and Welsh, RM (1995). Major histocompatibility complex class I antigens and the control of viral infections by natural killer cells. *J Virol* **69**: 3967–3971.
42. Orange, JS, Fassett, MS, Koopman, LA, Boyson, JE and Strominger, JL (2002). Viral evasion of natural killer cells. *Nat Immunol* **3**: 1006–1012.
43. Liu, C, Lou, Y, Lizée, G, Qin, H, Liu, S, Rabinovich, B *et al.* (2008). Plasmacytoid dendritic cells induce NK cell-dependent, tumor antigen-specific T cell cross-priming and tumor regression in mice. *J Clin Invest* **118**: 1165–1175.
44. Jarahian, M, Watzl, C, Fournier, P, Arnold, A, Djandji, D, Zahedi, S *et al.* (2009). Activation of natural killer cells by Newcastle disease virus hemagglutinin-neuraminidase. *J Virol* **83**: 8108–8121.
45. Shinozaki, K, Ebert, O and Woo, SL (2005). Eradication of advanced hepatocellular carcinoma in rats via repeated hepatic arterial infusions of recombinant VSV. *Hepatology* **41**: 196–203.
46. Altomonte, J, Braren, R, Schulz, S, Marozin, S, Rummeny, EJ, Schmid, RM *et al.* (2008). Synergistic antitumor effects of transarterial viroembolization for multifocal hepatocellular carcinoma in rats. *Hepatology* **48**: 1864–1873.
47. Cassel, WA and Garrett, RE (1965). Newcastle disease virus as an Antineoplastic Agent. *Cancer* **18**: 863–868.
48. Thasler, WE, Weiss, TS, Schillhorn, K, Stoll, PT, Irrgang, B and Jauch, KW (2003). Charitable State-Controlled Foundation Human Tissue and Cell Research: Ethic and Legal Aspects in the Supply of Surgically Removed Human Tissue For Research in the Academic and Commercial Sector in Germany. *Cell Tissue Bank* **4**: 49–56.
49. Nakaya, T, Cros, J, Park, MS, Nakaya, Y, Zheng, H, Sagrera, A *et al.* (2001). Recombinant Newcastle disease virus as a vaccine vector. *J Virol* **75**: 11868–11873.

Inhibition of the IFN-β Response in Hepatocellular Carcinoma by Alternative Spliced Isoform of IFN Regulatory Factor-3

Sabrina Marozin[1], Jennifer Altomonte[1], Florian Stadler[2], Wolfgang E Thasler[2], Roland M Schmid[1] and Oliver Ebert[1]

[1]II. Medizinische Klinik und Poliklinik, Klinikum rechts der Isar, Technical University of Munich, Munich, Germany; [2]Chirurgische Klinik und Poliklinik, Klinikum Großhadern, University of Munich, Munich, Germany

The intrinsic oncolytic specificity of vesicular stomatitis virus (VSV) is currently being exploited to develop alternative therapeutic strategies for hepatocellular carcinoma (HCC). We have observed earlier that, in contrast to cultured human HCC cells, primary human hepatocytes (PHHs) are refractory to VSV infection. Impairment of the type I interferon (IFN) pathway in HCC cells has been suggested to be the mechanism by which these cells become susceptible to VSV infection. The goal of this study was to elucidate the nature of the IFN defect in human HCC. We demonstrate here that the defect in IFN-β signaling in HCC cells results from a deregulated IFN regulatory factor-3 (IRF3) pathway. Expression of IRF3-spliced variant (IRF3-nirs3) was constitutively observed in HCC cells and, importantly, also in primary HCC samples. In contrast, IRF3 was readily activated in PHHs after stimulation with dsRNA or infection with VSV. In addition, overexpression of IRF3-nirs3 significantly abrogated the IFN-β response to VSV infection and improved viral growth. Our data provide evidence that aberrant splicing of IRF3 in HCC contributes to the defect in IFN-mediated antiviral defenses. This work may provide a potential molecular basis for selecting HCC patients for oncolytic VSV therapy in future clinical trials.

Received 18 June 2008; accepted 19 August 2008; published online 9 September 2008. doi:10.1038/mt.2008.201

INTRODUCTION

Hepatocellular carcinoma (HCC) accounts for the majority of primary liver cancers in adults. Potentially curative therapies such as liver transplantation and surgical resection can be applied only to a small percentage of patients, and while local-regional treatments (e.g., transarterial embolization, percutaneous ethanol injection, or radiofrequency ablation) may be beneficial for some HCC patients, recurrence is frequent and the long-term survival rate remains poor.[1] Given the limited treatment options and poor prognosis, the use of oncolytic viruses, which have the intrinsic property of selectively replicating in cancer cells and killing them, has found application in preclinical studies and early clinical trials for the treatment of primary and metastatic liver cancers.[2–8]

Vesicular stomatitis virus (VSV), a nonsegmented negative strand RNA virus belonging to the Rhabdoviridae family,[9] is one such oncolytic virus. It represents a promising agent for cancer treatment because of its tumor selectivity and rapid replication in many tumor cell types, including HCC.[7,10–12] We have previously demonstrated a prolongation of survival in rats bearing advanced multifocal HCC, using transarterial infusions of VSV-derived vectors,[13,14] and the same strategy is currently under development for investigation in human patients. Our current aim is to identify the molecular mechanism through which VSV exerts its tumor specificity. If we were to expand our understanding of the differences between HCC cells and normal hepatocytes, we could potentially use this knowledge in developing optimized VSV vectors with enhanced oncolytic properties in HCC cells, while simultaneously maintaining attenuation in the normal surrounding liver tissue, thereby resulting in a wider therapeutic index.

It is known that VSV growth is quite sensitive to the actions of type I interferons (IFNs), and that the lack of an intact IFN-system in cancer cells seems to promote the susceptibility of tumor cells to VSV;[10] however, the mechanism that causes the defects in IFN signaling in tumor cells remains to be clearly characterized. Wild-type (wt) VSV does not induce a robust antiviral response in infected cells because of an early block of nuclear export of cellular RNAs.[15,16] It has been reported that the VSV matrix protein is responsible for inhibiting host gene expressions, including those of various antiviral molecules.[17,18] Methionine at position 51 is critically important for this inhibitory activity, and substitution with an arginine, as in the mutant virus VSV-M51R, enhances the ability to trigger the IFN response.[17,19] Therefore wtVSV and VSV-M51R (the former being a weak inducer of IFN while the latter results in a strong IFN response) are useful tools for studying IFN responses in different cell types.

IFNs are a group of cytokines that exert pleiotropic effects on important cell functions, including cell proliferation and modulation of the immune system.[20,21] Because of their important biological activities, IFNs find application in the treatment of several diseases, including viral infection and cancer.[22] IFN-β and/or IFN-α

Correspondence: *Oliver Ebert, II. Medizinische Klinik und Poliklinik, Klinikum rechts der Isar, Technical University of Munich, Ismaningerstr. 22, 81675 München, Germany. E-mail: oliver.ebert@lrz.tum.de*

are rapidly induced following the detection of viral nucleic acids in the cytoplasm of cells by intracellular receptors such as retinoic-acid inducible gene-1 (*RIG-I*), or after engagement of Toll-like receptors (TLRs).[23] These cellular sensors induce the activation of a latent transcriptional factor IFN regulatory factor-3 (IRF3) by TANK-binding kinase 1 (TBK1) and IκB kinase ε kinases.[24] IRF3 is a protein of 55 kDa, which is constitutively expressed in most cell types. At its N-terminus it contains a highly conserved DNA binding domain, while the C-terminal region comprises a cluster of phosphoacceptor sites. Virus-induced phosphorylation at the C-terminal domain activates dimerization and translocation of IRF3 to the nucleus where, in cooperation with AP-1 and NF-κB transcription factors, it promotes the transcriptional activation of the IFN-β promoter.[25,26] An alternative spliced isoform (IRF3a) encoded by the *IRF3* gene has been described.[27] IRF3a is ubiquitously expressed in variable ratios to IRF3 mRNA in all tissues and several cell lines, and functions as a negative regulator of IRF3-transcriptional activity.[28]

In this study, we have characterized the defect in the IFN-induction associated with malignant transformation, tracing the deficit down to the level of the IRF3 protein. We demonstrate that expression of IRF3 can efficiently restore intracellular double-stranded RNA (dsRNA)-dependent IFN-signaling in HCC cells. Further, we observed that the HCC cell lines, HepG2 and Huh-7, as well as primary HCC samples from various donors, express impressively higher levels of splicing variant IRF3-nirs3 when compared with primary human hepatocytes (PHHs). By overexpressing the IRF3-nirs3 variant in IFN-competent cells, we were able to reverse the phenotype, and reproduce the scenario of poor IFN-induction and enhanced VSV replication observed in HCC cells. Therefore we concluded that the impairment of IFN-β expression in HCC cells might be due to constitutive IRF3-nirs3 expression.

RESULTS

The IFN-induction pathway is defective in HCC cells

In order to compare the IFN-induction properties of HCC hepatocytes with those of normal hepatocytes, we examined the extent to which Poly (I:C), a synthetic analogue of dsRNA, or viral infection can trigger expression of the IFN-β promoter in PHHs and the human HCC cell lines, HepG2 and Huh-7. Extracellular Poly (I:C), intracellular Poly (I:C), and viral infection are known to be recognized mainly by different cellular sensors (TLR3, MDA-5, and RIG-I, respectively), leading to transcriptional induction of IFN.[29–31] In the HCC cells, addition of Poly (I:C) to the culture medium, or VSV infection with wt or the mutant VSV-M51R, failed to induce IFN-β mRNA. However, transfection with Poly (I:C), which mimics generation of intracytoplasmatic dsRNA during viral infection, resulted in expression of IFN-β mRNA. No IFN-α mRNA was detected because HCC cell lines do not express IRF7 without a high-dose pretreatment with IFN-α.[32] The ability of PHHs to efficiently activate IFN-α/β transcription when exposed to either extracellular or intracellular Poly (I:C) or to VSV infection was demonstrated. As expected, VSV-M51R induced IFN-α/β mRNA to a greater degree than the wt strain did (**Figure 1a**).

In order to confirm these results, PHHs and HCC cells were transiently transfected with a reporter plasmid expressing luciferase under the control of the IFN-β promoter, and challenged with Poly (I:C) or VSV infection [multiplicity of infection (MOI) 1]. Consistent with the reverse transcriptase (RT)-PCR analysis, Huh-7 and HepG2 cells showed little, if any, IFN-β promoter activity in response to Poly (I:C) and viral infection, even with the use of the IFN-inducer VSV-M51R. In contrast, robust upregulation of IFN-β promoter activity over basal levels was observed in PHHs, with the greatest luciferase activity being in response to dsRNA (**Figure 1b**). In PHHs, the activity of an ISRE-promoter was induced upon infection with VSV-wt and VSV-M51R, thereby confirming the production of endogenous type I IFN. Although HCC cells were able to respond to IFN-α and -β, as confirmed by a dose-dependent ISRE-promoter activation, they expressed a significantly lower luciferase reporter activity following VSV infection than PHHs did (**Figure 1c**).

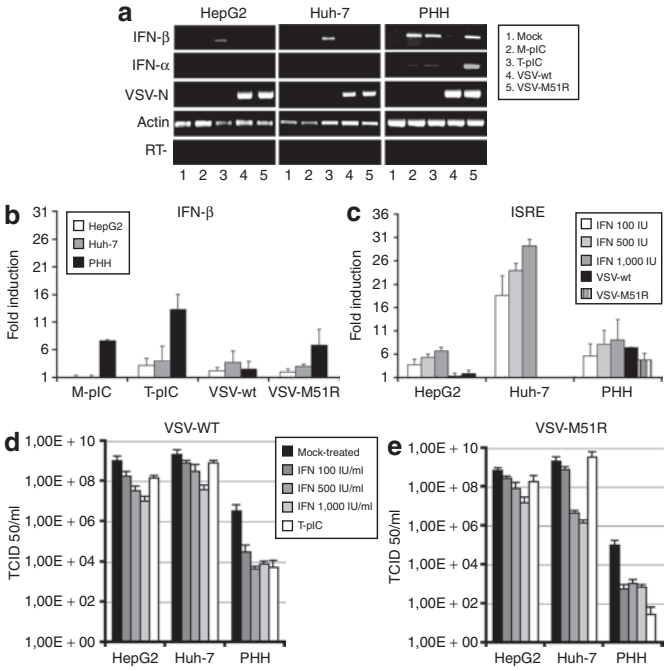

Figure 1 dsRNA and VSV infection do not activate interferon (IFN)-β-transcription in HCC cell lines. Two different human HCC cell lines, HepG2 and Huh-7, and control primary human hepatocytes (PHHs) derived from resected human liver tissue were left untreated, or treated with Poly (I:C) directly added to the culture medium (M-pIC; 50 µg/ml), or transfected with Lipofectamine (T-pIC; 1–5 µg/ml). Other cultures were treated with universal IFN type I (100–1,000 IU/ml), or infected with VSV-wt or VSV-M51R at a multiplicity of infection of 1, as indicated. (**a**) Semi-quantitative reverse transcriptase–PCR detection of IFN-α/β and housekeeping β-actin mRNAs. (**b**) IFN-β and (**c**) ISRE-promoter activation in PHHs and HCCs. Cells grown in a 24-well plate were co-transfected with pIFN-βLuc or pISRE Luc and pRL Luc, and stimulated under the conditions mentioned earlier, 24 hours after transfection. The increase in induction was calculated in terms of a multiple, by dividing the luciferase activity of stimulated cells with that of mock-treated cells. Error bars indicate standard deviations of experiments performed in triplicate. Primary hepatocytes and HepG2 and Huh-7 cells were seeded in 12-well-plates and treated with increasing concentrations of IFN type I (100–500–1,000 IU/ml) or transfected with Poly(I:C) overnight. Mock-treated and treated cultures were infected with (**d**) VSV-wt or (**e**) VSV-M51R at an MOI of 1 and viral titers were determined 24 hours after infection. The data represent the average value from experiments carried out in triplicate.

Treatment with escalating doses of IFN resulted in viral attenuation in both PHH cultures and HCC cell lines (**Figure 1d,e**). In PHHs, viral growth was already impaired at 100 IU/ml; in comparison, higher doses of IFN (1,000 IU/ml) were necessary in order to attain a comparable reduction in titers in HepG2 and Huh-7. Pretreatment with Poly I:C resulted in attenuation of viral growth in PHHs but not in HCC cells. VSV-wt and the mutant VSV-M51R were both sensitive to IFN and Poly (I:C) treatment.

Taken together, these results indicate that the IFN-induction pathways are altered in HCC cell lines. Interestingly, the TLR3-mediated response to dsRNA was completely abrogated in Huh-7 and HepG2, as indicated by the lack of *IFN* gene expression after administration of Poly (I:C) in the culture medium.

Type I IFN attenuates VSV replication in PHHs

In order to assess whether the deficits in IFN-β induction in HCC cells affect VSV replication, we compared HCC cell lines with PHHs as regards their respective abilities to support viral growth. PHHs and the two human HCC cell lines were infected with VSV-wt and the mutant VSV-M51R. HepG2 and Huh-7 strongly supported VSV-wt and VSV-M51R replication, with viral titers peaking at 16–24 hours after infection. PHHs did not show any visible cytopathic effect; in contrast, such an effect was marked in HCC cells (data not shown). Despite the recovery of infectious virions, titers in PHHs were 3–4 logs lower than in cancer cells, thereby indicating attenuation in the viral growth. No appreciable differences in growth kinetics were observed between the two viral strains (**Figure 2a**).

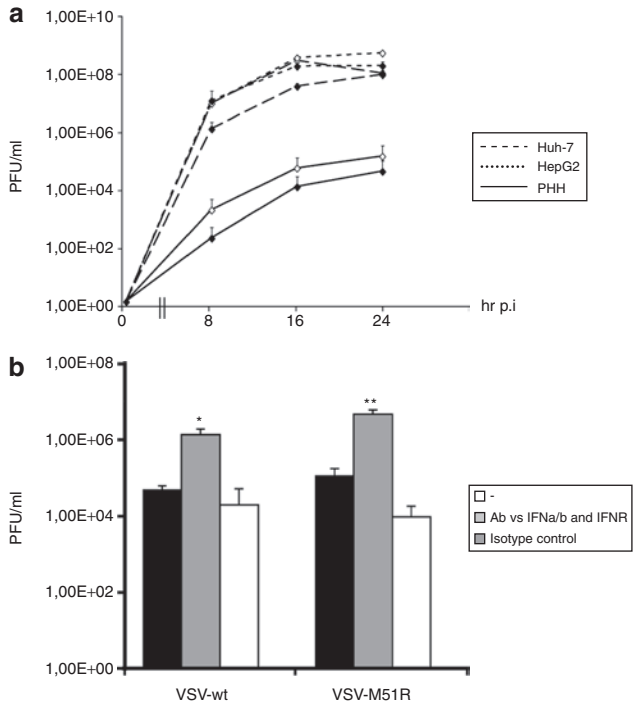

Figure 2 VSV growth in primary human hepatocytes is attenuated. (**a**) HepG2 and Huh-7 cultures and primary human hepatocytes were infected with VSV-wt (open diamonds) and VSV-M51R (closed diamonds) at a multiplicity of infection (MOI)of 0.01. Supernatants were collected at the indicated time points and viral replication was assessed by plaque assay. (**b**) Primary human hepatocyte cultures were incubated with a combination of blocking antibodies against human IFN-α, IFN-β, and IFN-α/β receptors. Cells were infected with VSV-wt and VSV-M51R at an MOI of 1, and titers were determined 24 hours after infection (one-step cycle). Assays were performed in triplicate; each bar indicates mean $*P \leq 0{,}05$; $**P \leq 0{,}001$.

In order to further confirm that IFN signaling is crucial for the control of VSV replication, PHHs were treated with a combination of neutralizing Abs to IFN-α, IFN-β, and IFN-α/β receptor. The blocking of IFN-signaling resulted in enhanced viral replication, with viral titers increasing by about 1.5 logs (e.g., VSV-wt titers increased from 8.8×10^4 to 2.5×10^6 pfu/ml in untreated and treated cells, respectively; **Figure 2b**). This suggested that endogenously produced IFN-α and -β are at least partly responsible for viral attenuation in PHHs.

The dsRNA-signaling pathway in HCC cells can be restored by overexpression of IRF3

In order to define the mechanisms underlying the defect in dsRNA-dependent signaling in HCC cells, we examined the effects of intracellular versus extracellular Poly (I:C) in their abilities to induce IFN-β-promoter activation. As additional controls, we included TBK1 and TRIF, which are known to stimulate IFN-β in IFN-competent cells. As expected in cancer cells, when Poly (I:C), TBK1, or TRIF were transfected, little or no effect on promoter activity was observed. However, transfection of human IRF3 restored stimulation of IFN-β expression, both in HepG2 and Huh-7 cells (**Figures 3a,b**). Strikingly, intracellular dsRNA as well as TBK1 and TRIF overexpression notably stimulated IFN-β-promoter-driven luciferase activity when IRF3 was

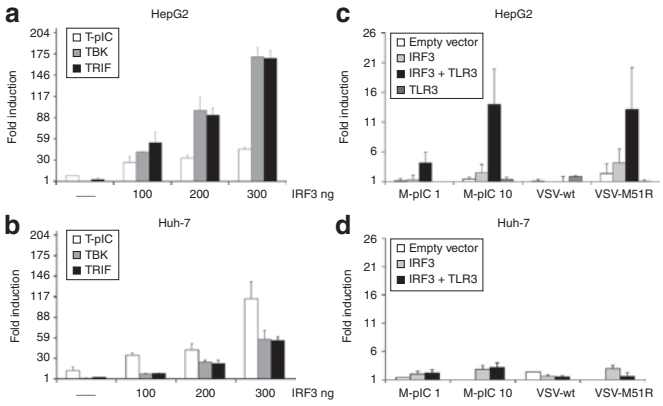

Figure 3 Expression of IRF3 restores activation of intracellular IFN-β signaling pathway in HCC cells. (**a**,**b**) Fold induction of an IFN-β promoter-Luciferase reporter gene in the presence of empty vector or IRF3 expression vector. HepG2 and Huh-7 cells were transfected with the reporter plasmid containing firefly luciferase gene under the control of IFN-β-Luc and increasing amounts (0–100, 200, and 300 ng) of an IRF3 expression vector, respectively. At 24 hours after transfection, the cultures were stimulated by a second round of transfection with Poly (I:C), (T-pIC), TBK1, or TRIF expression vectors. IFN-luciferase activities were measured and normalized to Renilla luciferase (RL) gene used as an internal control. (**c**,**d**) Expression of ectopic IRF3 alone is not sufficient to re-establish IFN-β expression by extracellular dsRNA or virus infection. HepG2 and Huh-7 were transfected with the IFN-β promoter reporter plasmid, or the IRF3 expression vector, or TLR3 alone, or in combination with IRF3 plasmid, respectively. At 24 hours after transfection Poly (I:C) was added to the culture medium (M-pIC: 1–10 μg/ml), or infection with VSV-wt or VSV-M51R at an MOI of 1 was performed.

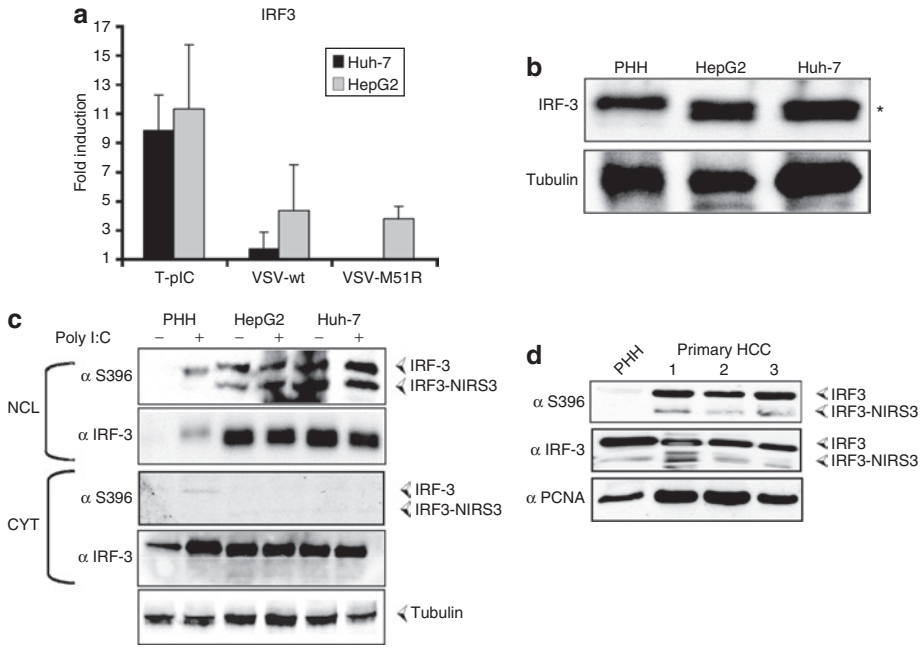

Figure 4 Constitutive expression of IRF3 and IRF3-nirs3 spliced variant in HCC cell lines and primary HCC samples from various donors. (**a**) IRF3 promoter activation in HCC cell lines by Poly (I:C) and virus infection. Luciferase activity increased substantially after transfection of dsRNA and to much lower extent in response to viral infection. Experiments were performed in triplicate; each bar indicates mean value ± SD. (**b**) Western blot showing the basal expression of IRF3 and the alternative IRF3-nirs3 form (,) in HCC cells and primary human hepatocytes. Whole protein lysates of mock cultures were separated by SDS/PAGE and transferred to polyvinylidene fluoride membrane. IRF3 was detected using a rabbit polyclonal antibody raised against the full-length human IRF3. (**c**) Phosphorylation of IRF3. Nuclear (NCL) and cytoplasmic (CT) extracts prepared from mock-transfected or Poly (I:C)-transfected primary hepatocytes, HepG2, and Huh-7 cells, were analyzed by immunoblotting. The membrane was probed with antibody recognizing the total IRF3 and the IRF3 phosphorylated form (phospho-S396). The lysates were also probed with anti-PCNA and antitubulin antibodies, respectively. (**d**) Protein expression of IRF3 in the same primary HCC samples as compared to unstimulated primary human hepatocytes (PHHs). Basal expression and the phosphorylation state were analyzed as described previously. Western blots are representatives of two independent experiments.

co-transfected with the reporter plasmids. Further, the extent of reporter activation was associated with IRF3 expression in a dose-dependent manner.

In addition to the restoration of intracellular dsRNA recognition and IFN signaling, IRF3 expression also played a role in the IFN response to extracellular dsRNA. While it is known that TLR3 is the major sensor of extracellular dsRNA, resulting in activation of the IFN pathway,[33] addition of Poly (I:C) to the culture medium does not induce IFN-β expression in HCC cells even when TLR3 is transfected (**Figure 3c**). However, coexpression of IRF3 with TLR3 resulted in restored IFN-β promoter activity by extracellular dsRNA stimulation in HepG2 cells (**Figure 3c**). In line with these results, the ability of VSV-M51R to evoke an antiviral response was rescued in the HepG2 cell line also only when IRF3 was co-transfected with TLR3. Interestingly, functional restoration of the TLR3-mediated signaling pathway in Huh-7 was not achieved by coexpression of IRF3 and TLR3 (**Figure 3d**), indicating the presence of a more complex defect involving other components of the pathway. This could be explained by a defect in TRIF, as previously described by others in Huh-7 cells.[32]

From these results, we conclude that cytoplasmatic IFN signaling is defective in Huh-7 and HepG2 cells as a consequence of a dysfunctional IRF3, and that its reconditioning is sufficient in HepG2 cells to re-establish an IFN response to extracellular synthetic dsRNA and VSV-M51R. As expected, VSV-wt did not induce expression of IFN-β even in the presence of a restored IFN-signaling pathway, because of the ability of the wt matrix protein to inhibit host gene expression.

IRF3 and IRF3-nirs3 spliced variant are constitutively activated in HCC

In order to determine whether the IRF3 promoter could be stimulated in HCC cells, we transfected a reporter plasmid driven by the IRF3 promoter, and observed an activation of the promoter by transfection of Poly (I:C) (**Figure 4a**). Next, for examining the possibility that the defect occurs at the post-transcriptional level, we compared IRF3 protein concentrations from the lysates of PHHs and HCC cells. Although total protein levels of IRF3 were comparable in both cell types, a second, faster-migrating band in the HCC cell lines was detected by western blotting (**Figure 4b**) using an antibody specific to human IRF3. The expression levels of this smaller band were notably higher in HepG2 and Huh-7 than in PHHs. We therefore hypothesized that this smaller band might correspond to a spliced variant of IRF3. In order to assess whether this isoform is involved in the impairment of dsRNA-induced *IFN* gene expression in HCC cells, we isolated the coding-regions of the full-length and truncated isoform (1,284 and 903 nucleotides, respectively) by RT-PCR from Huh-7 cells, and created IRF3 and IRF3-spliced isoform expression vectors by subcloning. Sequence analysis revealed that the shorter form of IRF3 corresponded to the spliced variant IRF3-nirs3 (GenBank accession number: AB102887). No differences were observed in the IRF3 sequence.

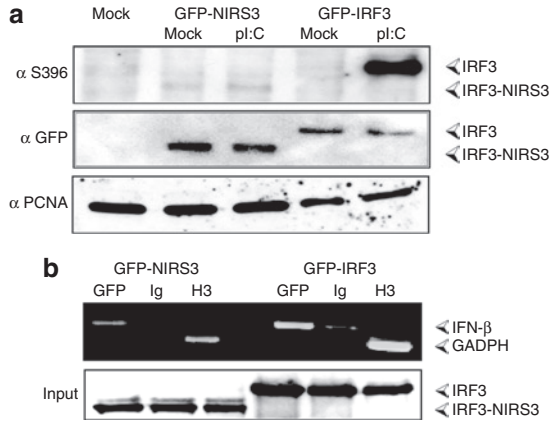

Figure 5 IRF3-nirs3 impairs the IFN-β response in HCC cell lines. (**a**) Fusion proteins GFP-IRF3 and GFP-IRF3nirs3 were expressed in Huh-7 cells. After mock- or Poly (I:C)–stimulation nuclear extracts were subjected to immunoblotting analyses for detection of basal expression and phosphorylation. (**b**) GFP-IRF3 and GFP-IRF3nirs3 association with IFN-β promoter sequence. The fusion proteins were transfected in Huh-7 cells and, following Poly (I:C) stimulation, chromatin immunoprecipitation was carried out in accordance with the manufacturer's instructions (EZ CHIP kit, Upstate). Chromatin was immunoprecipitated with α-GFP antibody (GFP); α-acetylated histone H3 (H3) and normal rabbit Ig (Ig) were used as controls. IFN-β promoter sequence and housekeeping control gene (*GAPDH*) associated with either IRF3 or IRF3-nirs3 spliced variant were amplified using standard PCR. The protein input was assessed by western blot, using an anti-GFP primary antibody.

In order to examine IRF3 activation, we utilized a phospho-specific antibody that reacts only with the form of IRF3 that is phosphorylated at serine 396. As expected, no phospho-IRF3 was detected in the nuclei of unstimulated PHHs, while its levels readily increased 3 hours after transfection of Poly (I:C). In mock-stimulated HCC cell lines, we found constitutively high levels of phoshorylated IRF3 and IRF3-nirs3 (**Figure 4c**). Importantly, clinical samples of primary human HCC from various donors (three representatives out of seven analyzed samples are shown) also revealed constitutive activation of IRF3 and IRF3-nirs3 by phosphorylation (**Figure 4d**), thereby indicating that our results in HCC cell lines are consistent with the scenario in primary HCC tissue.

Next, we hypothesized that phosphorylated IRF3-nirs3 shuttles to the nucleus and interferes with the binding of IRF3-dimers to the IFN promoter. For confirming this, fusion proteins GFP-IRF3 and GFP-IRF3nirs3 were overexpressed in Huh-7 cells. After stimulation with Poly (I:C), nuclear extracts were analyzed by western blot (**Figure 5a**). Using an antibody to GFP, both isoforms were detected in the nucleus even in the absence of stimulation. Poly (I:C) treatment resulted in strong phosphorylation of serine 396 of the transfected GFP-IRF3. Inexplicably, the spliced GFP-IRF3nirs3 appeared not to be phosphorylated on this residue, regardless of Poly (I:C) stimulation. Chromatin immunoprecipitation (ChIP) analyses revealed that IRF3-nirs3 maintains the ability to bind to the IFN-β promoter (**Figure 5b**).

IRF3-nirs3 impairs the IFN-β response and enhances viral replication in IFN-competent cells

While IFN-β promoter activation by intracellular Poly (I:C) was restored through expression of IRF3 in HepG2 and Huh-7 cells

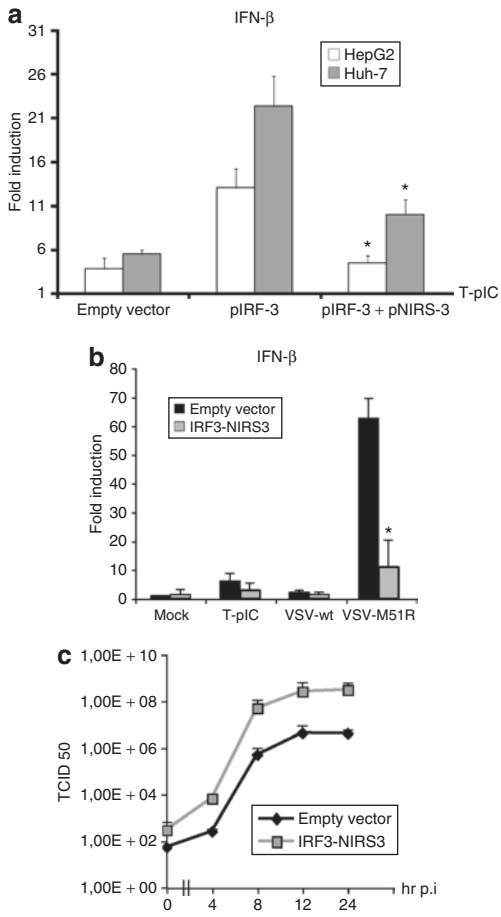

Figure 6 Restoration of IFN-β induction by expression of IRF3 in HCC cells is abrogated by IRF3-nirs3. (**a**) HepG2 and Huh-7 cells ectopically expressing IRF3, alone or in combination with IRF3-nirs3, were stimulated with Poly (I:C). Fold induction of the IFN-β promoter-dependent luciferase activity was calculated by normalizing with Renilla luciferase expression. *$P \leq 0{,}05$. (**b**) IRF3-nirs3 expression in A549 inhibits activation of the IFN-β promoter by Poly (I:C) and VSV-M51R infection. A549 cells transfected with an empty vector or IRF3-nirs3 expression plasmid (100 ng) were stimulated with Poly (I:C) or infected. Luciferase activity was calculated as explained earlier. (**c**) A549 cells were transfected with either IRF3-nirs3 or an empty vector. 48 hours after transfection, infection with VSV-M51R was carried out at a multiplicity of infection of 0.01, and viral titers were determined at 0, 4, 8,12, and 24 hours after infection.

(as shown earlier), the IFN-β response was almost completely abrogated by co-transfection with IRF3-nirs3 (**Figure 6a**). Similarly, when IRF3-nirs3 was expressed in IFN-competent A549 cells, a significantly impaired response ($P < 0.05$) to VSV-M51R was observed in comparison to mock-transfected cells (**Figure 6b**). In order to explore the hypothesis that IRF3-nirs3 enhance viral replication because of perturbation of the IFN response, we performed multi-step growth analysis of the mutant virus VSV-M51R in A549 cells. Given that A549 cells are able to respond to VSV-M51R infection by inducing IFN, we transfected cells with IRF3-nirs3 or an empty vector as a control and infected them at an MOI of 0.01. The altered growth kinetics in cells expressing IRF3-nirs3 resulted in an increase in viral titers by ~2 logs at 24 hours after infection (**Figure 6c**).

DISCUSSION

Initially described for their antiviral activities, type I IFNs have come to be recognized as important regulatory factors of several biological functions, including immunomodulation, cell growth and differentiation, angiogenesis, and apoptosis.[34] Alterations in cell proliferation and cell death are essential determinants in the pathogenesis and progression of malignancies. In this study, we have characterized type I IFN function in liver cells, comparing PHHs with HCC cell lines, namely HepG2 and Huh-7. As previously described, HCC cells are defective in their type I IFN signaling,[35] while PHHs possess a functional IFN pathway and can efficiently respond to stimulation by synthetic dsRNA and viral infection. In HCC cell lines a remarkable impairment in IFN induction is also accompanied by a weaker response. Therefore protection against viral infection is achieved only at higher IFN concentrations. It has been hypothesized that the defect in the IFN-induction pathway responsible for the unresponsiveness of HCC cell lines is related to impaired transcriptional factor activities such as IRF7.[35]

IRF3 is a member of the IFN regulatory transcription factor family. When stimulated it translocates to the nucleus and activates the transcription of IFN-α and -β as well as other IFN-inducible genes.[36] Given the requirement of IRF3 signaling for successful induction of type I *IFN* gene expression, we investigated the possibility that the impairment in IFN expression in HCC cells could be attributed to a defect in IRF3. For this purpose, we overexpressed human IRF3 by transfection of HepG2 and Huh7 cells and examined the effect on IFN-β promoter activity using a luciferase reporter plasmid. Because the ability of a cell to recognize and respond to intracellular, as distinct from extracellular, dsRNA involves different receptors, we investigated each of the pathways individually. When IRF3 was expressed, intracellular dsRNA successfully triggered induction of the IFN-β promoter, thereby indicating that the upstream pathway was intact. Also, the ability to induce IFN by overexpression of TBK1 or TRIF was re-established. We confirmed that the TLR3-TRIF pathway is functional in PHHs, while it is generally lacking in cultured HCC cells,[37] even after expression of IRF3. Further, extracellular Poly (I:C)-signaling, as well as the response to the IFN-inducing virus VSV-M51R, could be completely restored in HepG2 cells by coexpression of IRF3 with TLR3, the receptor for extracellular dsRNA recognition.[17,38] While this data suggests an involvement of TLR3 in antiviral innate immunity against VSV infection, our investigation thus far has revealed that the failure in type I IFN activation in HCC cells by dsRNA is caused mainly by a defect in the IRF3-dependent signaling pathway, and possibly also by defects in the TLR7-dependent signaling pathway (**Supplementary Figure S1**).

Next, we compared the levels of IRF3 at the mRNA and protein levels in PHHs and HCC cells. In PHHs IRF3 was activated by stimulation with Poly (I:C), while its mRNA and activated protein were undetected in mock-treated cells. In contrast, we observed constitutive upregulation of IRF3 mRNA transcription and its phosphorylated form in nuclear fractions of unstimulated HepG2 and Huh-7 cells. This phenomenon could be explained by a defect in the Ras signaling pathway, as described by others.[39] In addition, western blot analysis revealed the presence of a truncated form of IRF3, which was detected in abundance in the HCC cells. Encouragingly, it was found on analysis of primary HCC tumor tissue from seven individual clinical patients, that the IRF3 protein expression profiles in all the samples revealed nearly identical results to those observed in HepG2 and Huh-7 cells, thereby validating our *in vitro* results.

Intrigued by our observation of a truncated isoform of IRF3 in the HCC cell lines and primary HCC tissue, we investigated the possibility of alternative splicing. Several alternative-spliced variants of IRF3 have been recently reported in literature. Although their roles remain to be fully elucidated, their involvement in IRF3 activity has been postulated, and some of these spliced isoforms seem to exert dominant-negative functions.[27,28] Similarly, we identified the truncated form of IRF3 found in HCC cells as another spliced form of IRF3, known as IRF3-nirs3. This variant lacks 127 amino acids included in the highly conserved β-sandwich core of the IRF3 regulatory domain (RD).[40] This domain appears to be critically important for the signal-induced activation of IRF3. For example, mutations in the loop-helix region and in the acidic pocket (comprising residues Glu 200, 201, 203, and 205) impede dimer formation and binding to CBP/p300, respectively.[41] Although the spliced variant lacks the domain necessary for dimerization, the phosphorylation acceptors at its carboxyl terminus are conserved; this is consistent with our observation that, in addition to phosphorylated IRF3 in the nuclei of HCC cells, there was a second IRF3 protein, also phosphorylated at its carboxy-terminus, corresponding to the predicted size of IRF3-nirs3. This demonstrates that the phosphorylation of these serine residues is viable, allowing the translocation of IRF3-nirs3 to the nucleus. Further, according to our ChIP assay data, both IRF3 and IRF3-nirs3 have comparable binding affinity to the IFN-β promoter sequence, thereby suggesting that the interference in IRF3 signaling could be the result of competition with IRF3-nirs3 for limited binding sites. We speculate that the disruption of the regulatory domain in the central portion of the protein might influence the relative conformation of the DNA binding domain and the C-terminal region that are crucial for its transcription activity, as is the case for IRF2 and IRF1.[42,43] Taken together, our results indicate that competitive binding between functional full-length IRF3 and the defective IRF3-nirs3, could explain the malfunction in IRF3 signaling in HCC.

Given the abnormally high levels of IRF3-nirs3 in HCC cell lines and primary HCC tissue, we postulated that this splicing variant might be involved in the lack of virus- and dsRNA-induced *IFN-β* gene expression in cells derived from HCC. We confirmed this hypothesis by showing that IRF3-nirs3 isolated from Huh-7 was indeed able to counteract IFN-β promoter activation through dsRNA in IFN-competent A549 cells. Given the restricted transfection efficiency in PHHs, we used A549 cells in these experiments because they can efficiently induce IFN, and high expression levels of IRF3-nirs3 can be achieved by the transient transfection necessary for exerting its inhibitory effects. Expression of IRF3-nirs3 in A549 cells not only reduced luciferase activity of the IFN-β promoter upon infection with VSV-M51R, but also enhanced viral growth, presumably as a consequence of a delayed IFN response. These data verify our hypothesis and, collectively, demonstrate that the deregulation in IRF3 signaling caused by overexpression of IRF3-nirs3 contributes to the susceptibility of HCC cells to viral replication.

While it is encouraging that we could reproduce some of our *in vitro* findings in primary clinical samples, it is a valid concern

that, when testing a limited number of cell lines, one can be easily misled by products of *in vitro* artifacts. Although it would have been desirable to screen a larger panel of HCC cell lines, most of the available human HCC cells contain integrated viral DNA, which would introduce additional variables and likely interfere with the acquisition of reliable results.[44] Therefore, in order to eliminate these unknown variables, we selected HepG2 and Huh-7 as representatives of human HCC because they lack viral DNA.

In addition, it is noteworthy to mention that Huh-7 cells from different origins differ in their properties of IFN-β induction.[45] While some authors describe Huh-7 cells as IFN-competent, several authors have reported a weak or defective dsRNA-induced antiviral signaling pathway in this cell line.[32,46,47] Consistent with these observations, our Huh-7 cells revealed themselves to be similar to HepG2 cells, in that they were poor inducers of IFN.

In conclusion, our study demonstrates that, while reduced IFN-β expression in cancer cells is attributable to multiple defects in the type I IFN-induction pathways, the impairment of IRF3 activity seems to play a major role in HCC cells. The identification of differential expression of IRF3 and IRF3-nirs3 in HCC cells, described here for the first time, represents a critical step forward in the understanding of the IFN-signaling defects that contribute to the mechanism through which oncolytic viruses exert their tumor specificity. The expression profile of IRF3-nirs3 is an important determinant of the impaired IFN response to VSV infection in HCC, and may represent a potential marker to predict the magnitude of transformation, as well as to screen candidate tumors for susceptibility to VSV oncolytic therapy in future clinical applications.

MATERIALS AND METHODS

Cell lines, primary human HCC and hepatocytes, and viruses. Two human HCC cell lines (HepG2 and Huh-7), a kind gift of Dr Ulrich Lauer (University Hospital of Tübingen), and A549 (ATCC, Rockville, MD) were maintained in Dulbecco's modified Eagle's medium supplemented with 10% fetal bovine serum, 1% L-glutamine (200 mmol/l), 1% Penicillin/streptomycin, 1% nonessential amino acids, and 1% sodium pyruvate. BHK-21 cells were obtained from ATCC (Rockville, MD) and cultured in Glasgow MEM BHK-21 medium (GIBCO; Invitrogen, Karlsruhe, Germany) supplemented with 10% fetal bovine serum and 1% tryptose phosphate broth. All cell cultures were regularly tested for mycoplasma contamination.

Frozen primary HCC samples and short-term cultures of PHHs were derived from patients (negative for HBV, HCV, and HIV) who underwent surgical resections of liver tumors, in accordance with the guidelines of the charitable state controlled foundation Human Tissue and Cell Research (Regensburg, Germany).[48] PHHs were maintained in culture with HepatoZYME-SFM medium (GIBCO) containing 1% L-glutamine.

VSV-wt and the mutant strain VSV-M51R were generated as previously described.[7,49] Virus stocks were produced on BHK-21 cells and stored at −80 °C. Titers were determined by plaque assay on BHK-21 cells.

RT-PCR analysis. PHHs and HCC cells were grown in 6-well plates and were mock-treated, transfected with 5 μg Poly (I:C) (Invivogen, France), or infected at an MOI of 1 with VSV-wt or VSV-M51R. As a separate control, Poly (I:C) was applied to the culture medium at a concentration of 50 μg/ml. RNA was extracted using RNeasy Plus Kit (Qiagen, Hilden, Germany) in accordance with the manufacturer's instructions, 12–15 hours after treatment. RNA was DNase (Invitrogen, Karlsruhe, Germany)-treated and reverse transcribed. RT-PCR was carried out using the "one-step RT-PCR" kit (Qiagen, Hilden, Germany) with the specific primers listed in **Table 1**.

Table 1 Primer sets

IFN-β	5′-TTGAATGGGAGGCTTGAATA-3′
	5′-CTATGGTCCAGGCACAGTGA-3′
IFN-α	5′-TTTGCTTTACTGGTGGCCCT-3′
	5′- TTCTGCTCTGACAACCTCCCAG-3′
VSV-N	5′-ATCCTCTGCCGACTTGGCACAA-3′
	5′- TGTCAAATTCTGACAAAGCATACTTGCCAA-3′
huIRF3	5′-ATGAAGCTTGCCACCATGGGAACCCC AAAGCCACGG-3′
	5′-GAATTCCATCAGCTCTCCCCAGGGCCCT-3′
huIRF3 (partial)	5′-ATGGTGTTGGCCCCACTCCCAGATCC-3′
	5′-TCAGCTCTCGGCAGGGCCCT-3′
IFN-β promoter	5′-ATGACATAGGAAAACTGAAAGGGAGAAGTGA-3′
	5′-TGTAGGAATCCAAGCAAGTTGTAGCTCAT-3′
β-Actin	5′-GGCATCGTGATGGACTCC-3′
	5′- CCGCCAGACAGCACTGTGTTGGCGTA-3′

Western blotting. Whole-cell extracts and nuclear/cytoplasmatic extracts (NE-PER nuclear and cytoplasmic extraction reagents, Pierce) were run on a 7.5% SDS-PAGE and transferred to polyvinylidene fluoride membranes. Total cell lysates were prepared using lysing buffer [50 mmol/l Tris-HCl (pH 8.0), 150 mmol/l NaCl, 1% TX-100] containing a protease and phosphatase inhibitor cocktail. Protein concentrations in the samples were determined using the BCA protein assay kit (Biolynx, Brokeville, Canada). After blocking for 1 hour with 5% skim milk/TBS-tween, the membranes were blotted with the following primary antibodies overnight at 4 °C: IRF3 (sc-9082; Santa Cruz, Heidelberg, Germany), Phospho-IRF3-Ser396 (Cell Signalling, Frankfurt, Germany), GFP (ab290, Abcam, Cambridge, UK), PCNA (sc-7907, Santa Cruz, Heidelberg, Germany), and β-tubulin (Sigma, Taufkirchen, Germany). After secondary staining with anti-rabbit or anti-mouse peroxidase-conjugated Abs (Dianova, Hamburg, Germany), the blots were washed three times with TBS-Tween. Protein bands were visualized on Amersham Hyper-Max film with the ECL chemiluminescence system, in accordance with the manufacturer's instructions (Amersham, Buckinghamshire, UK).

Neutralization assay and IFN resistance. PHHs were plated on collagen-coated 24-well plates at the density of 2×10^5 cells/well. Monolayers were infected with VSV-wt and VSV-M51R at an MOI of 1 for 1 hour. After virus absorption, the cells were washed three times with PBS and, in order to block the effect of type I IFN, they were incubated with a mixture of 5,000 neutralizing U/ml rabbit anti-human IFN-α Ab, 2,000 U/ml rabbit anti-human IFN-β Ab and 20 μg/ml mouse anti-human IFN-α/β receptor mAb IFN-αR1β (PBL Biomedical Laboratories, Piscataway, NJ). A mouse IgG (DB Pharmingen, Heidelberg, Germany) was used as isotype control. At 24 hours after infection, supernatants were harvested and viral titers assessed by plaque assay.

PHHs and HCC cell lines (HepG2 and Huh-7) were seeded at a density of 1×10^6 cells/well. Monolayers were mock-treated or treated overnight with Universal type I IFN (PBL) at concentrations of 100, 500, and 1,000 IU/ml. Infection with VSV-wt or the VSV-M51R mutant, was performed for 1 hour, and viral titers were determined after 24 hours.

Viral growth. Multi-cycle growth curves of wt and M51R mutant strains of VSV were obtained for PHHs, HepG2, and Huh-7 cell lines. Cells (1×10^6/well) were infected with the viruses at an MOI of 0.01. After adsorption for 1 hour, monolayers were washed three times with PBS and fresh medium was added. Aliquots of culture media were taken and fresh media were added immediately at time points 0, 8, 16, and 24 hours after infection.

Viral titers were determined using a standard plaque assay, and each time point represents the average of triplicate experiments. For experiments to establish the activity of IRF3-nirs3 on viral growth, A549 cells were seeded at a density of 5×10^5/well and transfected with 1 μg of either pGFP-IRF3-nirs3 or the empty vector pGFP-C3. Twenty-four hours after transfection, the cells were infected with VSV-M51R at an MOI of 0.01 and viral titers were determined at time points 0, 4, 8, 12, and 24 hours after infection.

Luciferase assay. Transfection of plasmid DNA was carried out with Lipofectamine 2000 LTX (Invitrogen) as recommended by the manufacturer. Luciferase activity in cell lysates was quantified using the Dual-Luciferase Assay system (Promega, Mannheim, Germany) with a luminometer (Turner Designs, Sunnyvale, CA). The relative light units were normalized by co-transfection of constitutively active Renilla luciferase and presented as a multiplying factor of induction relative to the basal expression level. For luciferase assays, cells seeded in 24-well plates were co-transfected with the IFN-β, IRF3, and ISRE promoter-luciferase reporter plasmids (100 ng), and with the Renilla reniformis plasmid (10 ng). The following expression vectors were used for the various experiments as appropriate: phuTBK1, phuTRIF, phuIRF3, phuTLR7, phuTLR3, and phuIRF3nirs3 in the indicated amounts. Twenty-four hours later, the cells were mock-treated or challenged with Poly (I:C), treated with different concentrations of recombinant Universal type I IFN (PBL Biomedical), or virus-infected according to the requirements of the relevant experiment.

Cloning of GFP-IRF3 and GFP-IRF3nirs3 fusion plasmids. The GFP-IRF3 and the GFP-IRF3nirs3 fusion plasmids were prepared by cloning the HindIII-EcoRI fragments containing the full-length complementary DNAs, amplified by RT-PCR from Huh-7 mRNA, in the pGFP-C3 vector (Invitrogen). The sequencing of the plasmids was conducted at MWG Biotech, Germany.

Chromatin immunoprecipitation (ChIP) assay. Huh-7 cells were transfected with the fusion plasmids GFP-IRF3 and GFP-IRF3nirs3. Chromatin immunoprecipitation was performed from unstimulated and Poly (I:C)-treated cells using an assay kit in accordance with the manufacturers' instructions (Upstate Biotechnology, Lake Placid, NY). Chromatin was immunoprecipitated with an antibody against GFP (Ab290, Abcam). Controls were obtained with an antiacetyl histone H3 or normal rabbit Ig as the immunoprecipitating antibodies. The immunoprecipitated DNAs were amplified by PCR, using primers for amplifying the human IFN-β promoter (**Table 1**) and GADPH as internal control. The samples were amplified for 35 cycles and analyzed by electrophoresis on a 1.5% agarose gel.

ACKNOWLEDGMENTS

We thank Adolfo García-Sastre for his critical review of the manuscript, Stephan Bauer for providing the phuTLR3 and phuTLR7 vectors, and Barbara Lindner for her excellent technical assistance. We express our appreciation to Human Tissue and Cell Research (Regensburg, Germany) for providing human primary hepatocytes and primary HCC samples. Our special gratitude goes to Laurent Lariviere for useful discussions about IRF3 structure. The study was partly supported by the German Cancer Aid (Max-Eder Research Program) (O.E.), and the German Federal Ministry of Education and Research Grant 01GU0505 (O.E.).

SUPPLEMENTARY MATERIAL

Figure S1. The TLR7-dependent pathway malfunctions in HCC cells.

REFERENCES

1. Giannelli, G and Antonaci, S (2006). Novel concepts in hepatocellular carcinoma: from molecular research to clinical practice. *J Clin Gastroenterol* **40**: 842–846.
2. Vollmer, CM, Ribas, A, Butterfield, LH, Dissette, VB, Andrews, KJ, Eilber, FC *et al.* (1999). p53 selective and nonselective replication of an E1B-deleted adenovirus in hepatocellular carcinoma. *Cancer Res* **59**: 4369–4374.
3. Hallenbeck, PL, Chang, YN, Hay, C, Golightly, D, Stewart, D, Lin, J *et al.* (1999). A novel tumor-specific replication-restricted adenoviral vector for gene therapy of hepatocellular carcinoma. *Hum Gene Ther* **10**: 1721–1733.
4. Huang, TG, Savontaus, MJ, Shinozaki, K, Sauter, BV and Woo, SL (2003). Telomerase-dependent oncolytic adenovirus for cancer treatment. *Gene Ther* **10**: 1241–1247.
5. Miyatake, SI, Tani, S, Feigenbaum, F, Sundaresan, P, Toda, H, Narumi, O *et al.* (1999). Hepatoma-specific antitumor activity of an albumin enhancer/promoter regulated herpes simplex virus *in vivo*. *Gene Ther* **6**: 564–572.
6. Pawlik, TM, Nakamura, H, Yoon, SS, Mullen, JT, Chandrasekhar, S, Chiocca, EA *et al.* (2000). Oncolysis of diffuse hepatocellular carcinoma by intravascular administration of a replication-competent, genetically engineered herpes virus. *Cancer Res* **60**: 2790–2795.
7. Ebert, O, Shinozaki, K, Huang, TG, Savontaus, MJ, Garcia-Sastre, A and Woo, SL (2003). Oncolytic vesicular stomatitis virus for treatment of orthotopic hepatocellular carcinoma in immune-competent rats. *Cancer Res* **63**: 3605–3611.
8. Kemeny, N, Brown, K, Covey, A, Kim, T, Bhargava, A, Brody, L *et al.* (2006). Phase I, open-label, dose-escalating study of a genetically engineered herpes simplex virus, NV1020, in subjects with metastatic colorectal carcinoma to the liver. *Hum Gene Ther* **17**: 1214–1224.
9. Rose, JK and Whitt, MA (2001). Rhabdoviridae: the viruses and their replication. In: Knipe, DM and Howley, PM (eds). *Fields Virology*, 4th edn. Lippincott Williams & Wilkins: Philadelphia. pp. 1221–1242.
10. Stojdl, DF, Lichty, B, Knowles, S, Marius, R, Atkins, H, Sonenberg, N *et al.* (2000). Exploiting tumor-specific defects in the interferon pathway with a previously unknown oncolytic virus. *Nat Med* **6**: 821–825.
11. Balachandran, S and Barber, GN (2000). Vesicular stomatitis virus (VSV) therapy of tumors. *IUBMB Life* **50**: 135–138.
12. Ebert, O, Shinozaki, K, Kournioti, C, Park, MS, Garcia-Sastre, A and Woo, SL (2004). Syncytia induction enhances the oncolytic potential of vesicular stomatitis virus in virotherapy for cancer. *Cancer Res* **64**: 3265–3270.
13. Shinozaki, K, Ebert, O, Kournioti, C, Tai, YS and Woo, SL (2004). Oncolysis of multifocal hepatocellular carcinoma in the rat liver by hepatic artery infusion of vesicular stomatitis virus. *Mol Ther* **9**: 368–376.
14. Shinozaki, K, Ebert, O and Woo, SL (2005). Eradication of advanced hepatocellular carcinoma in rats via repeated hepatic arterial infusions of recombinant VSV. *Hepatology* **41**: 196–203.
15. Petersen, JM, Her, LS, Varvel, V, Lund, E and Dahlberg, JE (2000). The matrix protein of vesicular stomatitis virus inhibits nucleocytoplasmic transport when it is in the nucleus and associated with nuclear pore complexes. *Mol Cell Biol* **20**: 8590–8601.
16. von Kobbe, C, van Deursen, JM, Rodrigues, JP, Sitterlin, D, Bachi, A, Wu, X *et al.* (2000). Vesicular stomatitis virus matrix protein inhibits host cell gene expression by targeting the nucleoporin Nup98. *Mol Cell* **6**: 1243–1252.
17. Ahmed, M, McKenzie, MO, Puckett, S, Hojnacki, M, Poliquin, L and Lyles, DS (2003). Ability of the matrix protein of vesicular stomatitis virus to suppress beta interferon gene expression is genetically correlated with the inhibition of host RNA and protein synthesis. *J Virol* **77**: 4646–4657.
18. Stojdl, DF, Lichty, BD, tenOever, BR, Paterson, JM, Power, AT, Knowles, S *et al.* (2003). VSV strains with defects in their ability to shutdown innate immunity are potent systemic anti-cancer agents. *Cancer Cell* **4**: 263–275.
19. Desforges, M, Charron, J, Berard, S, Beausoleil, S, Stojdl, DF, Despars, G *et al.* (2001). Different host-cell shutoff strategies related to the matrix protein lead to persistence of vesicular stomatitis virus mutants on fibroblast cells. *Virus Res* **76**: 87–102.
20. Stetson, DB and Medzhitov, R (2006). Type I interferons in host defense. *Immunity* **25**: 373–381.
21. Dunn, GP, Koebel, CM and Schreiber, RD (2006). Interferons, immunity and cancer immunoediting. *Nat Rev Immunol* **6**: 836–848.
22. Parmar, S and Platanias, LC (2003). Interferons: mechanisms of action and clinical applications. *Curr Opin Oncol* **15**: 431–439.
23. Yoneyama, M, Kikuchi, M, Natsukawa, T, Shinobu, N, Imaizumi, T, Miyagishi, M *et al.* (2004). The RNA helicase RIG-I has an essential function in double-stranded RNA-induced innate antiviral responses. *Nat Immunol* **5**: 730–737.
24. Fitzgerald, KA, McWhirter, SM, Faia, KL, Rowe, DC, Latz, E, Golenbock, DT *et al.* (2003). IKKepsilon and TBK1 are essential components of the IRF3 signaling pathway. *Nat Immunol* **4**: 491–496.
25. Sharma, S, tenOever, BR, Grandvaux, N, Zhou, GP, Lin, R and Hiscott, J (2003). Triggering the interferon antiviral response through an IKK-related pathway. *Science* **300**: 1148–1151.
26. Servant, MJ, Grandvaux, N, tenOever, BR, Duguay, D, Lin, R and Hiscott, J (2003). Identification of the minimal phosphoacceptor site required for *in vivo* activation of interferon regulatory factor 3 in response to virus and double-stranded RNA. *J Biol Chem* **278**: 9441–9447.
27. Karpova, AY, Howley, PM and Ronco, LV (2000). Dual utilization of an acceptor/donor splice site governs the alternative splicing of the IRF-3 gene. *Genes Dev* **14**: 2813–2818.
28. Karpova, AY, Ronco, LV and Howley, PM (2001). Functional characterization of interferon regulatory factor 3a (IRF-3a), an alternative splice isoform of IRF-3. *Mol Cell Biol* **21**: 4169–4176.
29. Jiang, Z, Mak, TW, Sen, G and Li, X (2004). Toll-like receptor 3-mediated activation of NF-κB and IRF3 diverges at Toll-IL-1 receptor domain-containing adapter inducing IFN-β. *Proc Natl Acad Sci USA* **101**: 3533–3538.
30. Le Goffic, R, Pothlichet, J, Vitour, D, Fujita, T, Meurs, E, Chignard, M *et al.* (2007). Cutting Edge: Influenza A virus activates TLR3-dependent inflammatory and RIG-I-dependent antiviral responses in human lung epithelial cells. *J Immunol* **178**: 3368–3372.
31. Loo, YM and Gale, M Jr. (2007). Viral regulation and evasion of the host response. *Curr Top Microbiol Immunol* **316**: 295–313.
32. Li, K, Chen, Z, Kato, N, Gale, M Jr. and Lemon, SM (2005). Distinct poly(I-C) and virus-activated signaling pathways leading to interferon-β production in hepatocytes. *J Biol Chem* **280**: 16739–16747.
33. Alexopoulou, L, Holt, AC, Medzhitov, R and Flavell, RA (2001). Recognition of double-stranded RNA and activation of NF-κB by Toll-like receptor 3. *Nature* **413**: 732–738.

34. Maher, SG, Romero-Weaver, AL, Scarzello, AJ and Gamero, AM (2007). Interferon: cellular executioner or white knight? *Curr Med Chem* **14**: 1279–1289.
35. Keskinen, P, Nyqvist, M, Sareneva, T, Pirhonen, J, Melen, K and Julkunen, I (1999). Impaired antiviral response in human hepatoma cells. *Virology* **263**: 364–375.
36. Hiscott, J, Pitha, P, Genin, P, Nguyen, H, Heylbroeck, C, Mamane, Y *et al.* (1999). Triggering the interferon response: the role of IRF-3 transcription factor. *J Interferon Cytokine Res* **19**: 1–13.
37. Li, XD, Sun, L, Seth, RB, Pineda, G and Chen, ZJ (2005). Hepatitis C virus protease NS3/4A cleaves mitochondrial antiviral signaling protein off the mitochondria to evade innate immunity. *Proc Natl Acad Sci USA* **102**: 17717–17722.
38. Trottier, MD, Lyles, DS and Reiss, CS (2007). Peripheral, but not central nervous system, type I interferon expression in mice in response to intranasal vesicular stomatitis virus infection. *J Neurovirol* **13**: 433–445.
39. Noser, JA, Mael, AA, Sakuma, R, Ohmine, S, Marcato, P, Wk Lee, P *et al.* (2007). The RAS/Raf1/MEK/ERK signaling pathway facilitates VSV-mediated oncolysis: implication for the defective interferon response in cancer cells. *Mol Ther* **15**: 1531–1536.
40. Qin, BY, Liu, C, Lam, SS, Srinath, H, Delston, R, Correia, JJ *et al.* (2003). Crystal structure of IRF-3 reveals mechanism of autoinhibition and virus-induced phosphoactivation. *Nat Struct Biol* **10**: 913–921.
41. Takahasi, K, Suzuki, NN, Horiuchi, M, Mori, M, Suhara, W, Okabe, Y *et al.* (2003). X-ray crystal structure of IRF-3 and its functional implications. *Nat Struct Biol* **10**: 922–927.
42. Koenig Merediz, SA, Schmidt, M, Hoppe, GJ, Alfken, J, Meraro, D, Levi, BZ *et al.* (2000). Cloning of an interferon regulatory factor 2 isoform with different regulatory ability. *Nucleic Acids Res* **28**: 4219–4224.
43. Lee, EJ, Jo, M, Park, J, Zhang, W and Lee, JH (2006). Alternative splicing variants of IRF-1 lacking exons 7, 8, and 9 in cervical cancer. *Biochem Biophys Res Commun* **347**: 882–888.
44. Shamay, M, Agami, R and Shaul, Y (2001). HBV integrants of hepatocellular carcinoma cell lines contain an active enhancer. *Oncogene* **20**: 6811–6819.
45. Binder, M, Kochs, G, Bartenschlager, R and Lohmann, V (2007). Hepatitis C virus escape from the interferon regulatory factor 3 pathway by a passive and active evasion strategy. *Hepatology* **46**: 1365–1374.
46. Lanfor, RE, Guerra, B, Lee, H, Averett, DR, Pfeiffer, B, Chavez, D *et al.* (2003). Antiviral effect and virus-host interactions in response to alpha interferon, gamma interferon, Poly(I)-Poly(C), tumor necrosis factor alpha, and Ribavirin in hepatitis C virus subgenomic replicons. *J Virol* **77**: 1092–1104.
47. Dansako, H, Ikeda, M and Kato, N (2007). Limited suppression of the interferon-β production by hepatitis C virus serine protease in cultured human hepatocytes. *FEBS J* **274**: 4161–4176.
48. Thasler, WE, Weiss, TS, Schillhorn, K, Stoll, PT, Irrgang, B and Jauch, KW (2003). Charitable state-controlled foundation human tissue and cell research: ethic and legal aspects in the supply of surgically removed human tissue for research in the academic and commercial sector in Germany. *Cell Tissue Bank* **4**: 49–56.
49. Ebert, O, Harbaran, S, Shinozaki, K and Woo, SL (2005). Systemic therapy of experimental breast cancer metastases by mutant vesicular stomatitis virus in immune-competent mice. *Cancer Gene Ther* **12**: 350–358.

Personal Information

Name: **Jennifer E. Altomonte**
Birthdate: 22.01.1976 in N.Y., USA

Education and research experience

1994-1999 Bachelor of Science, Microbiology with minor in biochemistry and molecular biology; Pennsylvania State University, University Park, PA

1999-2006 Research Coordinator, laboratory of Prof. Savio Woo; Institute for Gene and Cell Medicine, Mount Sinai School of Medicine, New York, NY, USA

2003-2005 Master of Science, Forensic Science; John Jay College of Criminal Justice, New York, NY (Thesis work: 2009, Helmholtz Zentrum München; Supervisor: Dr. Arne Pfeufer)

2006-present Research Scientist, laboratory of Dr. med. Oliver Ebert; 2nd Medical Clinic, Klinikum rechts der Isar at the Technical University of Munich, Munich, Germany

Skills

- **Molecular biology:** molecular cloning, site-directed mutagenesis, SDS-PAGE, Western blot, Northern blot, ELISA, RIA, ChIP, immunoprecipitation, PCR, RT-PCR, qRT-PCR, DNA and RNA isolation, virus purification, reporter assays
- **Cell culture:** propagation of primary and immortalized cell lines, transfection, infection experiments, virus rescue and amplification, plaque assay, TCID50, MTT assay, immunofluorescent staining, photomicroscopy
- **Animal procedures:** establishment of implanted and spontaneous tumor models, microsurgery, suturing, catheter placement, tail vein injection, blood collection, anesthesia and post-operative care, isolation of primary hepatocytes, necropsy, histology, immunohistochemistry
- **Computer skills:** Microsoft Office, Endnote, ImageJ, MacVector (for analyzing DNA, RNA, and protein sequences, and design of primers), GraphPad Prism (for statistical analysis), Photoshop, Illustrator

Volunteer Work

2000-2002 Emergency Medical Technician; Bellore-Merrick EMS, Bellmore, NY, USA

2001-2003 Child-Life Volunteer, Northshore University Hospital, Manhasset, NY, USA

Publications

Dong, H., **Altomonte, J.**, Morral, N., Meseck, M., Thung, S.N. and Woo, S.L.C. (2002). Basal Insulin Gene Expression Significantly Improves Conventional Insulin Therapy in Type 1 Diabetes. *Diabetes*. 51, 130-139.

Morral, N., McEvoy, R., Dong, H., Meseck, M., **Altomonte, J.**, Thung, S., and Woo, S.L.C. (2002). Adenovirus-Mediated Expression of Glucokinase in the Liver as an Adjuvant Treatment for Type 1 Diabetes. *Human Gene Therapy*. 13, 1561-1570.

Hofmann, S., Dong, H., Li, Z., Cai, W., **Altomonte, J.**, Thung, S.N., Zeng, F., Fisher, E.D., and Vlassara, H. (2002). Improved Insulin Sensitivity is Associated With Restricted Intake of Dietary Glycoxidation Products in the db/db Mouse. *Diabetes*. 51, 2082-2089.

Altomonte, J., Harbaran, S., Richter, A., and Dong, H. (2003). Fat Depot-Specific Expression of Adiponectin is Impaired in Zucker Fatty Rats. *Metabolism*. Aug;52(8):958-63.

Altomonte, J., Richter, A., Harbaran, S., Nakae, J., Meseck, M., Accili, D., and Dong, H. (2003). Inhibition of Foxo1 Function is Associated with Improved Fasting Glycemia in Diabetic Mice. *American Journal of Physiology, Endocrinology, and Metabolism*. 285(4):E718-28

Puigserver, P., Rhee, J., Donovan, J., Yoon, J.C., Walkey, C.J., Oriente, F., Kitamura, Y., **Altomonte, J.**, Dong, H., Accili, D., and Spiegelman, B.M. (2003). Insulin-Regulated Hepatic Gluconeogenesis Through FOXO1-PGC1alpha Interaction. *Nature*. 423(6939):550-5.

Altomonte, J., Cong, L., Harbaran, S., Richter, A., Xu, J., Meseck, M., and Dong, H. (2004). Foxo1 mediates insulin action on apoC-III and triglyceride metabolism. *J Clin Invest*. 114(10):1493-503.

Zhang, N., Richter, A., Suriawinata, J., Harbaran, S., **Altomonte, J.**, Cong, L., Zhang, H., Song, K., Meseck, M., Bromberg, J., and Dong, H. (2004). Elevated vascular endothelial growth factor production in islets improves islet graft vascularization. *Diabetes*. 53(4)963-70.

Dong, H., Maddux, B.A., **Altomonte, J.**, Meseck, M., Accili, D., Terkeltaub, R., Johnson, K., Youngren, J.F., and Goldfine, I.D. (2005). Increased hepatic levels of the insulin receptor inhibitor, PC-1/NPP1, induce insulin resistance and glucose intolerance. *Diabetes*. 54(2):367-72.

Qu, S., **Altomonte, J.**, Perdomo, G., He, J., Fan, Y., Kamagate, A., Meseck, M., and Dong, H. (2006) Aberrant Forkhead box 01 function is associated with impaired hepatic metabolism. *Endocrinology* . 147(12):5641-52

Qu, S., Su, D., **Altomonte, J.**, Kamagate, A., He, J., Perdomo, G., Tse, T., Jiang, Y., and Dong, H. (2007) PPARalpha mediates the hypolipidemic action of fibrates by antagonizing FoxO1. *Am J Physiol Endocrinol Metab*. 292(2):E421-34

Morral. N., Edenberg, H., Witting, SR., **Altomonte, J.**, Chu, T., and Brown, M. (2007). Effects of glucose metabolism on the regulation of genes of fatty acid synthesis and triglyceride secretion in the liver. *J Lipid Res*. 48(7)1499-510.

Altomonte, J., Wu, L., Chen, L., Meseck, M., Ebert, O., Garcia-Sastre, A., Fallon, J., and Woo, SL. (2008). Exponential enhancement of oncolytic Vesicular stomatitis virus potency by vector-mediated suppression of inflammatory responses in vivo. *Mol Ther*. 16(1):146-53

Wu, L., Huang, TG, Meseck, M., **Altomonte, J.**, Ebert, O., Shinosaki, K., Garcia-Sastre, A., Fallon, J., Mandeli, J., and Woo, SL. (2008). rVSV(MD51)-M3 is an effective and safe oncolytic virus for cancer therapy. *Hum Gene Ther* 19(6):635-47.

Altomonte, J., Braren, R., Schulz, S., Marozin, M., Rummeny, EJ, Schmid, RM, and Ebert, O. (2008) Synergystic antitumor effects of transarterial viroembolization for multifocal hepatocellular carcinoma in rats. *Hepatology*, 48(6):1864-73.

Marozin, S., **Altomonte, J.**, Stadler, F., Thasler, WE, Schmid, RM, and Ebert, O. (2008). Inhibition of the IFN-b response in hepatocellular carcinoma by alternative spliced isoform of IFN regulatory factor 3. *Mol Ther,* 16(11):1789-97.

Altomonte, J., Wu, L., Meseck, M., Ebert, O., Garcia-Sastre, A., Fallon, J., and Woo, SL. (2009) Enhanced oncolytic potency of vesicular stomatitis virus via vector-mediated inhibition of NK and NKT cells. *Cancer Gene Ther*, 16(3):266-78.

Altomonte, J., Marozin, S., Schmid, RM, and Ebert, O. (2010). Engineered Newcastle Disease Virus as an improved oncolytic agent against hepatocellular carcinoma. *Mol Ther*. 18(2):275-84.

Abstracts and Presentations:

Hofmann, S., Dong, H., Cai, W., Li, Z., **Altomonte, J.**, Fischer, E., and Vlassara, H. Restricted intake of glycoxidants leads to elevated serum HDL-C levels in db/db (+/+) mice. Poster presentation at *ADA 62nd Annual Scientific Sessions*. San Francisco, CA 2002.

Dong, H., **Altomonte, J.**, Richter, A., Meseck, M., and Woo, S. Suppression of hepatic gluconeogenesis by liver-targeted gene transfer. Poster presentation at *ADA 62nd Annual Scientific Sessions*. San Francisco, CA. 2002.

Altomonte, J., Harbaran, S., Richter, A., Meseck, M., and Dong, H. Foxo1 (FKHR) functionally mediates insulin action in regulating hepatic Apolipoprotein C-III Production. Oral presentation at *ADA 63rd Annual Scientific Sessions*. New Orleans, LA. 2003.

Richter, A., **Altomonte, J.**, Harbaran, S., Meseck, M., Accili, D., and Dong, H. Suppression of hepatic Foxo1 (FKHR) expression improves insulin sensitivity in db/db mice. Oral presentation at *ADA 63rd Annual Scientific Sessions*. New Orleans, LA. 2003.

Altomonte, J., Harbaran, S., Richter, A., and Dong, H. Differential production of adiponectin in visceral vs. subcutaneous fat in relation to the pathogenesis of insulin resistance in Zucker fatty rats. Poster presentation at *ADA 63rd Annual Scientific Sessions*. New Orleans, LA. 2003

Zhang, N., Richter, A., Suriawinata, J., **Altomonte, J.**, Meseck, M., and Dong, H. Elevated VEGF production in islet cells enhances islet graft vascularization and improves functional islet mass post transplantation. Oral presentation at *ADA 63rd Annual Scientific Sessions*. New Orleans, LA. 2003.

Altomonte, J., Anthony, K., Baliga, S., Xu, J., and Dong, H. Foxo1 plays a role in mediating the effect of fibrates on diabetic dyslipidemia. Poster presentation at *ADA 64th Annual Scientific Sessions*. Orlando, FL. 2004.

Zhang, N., Richter, A., Harbaran, S., **Altomonte, J.**, Zhang, H., et al. Intra-graft production of VEGF is associated with enhanced islet neovascularization and improved outcome of marginal islet transplantation in diabetic mice. Poster presentation in *ADA 64th Annual Scientific Sessions*. Orlando, FL. 2004.

Altomonte, J., Qu, S., and Dong, H. Aberrant Foxo1 expression is associated with intrahepatic fat deposition and impaired insulin action in liver. Poster presentation at *ADA 65th Annual Scientific Sessions*. San Diego, CA. 2005.

Qu, S., **Altomonte, J.**, and Dong, H. Insulin gene therapy corrects hypertriglyceridemia in diabetic mice. Poster presentation at *ADA 65th Annual Scientific Sessions*. San Diego, CA. 2005.

Altomonte, J., Qu, S., and Dong, H. Fibrates down-regulate Foxo1 expression and ameliorate hypertriglyceridemia in high fructose diet-fed hamsters. Oral presentation in *ADA 65th Annual Scientific Sessions*. San Diego, CA. 2005.

Qu, S., **Altomonte, J.**, He, J., Meseck, M., and Dong, H. Aberrant Foxo1 expression in liver associated with intrahepatic fat infiltration and hepatic insulin resistance. Accepted for presentation at 2006 Keystone Symposia: Diabetes Melitus and the Control of Cellular Energy Metabolism.

Qu, S.,, Altomonte, J., He, J., Su, D., Perdomo, G., Baliga, S., and Dong, H. Fibrates downregulate Foxo1 and PGC-1B expression and ameliorate hypertriglyceridemia in high fructose diet-fed hamsters. Accepted for presentation at 2006 Keystone Symposia: Diabetes Melitus and the Control of Cellular Energy Metabolism.

Qu, S., **Altomonte, J.**, Su, D., and Dong, H. ApoA-V counteracts ApoC-III in improving triglyceride metabolism in hypertriglyceridemic APOC3 transgenic mice. Accepted for presentation at 2006 Keystone Symposia: Diabetes Melitus and the Control of Cellular Energy Metabolism.

Marozin, S., **Altomonte, J.**, Stadtler, F., Thasler, W., Schmid, R., and Ebert, O. Inhibition of the IFN-beta response to dsRNA and VSV infection in hepatocellular carcinoma by alternative spliced isoform interferon regulatory factor 3. Poster presentation at *German Society of Gene Therapy (DG-GT) 14th Annual Meeting.*

Altomonte, J., Braren, R., Rummeny, E.J., Schmid, R.M., and Ebert, O. Enhancement of transarterial oncolytic VSV therapy by transient reduction of intratumoral blood flow with degradable starch microspheres in multifocal HCC-bearing rats. Poster presentation at *In Vivo Barriers to Gene Delivery*, 2007, Cold Spring Harbor.

Altomonte, J., Marozin, S., Schmid, R.M., and Ebert, O. Engineered Newcastle Disease Virus as a novel oncolytic agent against hepatocellular carcinoma. Poster presentation at *The 5th International Meeting on Replicating Oncolytic Virus Therapeutics*. March 18-22, 2009, Banff, Canada.